ABSTRACT

The Effects of Vancomycin on the Structure of Cell Wall Peptidoglycan of *vanB*-type Vancomycin-Resistant *Enterococcus faecalis* by Liquid Chromatography-Mass Spectrometry

Erin E. Foster

Director: Sung Joon Kim, Ph.D.

Enterococcus faecalis is a leading cause of nosocomial infections, and the clinical emergence of vancomycin-resistant *E. faecalis* (VRE) makes studying this bacterium increasingly urgent. This study investigates a *vanB*-type strain of VRE (ATCC 51299), which is vancomycin-resistant upon vancomycin's induction of the *vanB* operon and subsequent changes in the structure of cell wall peptidoglycan that result in reduced affinity of vancomycin for peptidoglycan. This study explored the effects of vancomycin (at 6 μg/mL) on peptidoglycan structure of VRE using a novel approach that involved a combinatorial, *in silico* peptidoglycan mass library paired with liquid chromatography-mass spectrometry. In addition to observing the *vanB*-related changes of the presence of terminal D-Ala-D-Lac and increased D,D-carboxypeptidase activity, increased L,D-carboxypeptidase activity and increased O-acetylation were also observed upon the presence of vancomycin, findings which suggest additional mediating roles of vancomycin in the creation and editing of cell wall peptidoglycan.

APPROVED BY DIRECTOR OF HONORS THESIS

_____

Dr. Sung Joon Kim, Department of Chemistry and Biochemistry

APPROVED BY THE HONORS PROGRAM

_____

Dr. Andrew Wisely, Director

DATE: _____

THE EFFECTS OF VANCOMYCIN ON THE STRUCTURE OF CELL WALL PEPTIDOGLYCAN OF *VANB*-TYPE VANCOMYCIN-RESISTANT *ENTEROCOCCUS FAECALIS* BY LIQUID CHROMATOGRAPHY-MASS SPECTROMETRY

A Thesis Submitted to the Faculty of

Baylor University

In Partial Fulfillment of the Requirements for the

Honors Program

By

Erin E. Foster

Waco, Texas

May 2015

TABLE OF CONTENTS

ACKNOWLEDGEMENTS

I would like to express my deepest gratitude to my thesis director, Dr. Sung Joon Kim, for giving me the invaluable opportunity to learn about research through participation in his lab, for his limitless generosity with his time, and for his kind mentorship and guidance. I would also like to express profound gratitude to James Chang, my graduate student mentor, who taught me everything that I know about lab research and who guided me, assisted me, and encouraged me through every single step of the process of designing, executing, and writing this thesis. Working alongside and observing Dr. Kim and James has taught me an appreciation for lab research and for those who devote their lives and careers to the furthering of scientific knowledge, and I am grateful for getting to see their examples of Christian scholarship at its best. I would also like to thank Dr. Kevin Shuford and Dr. Cheolho Sim for generously volunteering their time and assistance to serve on my thesis defense committee. In addition, I would like to acknowledge all of the invaluable support, encouragement, advice, and prayers that I received from many others throughout the thesis process, including from my family, friends, roommates, neighbors, and current and former colleagues in the Kim Lab Group. Furthermore, I would like to thank Stephanie Harmon, my high school honors chemistry teacher, for initially inspiring my interest in chemistry and in science in general, an interest that has since grown into the passion that motivated the initiation and completion of this project.

CHAPTER ONE

Introduction

Enterococcus faecalis and the Clinical Relevance of VRE

Enterococcus faecalis (*E. faecalis*) is a gram-positive bacterium that inhabits the gastrointestinal (GI) tract of humans and other animals (Arias and Murray, 2012) (Figure 1). *E. faecalis* is clinically important because it is one of the leading causes of nosocomial infections, and the clinical emergence of *E. faecalis* strains resistant to vancomycin, the so-called antibiotic of last resort, only makes studying the bacterium more urgent.

Figure 1: Enterococcal Bacteria (Centers for Disease Control and Prevention, 2013).

According to the CDC, there were about 66,000 enterococcus infections annually as of 2013. 20,000 of those annual infections (or about 30%) were caused by vancomycin-resistant enterococci, and 1,300 of the vancomycin-resistant cases resulted in mortality. Since vancomycin is the antibiotic that is considered the drug of last resort for gram-positive pathogens, only very few (if any) treatment options are available for

patients contracting vancomycin-resistant enterococcal infections. The CDC has therefore classified vancomycin-resistant enterococcus as having a threat level of "serious," meaning that the CDC believes that vancomycin-resistant enterococcus is a pressing health concern that warrants research to address the problem and prevent it from escalating further (Centers for Disease Control and Prevention, 2013). Although these statistics are for enterococcus in general and include all enterococcal strains, *E. faecalis* is a particularly important strain to study because it causes 80-90% of enterococcal infections (Betinkaya, Falk, and Mayhall, 2000).

Vancomycin-Resistant *E. faecalis* (VRE) is particularly problematic due to its occurrence and transmission in the hospital setting, and it is particularly well-known for causing endocarditis, skin and wound infections, and infections arising from the use of an indwelling catheter, such as urinary tract infections (UTI's) from the use of urinary catheters and systemic infections of the bloodstream (bacteremia) from central venous catheters. While enterococcal bacteria normally exist innocuously in the GI tract of humans and other animals as part of the gut microbiota, antibiotic treatment of hospitalized patients can selectively promote the colonization of the GI tract by antibiotic resistant enterococcus, such as VRE. Once VRE colonizes the GI tract, the GI tract can serve as a steady source of the bacteria and lead to the opportunistic infection of other sites. For instance, VRE can move from the GI tract into the bloodstream by crossing the intestinal lining and going through the liver. After the bacteria enter and proliferate in the bloodstream, bacteremia leading to sepsis and endocarditis can occur. Transmission to the patient's skin and to the hospital environment can occur when VRE exits the body via contaminated fecal matter. VRE on the skin can cause localized infections of the skin

and wounds and can participate in catheter-associated infections of the urinary tract and bloodstream (Figure 2a) (Arias and Murray, 2012).

The transmission of VRE to other hospitalized patients is facilitated by the ability of enterococcal bacteria to survive harsh conditions, including high salt concentrations and temperatures ranging from as low as 10°C to higher than 45°C. When proper sanitization protocols are not followed, VRE is therefore easily transmitted between patients within a hospital environment since it is able to survive for prolonged periods of time on the hands of hospital staff and visitors, on contaminated medical equipment, and on other inanimate objects in the hospital (Figure 2b) (Arias and Murray, 2012).

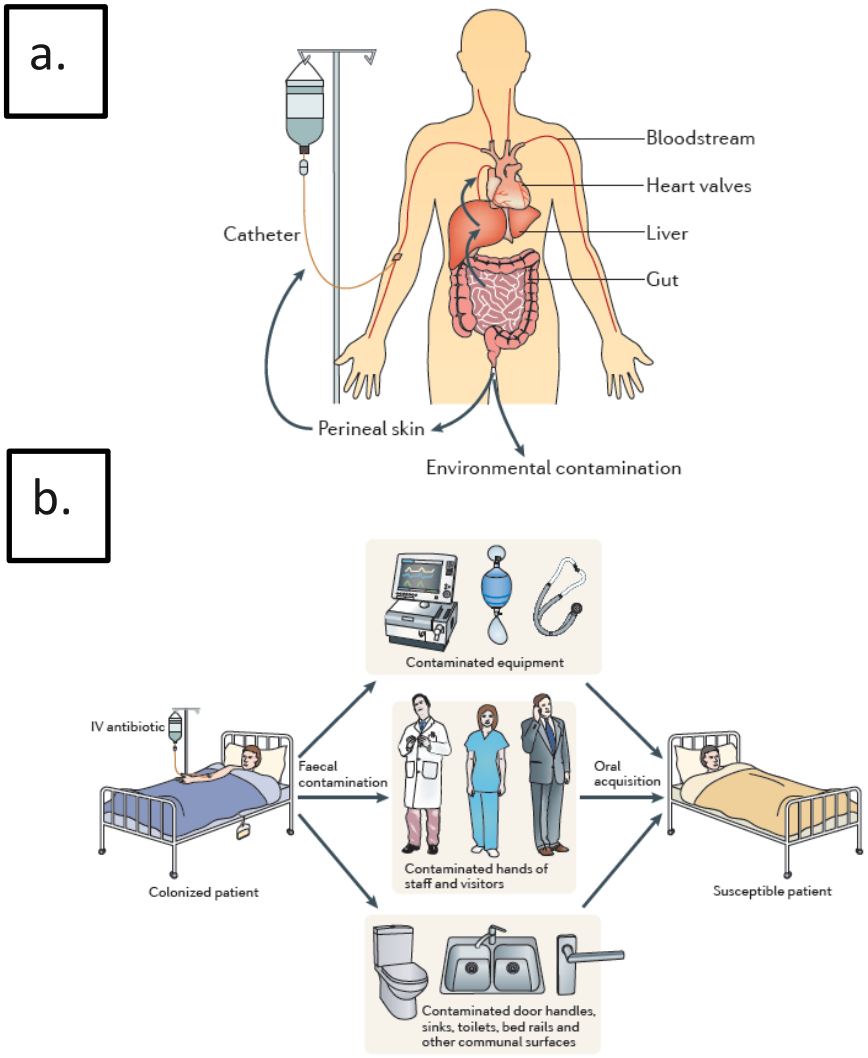

Figure 2: Nosocomial Acquisition and Transmission of VRE (Arias and Murray, 2012). Part (a) shows the colonization of VRE in the GI tract in response to antibiotic treatment and the possible flow of VRE into the circulation (via the intestinal lining and liver) and out of the body (via fecal matter) to contaminate the skin and environment. Part (b) highlights the easy transmission of VRE between hospital inpatients due to its ability to survive harsh conditions.

Vancomycin and Cell Wall Peptidoglycan

Enterococcus faecalis, like all other gram-positive bacteria, contains a thick cell wall outside of the cell membrane that encases the entire cell (Figure 3). The cell wall is a cage-like macromolecule that simultaneously provides structural rigidity and flexibility

for the cell, in addition to protecting the cell from osmotic stress. The key building block and major component of the cell wall is peptidoglycan (PG). Each PG unit contains a sugar backbone composed of a disaccharide of N-acetylglucosamine (GlcNAc or NAG) and N-acetylmuramic acid (MurNAc or NAM), which are joined by a β(1-4) glycosidic linkage. The NAM of PG is bound to a peptide portion, which is variable across gram-positive bacteria (Tong, Pan, Dong, Pryor, Wilson, and Schaefer, 1997). In *E. faecalis*, cell wall PG includes a pentapeptide stem (L-Ala, D-iGln, L-Lys, D-Ala, D-Ala) and a dipeptide cross-linker (L-Ala, L-Ala) (Figure 4) (Bouhss, Josseaume, Severin, Tabei, Hugonnet, Shlaes, Mengin-Lecreulx, Heijenoort, and Arthur, 2002).

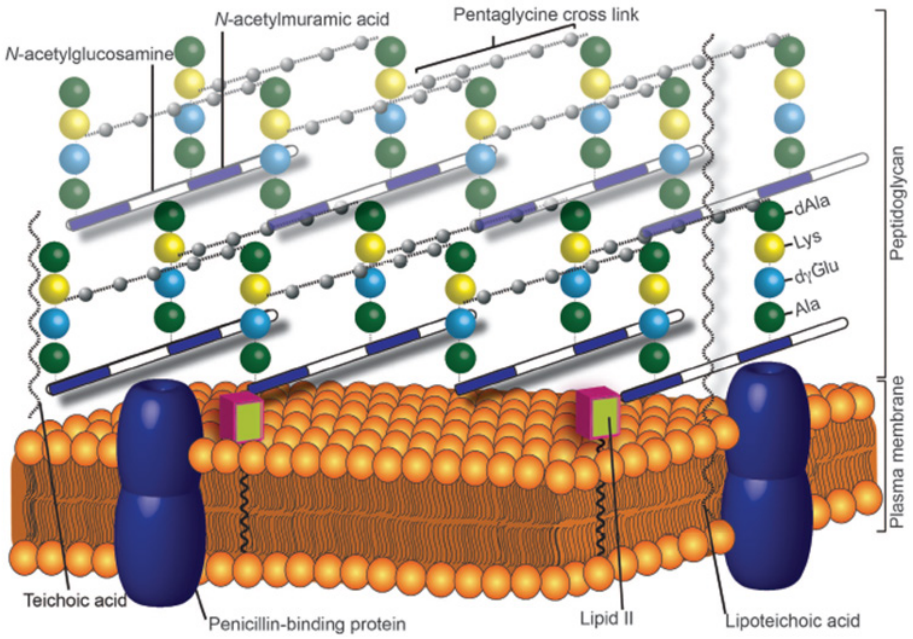

Figure 3: Gram-Positive Cell Wall (Butler, Hansford, Blaskovich, Halai, and Cooper, 2014). The figure shows the thick cell wall that exists outside of the plasma membrane in all gram-positive bacteria. The main component of the bacterial cell wall is peptidoglycan, which is sugar-linked and cross-linked to form the lattice structure shown in the figure.

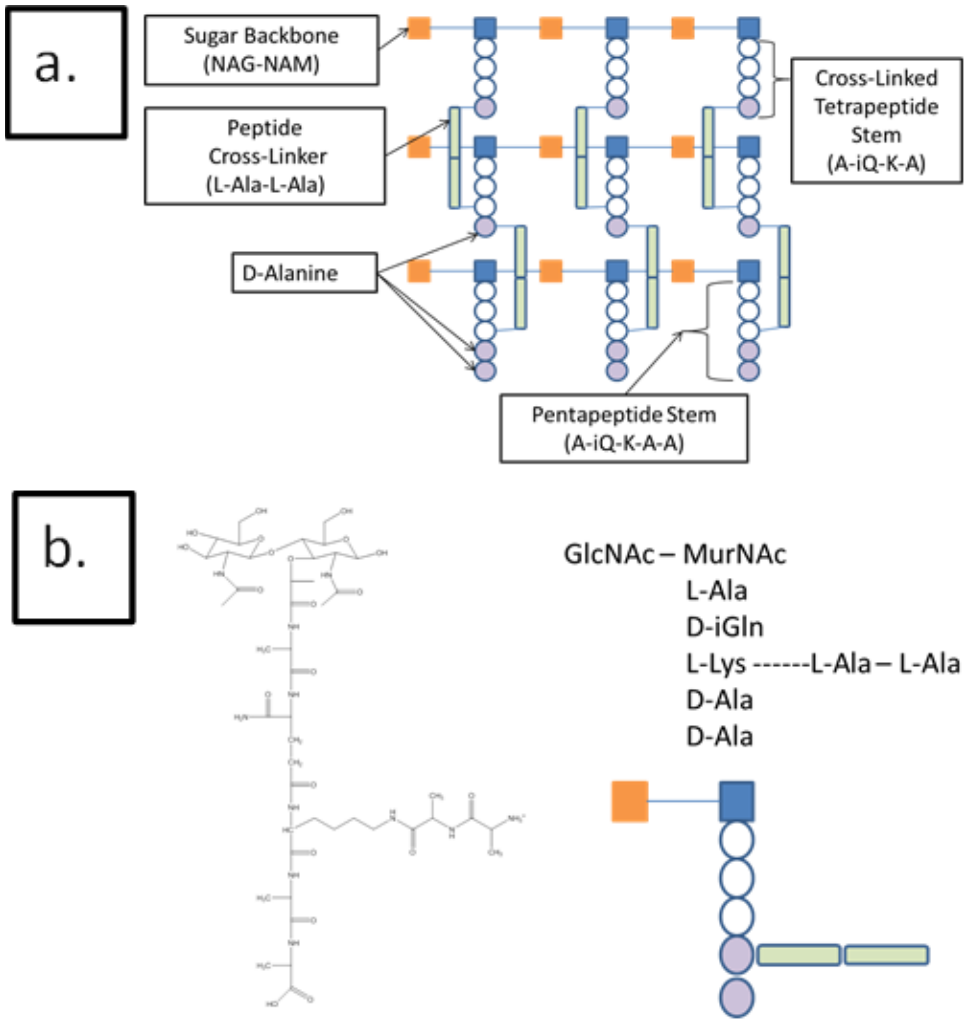

Figure 4: *E. faecalis* Cell Wall and Cell Wall Peptidoglycan. Part (a) gives a diagram of the mature cross-linked and sugar-linked peptidoglycan in *E. faecalis* (figure adapted from a drawing of *S. aureus* cell wall PG in Tong, Pan, Dong, Pryor, Wilson, and Schaefer, 1997) and part (b) shows the structure of the PG monomer. In *E. faecalis*, the PG monomer has a pentapeptide stem with the following amino acids in the following order: L-Ala, D-iGln, L-Lys, D-Ala, D-Ala. The cross-linking bridge on the *E. faecalis* PG is composed of two L-alanines.

Cell wall biosynthesis can be summarized as a process that includes the production of PG units and their subsequent incorporation into the cell wall (Figure 5). A PG precursor, called Lipid II, is first assembled inside the cytoplasmic side of the cell membrane. Lipid II is then transported to outside of the cell membrane (perhaps by an enzyme called a flippase or by another unknown mechanism). Outside of the cell

membrane, lipid II is incorporated into nascent peptidoglycan through transglycosylation (sugar-linking of the disaccharide backbone) and transpeptidation (cross-linking of the peptide cross-linkers) by penicillin-binding proteins (PBP's) (Bugg, Braddick, Dowson, and Roper, 2011). Although there are many additional steps and intermediates in the cell wall biosynthesis pathway not mentioned here, understanding only these few key steps gives insights into 1) the way in which vancomycin functions as an antibiotic to prevent cell wall biosynthesis and 2) the ways in which vancomycin-resistant bacteria evade the antibiotic activity of vancomycin by modifying the cell wall biosynthesis process.

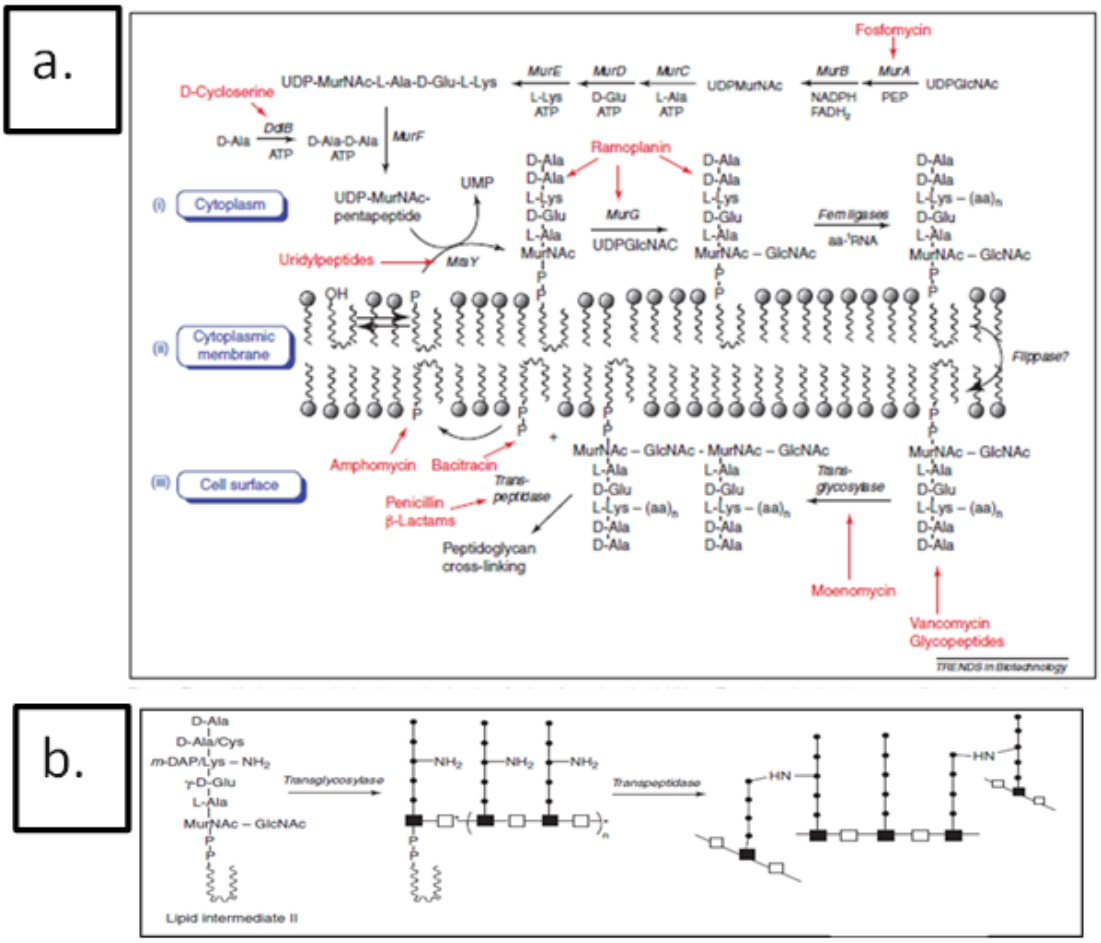

Figure 5: Cell Wall Biosynthesis (Bugg, Braddick, Dowson, and Roper, 2011). Part (a) gives an overview of the complete process of cell wall biosynthesis, including the steps that take place in the cytoplasm and those that take place outside the cell membrane. Part (b) highlights only the stages of cell wall biosynthesis that are most important to vancomycin's mechanism of action, including the lipid II PG precursor that is present on the cell surface and that is then involved in transglycosylation, and transpeptidation.

Vancomycin is a glycopeptide antibiotic that functions by preventing cell wall biosynthesis. The binding site of vancomycin is able to interact with the terminal D-Alanyl-D-Ala amino acid residues of the pentapeptide stem through forming five hydrogen-bonds (Figure 6). Both lipid II and the nascent PG contain unedited D-Alanyl-D-Ala residues that vancomycin is known to bind, and thus vancomycin is able to inhibit cell wall biosynthesis through the following two mechanisms: 1) through binding to

exported lipid II, vancomycin sequesters the lipid II, which effectively causes depletion of the lipid II substrate and arrests the elongation of the glycan chain by transglycosylation, and 2) by binding to the nascent PG, vancomycin sterically hinders the PBP's to prevent their participation in transglycosylation of the nascent PG, thus preventing the formation of the mature PG lattice (Heijenoort, 2007).

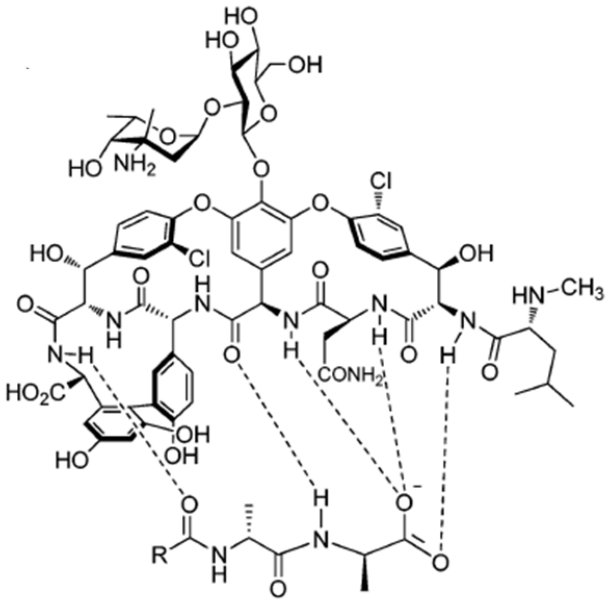

Figure 6: Vancomycin's Mechanism of Action (Ashford and Bew, 2012). Vancomycin is a glycopeptide antibiotic that functions to prevent cell wall biosynthesis by binding to the terminal D-Alanyl-D-Ala residues of peptidoglycan through forming five hydrogen bonds, as shown.

Vancomycin Resistance in Enterococcus faecalis

Vancomycin-Resistant strains of *E. faecalis* are able to evade destruction by vancomycin due to the activity of a *van*-type gene cluster, such as *vanA*, *vanB*, *vanC*, *vanD*, *vanE*, or *vanG*. The strain of VRE tested in this experiment (ATCC 51299) contains the *vanB* operon, so this review will focus on *vanB*. The *vanB* operon includes the following genes: $vanS_B$, $vanR_B$, $vanY_B$, *vanW*, $vanH_B$, *vanB*, and $vanX_B$ (Figure 7)

(Rice, 2001). The *vanB* operon can be subdivided into a regulatory region and an effector region.

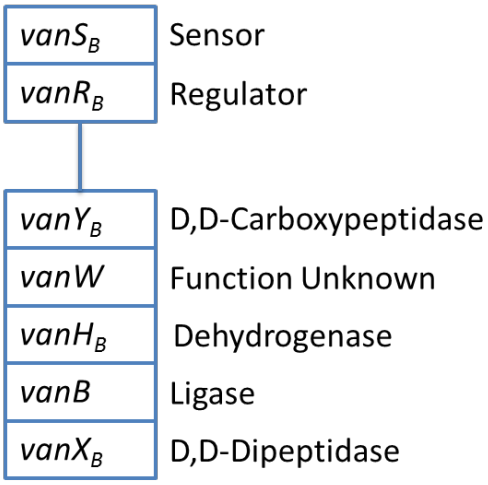

Figure 7: *vanB* Operon in VRE. The *vanB* operon is the genetic basis for vancomycin resistance in the strain of VRE studied in this experiment. The *vanB* operon contains a regulatory region with genes $vanS_B$ and $vanR_B$ and an effector region with $vanY_B$, *vanW*, $vanH_B$, *vanB*, and *vanX*. The functions of the proteins encoded by each gene of the *vanB* operon are noted in the figure.

The regulatory region controls the expression of *vanB* and includes $VanS_B$, a histidine kinase that senses the presence and activity of vancomycin, and $VanR_B$, a transcriptional regulator protein that causes the induction of *vanB* gene activity upon phosphorylation by $VanS_B$ (Depardieu, Courvalin, and Msadek, 2003; Kwun, Novotna, Hesketh, Hill, and Hong, 2013). More specifically, when vancomycin that is bound to the terminal D-Alanyl-D-Ala of lipid II or nascent PG binds to $VanS_B$, $VanS_B$ is converted into its active form. Activated $VanS_B$ is a kinase that phosphorylates $VanR_B$, which causes expression of the rest of *vanB*. When $VanS_B$ is not bound to vancomycin with D-Alanyl-D-Ala of lipid II or PG, $VanS_B$ acts as a phosphatase that dephosphorylates $VanR_B$ to suppress the expression of the rest of *vanB* (Figure 8) (Kwun, Novotna, Hesketh, Hill, and Hong, 2013).

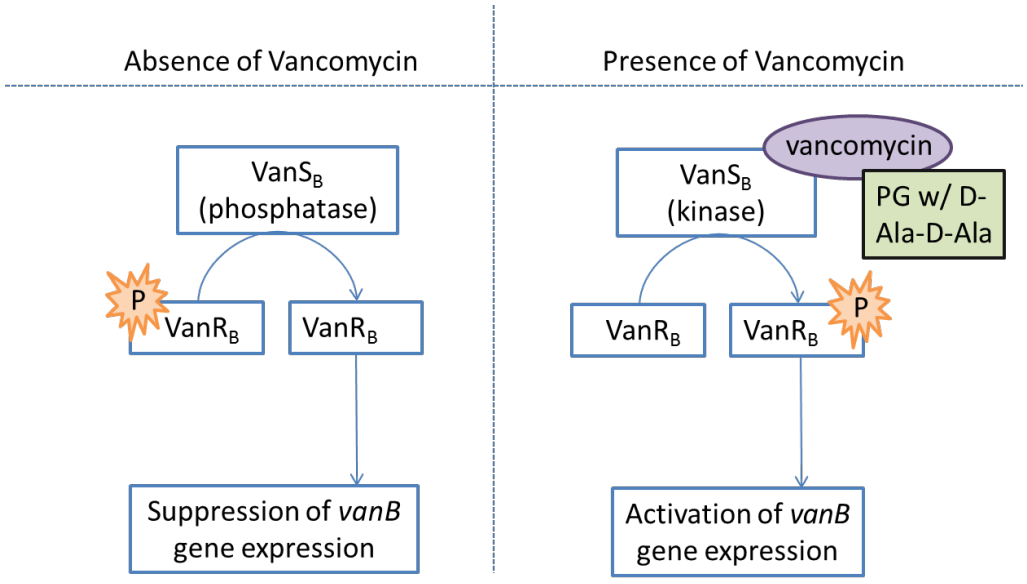

Figure 8: Induction of the *vanB* Operon in VRE by the Presence of Vancomycin Bound to D-Alayl-D-Ala. *vanB* expression is induced by the binding of the vancomycin/PG complex to VanS$_B$. When vancomycin/PG is bound to VanS$_B$, VanS$_B$ acts as a kinase to phosphorylate VanR$_B$, leading to expression of the rest of the *vanB* operon. When vancomycin is not bound to VanS$_B$, VanS$_B$ functions as a phosphatase and dephosphorylates VanR$_B$, leading to suppression of the rest of the *vanB* operon.

The effector portion of *vanB* includes the following genes: *vanY$_B$*, *vanW*, *vanH$_B$*, *vanB*, and *vanX$_B$*. VanH$_B$, VanX$_B$, and VanB function together to manufacture PG with terminal D-Ala-D-Lac residues instead of the normal D-Alanyl-D-Ala residues. VanX$_B$ is a D,D-dipeptidase that functions to cleave D-Ala-D-Ala precursors into D-Ala residues. VanH$_B$ is a dehydrogenase that produces D-Lac from pyruvate. VanB is the ligase that connects the D-Ala with the D-Lac to form the D-Ala-D-Lac complex that is later incorporated into the terminal portion of peptidoglycans (Figure 9a) (Werner, Strommenger, and Witte, 2008). VanY$_B$ is a D,D-carboxypeptidase that edits off the terminal alanine of pentapeptide peptidoglycan precursors, converting them into tetrapeptide peptidoglycan precursors (Figure 9b) (Meziane-Cherif, Stogios, Evdokimova, Savchenko, and Courvalin, 2014). The function of VanW is still unknown (Werner, Strommenger, and Witte, 2008).

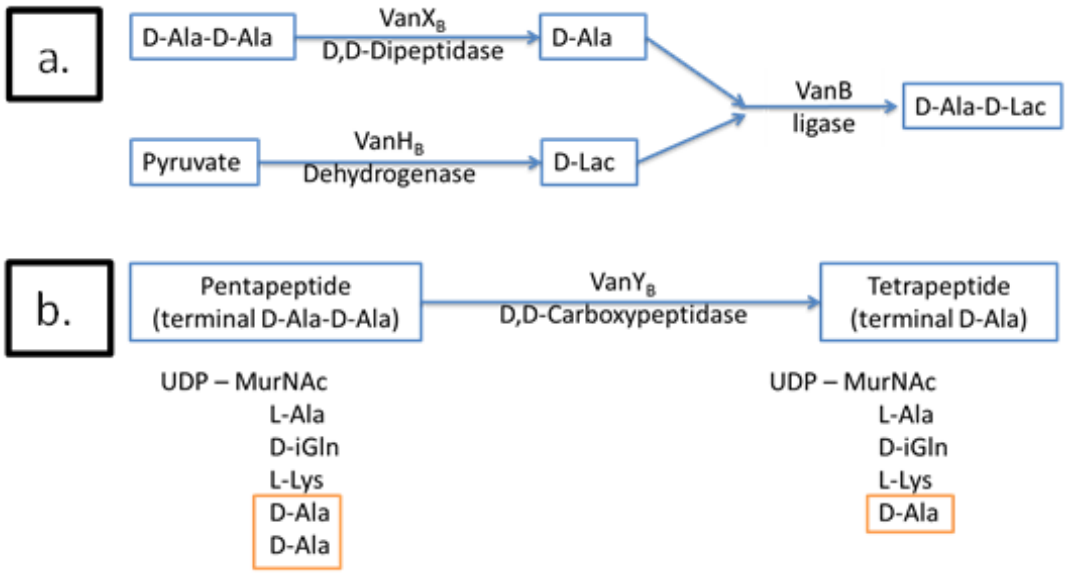

Figure 9: *vanB* Activity in PG Biosynthesis. Part (a) shows the involvement of *vanB* in synthesizing PG with terminal D-Ala-D-Lac instead of the normative D-Alanyl-D-Ala. $VanX_B$ is a D,D-dipeptidase that cleaves D-Ala-D-Ala into D-Ala, while $VanH_B$ is a dehydrogenase that converts pyruvate to D-Lac. VanB is a ligase that synthesizes the D-Ala-D-Lac from D-Ala and D-Lac precursors. Part (b) shows the involvement of *vanB* in editing PG precursors. $VanY_B$ is a D,D-carboxypeptidase that converts UDP-MurNAc-pentapeptides to UDP-MurNAc-tetrapeptides by cleaving the terminal D-Ala residue.

Vancomycin can bind with high affinity to the terminal D-Alanyl-D-Ala of normal peptidoglycan by forming five hydrogen bonds. However, when *vanB* causes PG to terminate in D-Ala-D-Lac instead of D-Alanyl-D-Ala, an oxygen takes the place of an amine group, which allows only four hydrogen bonds to form between PG and vancomycin while also adding a lone pair-lone pair repulsion between the carbonyl carbon of vancomycin and the substituted oxygen in D-Lac (Figure 10) (Ashford and Bew, 2012). Upon the substitution of D-Alanyl-D-Ala for D-Ala-D-Lac, the affinity of vancomycin for PG shows a decrease by three orders of magnitude (a 1000-fold decrease), resulting in the bacteria's ability to evade the antibacterial effects of vancomycin (Arias and Murray, 2012).

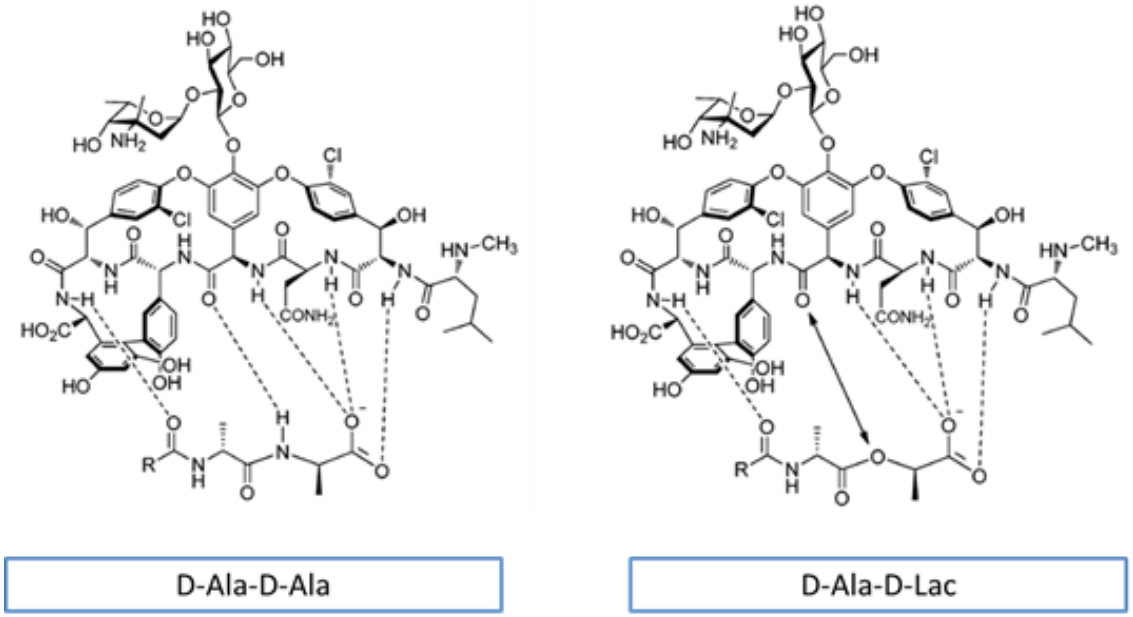

Figure 10: Vancomycin Resistance Due to the Reduced Binding Affinity of Vancomycin for D-Ala-D-Lac (Ashford and Bew, 2012). Vancomycin binds to terminal D-Ala-D-Ala in PG with five hydrogen bonds. Vancomycin is only able to form four hydrogen bonds with D-Ala-D-Lac and also experiences repulsion between the two lone-pairs of the oxygen atoms, resulting in a 1000-fold decrease in binding affinity.

Additional PG Modifications Associated with Bacterial Pathogenicity

In addition to modifications to the terminal peptide portion of the peptidoglycan that enables antibiotic-resistant bacteria to survive in the presence of antibiotics, many pathogenic bacteria also possess modifications to the glycan backbone of peptidoglycan that contribute to the pathogenicity of bacteria by enabling the bacteria to evade defense factors of host immune systems, such lysozyme. Common modifications to the glycan backbone include the following: N-deacetylation (of GlcNAc and MurNAc), N-glycolyation (at MurN), and O-acetylation (of MurNAc) (Figure 11) (Vollmer, 2008). N-deacetylation has been observed in *E. faecalis* in the presence of lysozyme, and the mechanism of N-deacetylation in *E. faecalis* is thought to occur via the N-acetylglucosamine deaccetylase PgdA (EF1843) (Benachour, Labjouzi, Jeune, Hébert,

Thorpe, Courtin, Chapot-Chartier, Prajsnar, Foster, and Mesnage, 2012). N-glycolyation has not yet been identified in *E. faecalis*. O-acetylation, however, not only has been identified in *E. faecalis* bacteria, but O-acetylation of peptidoglycan was first discovered in a strain of *E. faecalis*. Moreover, O-acetylation is thought to be relatively common in *E. faecalis*, with a prevalence ranging from 20 to 60% of the MurNAc being O-acetylated (depending on the strain). O-acetylation has thus far only been observed to occur on MurNAc and has never been seen on GlcNAc, and it is thought to occur only on polymerized peptidoglycan outside of the cell membrane by a membrane-associated O-acetyltransferase. The acetyltransferase gene in *S. aureus* is *oatA*, and *E. faecalis* possesses a homologous gene (EF_0783) (Vollmer, 2008).

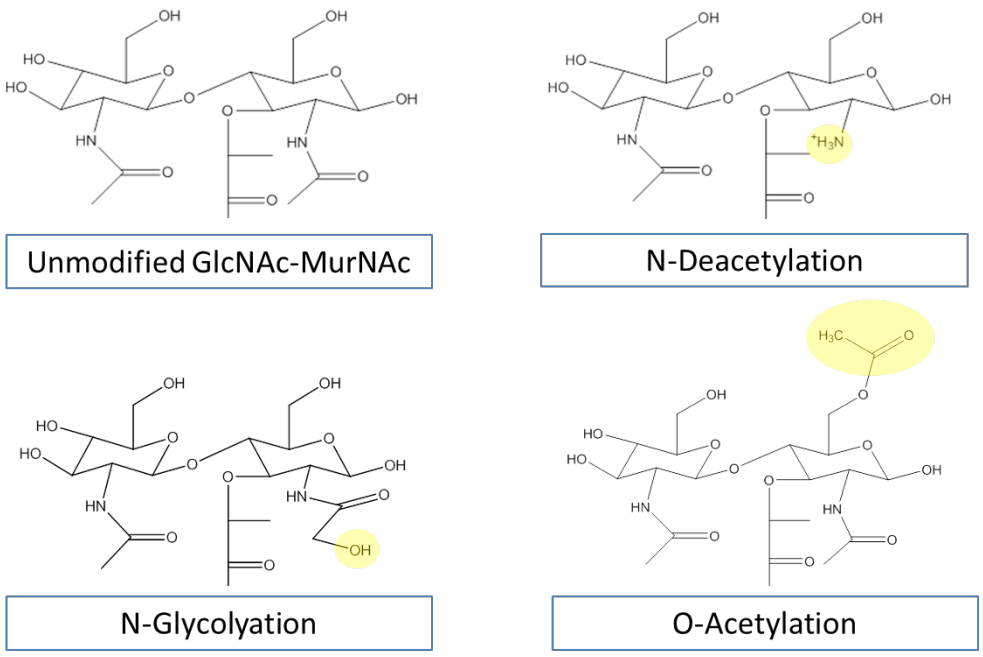

Figure 11: Additional PG Modifications Associated with Virulence. The figure shows the structure of the unmodified GlcNAc-MurNAc disaccharide portion of a PG monomer and shows the structure of the following modifications commonly found in pathogenic bacteria: N-deacetylation, N-glycolyation, and O-acetylation. All of these modifications to the glycan backbone are thought to be associated with bacterial pathogenicity due to their ability to help bacteria survive elements of the host immune system, such as lysozyme.

Experimental Goals and Hypotheses

This experiment seeks to explore the effects of the presence of vancomycin on peptidoglycan structure in a *vanB*-type strain of vancomycin-resistant *Entercoccus faecalis* (ATCC 51299) through a novel approach that involves pairing liquid chromatography-mass spectrometry (LC-MS) with a combinatorial *in silico* peptidoglycan mass library. Since every change to the peptidoglycan structure is associated with a predictable change in mass, peptidoglycan structure can be inferred by comparing the m/z values from MS data with pre-calculated values from a peptidoglycan mass library that includes peptidoglycans with all the possible combinations of known and hypothetical modifications. Additionally, any modification to the peptidoglycan that changes its size or chemical properties is likely to result in a discernable change in the elution profile of that particular species from the chromatography column.

Due to the known induction of the *vanB* gene by vancomycin, it was expected that the presence of vancomycin would cause changes in the PG structure associated with induction of *vanB*, including the presence of terminal D-Ala-D-Lac instead of D-Ala-D-Ala and increased editing of the terminal D-alanine residue of PG. Other modifications of the peptidoglycan unit, such as the degrees of cross-linking, sugar-linking, O-acetylation, N-deacetylation, and N-glycolyation, are not thought to be associated with *vanB* and thus were not expected to change based on the presence or absence of vancomycin during the growth of VRE.

CHAPTER TWO

Materials and Methods

Bacterial Growth

Peptidoglycans from a clinical strain of vancomycin-resistant *Enterococcus faecalis* (VRE), American Type Culture Collection (ATCC) strain 51299 (strain designation NJ-3), were isolated in the absence and in the presence of vancomycin (6 μg/mL) during growth. The peptidoglycan composition of VRE was compared to a vancomycin-susceptible strain of *Enterococcus faecalis* (VSE), ATCC 29212 (strain designation Portland), as the control.

Overnight cultures were each prepared in brain-heart infusion (BHI, BD Biosciences) media with 1% inoculum of frozen stock. Vancomycin resistance was induced in VRE (ATCC 51299) by the addition of vancomycin to a final concentration of 6 μg/mL during the growth. The cultures were grown for 24 hours at 37°C at 180 RPM.

The overnight cultures were used to inoculate 100 mL of tryptic soy broth (TSB) media for each condition, each with 1% inoculum. Vancomycin resistance was continuously induced in the VRE (ATCC 51299) being tested in the presence of vancomycin by the addition of vancomycin to a final concentration of 6 μg/mL at the start of the incubation period. The cultures were grown for 24 hours at 37°C and 180 RPM orbital shaking.

Pelleting and Sterilization of Bacteria

The bacteria were harvested at the stationary phase (OD_{600} > 0.8). The cells were pelleted by centrifugation (Beckman Coulter Allegra X-15R centrifuge with a SX4750 rotor) for 12 minutes at 4°C at 4750 RPM. The supernatants were discarded, leaving pellets of bacteria that were then resuspended in phosphate buffered saline (PBS). The PBS contained 8 mg/mL NaCl, 0.2 mg/mL KCl, 1.44 mg/mL Na_2HPO_4, and 0.24 mg/mL KH_2PO_4. The samples were sterilized by immersing in a boiling water bath for 30 minutes.

Disruption of Bacterial Cell Wall by Bead Beating

After the samples were cooled, they were divided equally into multiple microcentrifuge tubes with each containing approximately 400 μL (0.65g) of 0.5 mm glass beads. The glass beads were vigorously agitated to disrupt the cell wall in order to liberate and purify the PG for the analysis. The samples were agitated (Disruptor Genie, Scientific Industries) with the beads for 13 minutes in an alternating cycle of one minute of bead-beating and one minute of rest, giving a total of 7 cycles of 1-minute bead-beating and 6 cycles of 1-minute rest. The samples with the beads were combined together using additional PBS to facilitate complete transfer of the samples, and the beads were filtered out of the samples using the Steriflip 20 μm nylon net vacuum filtration system (EMD Millipore).

Isolation of Cell Wall from Lysed Bacteria

The disrupted cells were divided into microcentrifuge tubes and spun down with a microcentrifuge (VWR 1207 microcentrifuge). The supernatants were discarded, and the disrupted cells were combined and suspended in 1.5 mL of PBS. To remove the lipids in the sample and to denature the proteins before trypsin digestion, the sample was combined with an 8.5 mL solution of 2% sodium dodecyl sulfate (SDS) in autoclaved DI water, which was submerged in a boiling water bath for 30 minutes. The samples were divided into multiple microcentrifuge tubes and were washed with autoclaved DI water 5 times, once with 500 µL and four times with 1000 µL. The samples were spun down for 2 minutes in between each wash to separate the pelleted cell walls from the supernatant, and the supernatants were discarded. The washed sample was suspended in 20 mM Tris pH 8.0 buffer made with HPLC-grade water.

The nucleic acids in the crude isolated cell wall were digested by the addition of 200 µg DNase (Sigma-Aldrich) for 24 hours at 37°C and 180 RPM. The subsequent protein digestion was done for 24 hours at 37°C at 180 RPM following the addition of 300 µg trypsin (Sigma-Aldrich). The samples were completely frozen at -80°C and then lyophilized at -55°C (Labconco FreeZone 1).

Cell Wall Digestion with Mutanolysin

The lyophilized samples were each dissolved in 2 mL of 20 mM Tris pH 8.0 buffer made with HPLC-grade water. Cell walls were digested by hydrolysis of peptidoglycan β-(1,4) sugar-links with the addition of 100 units of mutanolysin (Sigma-Aldrich) to each sample at room temperature. Following 24 hours of digestion, an

additional 100 units of mutanolysin was added to each sample, and the samples were further digested at room temperature for an additional 24 hours.

Filtration

To remove any large undigested components, the samples were centrifuge filtered first through a 0.45 μm filter (Amicon) and next through a 30 kDa molecular weight cutoff filter (VWR) for 3-5 minutes as needed at 14800 RPM (Thermo Scientific Legend Micro 21 Centrifuge). The filtered samples were completely frozen at -80°C and then lyophilized at -55°C.

Reduction

To facilitate chromatographic separation, the sugars of the mutanolysin-digested muropeptides were reduced by adding sodium borohydride. The optimum sodium borohydride reduction is accomplished at a pH around 9.0, so each lyophilized sample were resuspended in 1 mL 0.5 M borate pH 9.0 buffer made with HPLC-grade water. The muropeptides were reduced by adding 10 mg of sodium borohydride (Fisher Scientific) in 20 μL of 0.5 M borate pH 9.0 buffer, giving a final concentration of approximately 10 mg/mL of sodium borohydride to borate buffer. The centrifuge tubes were inverted to ensure thorough mixing, and the samples were left to reduce at room temperature for 30 minutes. The reduction was quenched by the addition of 120 μL of 85% phosphoric acid (Acros). The reduced cell wall isolate digest was completely frozen at -80°C and then lyophilized at -55°C.

Sample Preparation for LC-MS

20 to 40 mg of each lyophilized sample was added to 500 µL of 20 mM Tris pH 8.0 buffer made with HPLC-grade water. To eliminate any large remaining particulates that could interfere with the optimal performance of the UPLC column, each reduced sample of cell wall isolate was again centrifuge filtered through a 0.45 µm filter. The filtered samples of reduced cell wall isolate were diluted 1:10, using methanol with 0.1% formic acid, and 200 µL of each diluted sample was added to an MS insert within an MS sample vial.

Liquid Chromatography-Mass Spectrometry

Liquid chromatography-mass spectrometry was used to analyze the structure and composition of cell wall peptidoglycans. The mutanolysin-digested peptidoglycan fragments were first separated by elution time based on their physical and chemical properties using ultra performance liquid chromatography (UPLC). Subsequent ionization of the peptidoglycans and separation by their mass-per-charge ratios (m/z) was achieved through mass spectrometry (MS). Fragmentation of the peptidoglycans and separation of the fragmented peptidoglycans by m/z for verification of the methods was done by tandem mass spectrometry (MS/MS). MS and MS/MS were run concurrently, alternating with intervals of 50 ms.

UPLC: The Waters C18 ACUITY Ultra Performance Liquid Chromatography system was used with an injection volume of 1 µL. The column had a length of 100 mm, a bead size of 1.7 µm, and a pore size of 130 Å. The chromatography elution gradient used 0.1 % formic acid in methanol as solvent A and acetonitrile as solvent B. The

elution gradient changed in a linear fashion, and the details of the elution profile are shown in Table 1. Total run time was 60.00 minutes.

Table 1: UPLC Elution Profile.

Time (Minutes)	Relative Amount of Solvent A: 0.1% Formic Acid in Methanol	Relative Amount of Solvent B: Acetonitrile
0.00	99.0 %	1.0 %
1.00	99.0 %	1.0 %
30.00	50.0 %	50.0 %
31.00	15.0 %	85.0 %
36.00	15.0 %	85.0 %
37.00	99.0 %	1.0 %

MS: Ionization of the sample was done through electrospray ionization (ESI) with a spray voltage of 35 V, a capillary voltage of 3.5 kV, and a flow rate of 0.450 µL/min. The Waters Synapt G2 High Definition Mass Spectrometer (HDMS) Time-of-Flight (TOF) mass analyzer was used. It was run in positive ion mode. The TOF mass analyzer was optimized prior to the runs for m/z values ranging from 100 to 2000. Under optimal conditions, the resolving power of the calibrated mass analyzer was over 40,000 FWHM with the exact mass determined within 1 ppm RMS error. Fibrinopeptide B (Glu-Fib) was used as the lock mass to serve as an internal reference for the TOF mass analyzer.

MS/MS: Fragmentation of the sample was accomplished through collision-induced dissociation (CID) with nitrogen gas at 120°C and 2.00 Bar. The transfer collision energy was 5 V, and the trap collision energy was 30 V.

Data Analysis

MassLynx Mass Spectrometry Software (Waters) was used to control the LC-MS instrument and was also used for data analysis.

CHAPTER THREE

Results

Combinatorial Generation of a PG Mass Library in silico

A bottom-up LC-MS approach was used to identify the chemical composition and structure of peptidoglycan (PG) fragments in mutanolysin-digested cell wall of *E. faecalis*. The observed m/z values were compared with pre-calculated theoretical values from an *in silico* PG library. Known and hypothetical modifications were considered in generating a combinatorial library of all possible PG fragments using a MATLAB script. Formulas were derived to provide the exact masses (and the corresponding mass-per-charge ratios) for each entry in the library of a possible modified PG fragment.

The following known and hypothetical modifications to the PG repeat unit (Figure 12, a) were considered for combinatorial *in silico* PG library generation: 1) cross-inking, 2) sugar-linking, 3) D-alanylation of stem, 4) removal of pentapeptide stems, 5) removal of NAG (possible editing or as an artifact), 6) O-acetylation of NAM, 7) N-deacetylation of NAG and/or NAM, 8) N-glycolyation NAM, 9) O-glycosylation of NAG and/or NAM, 10) incomplete reduction of NAM by sodium borohydride, 11) stem terminal D-Ala replaced by D-Lac (the mechanism of vancomycin resistance in vancomycin-resistant *E. faecalis*), and 12) the absence of L-Ala-L-Ala bridge structure (Figure 12, b-e).

a.

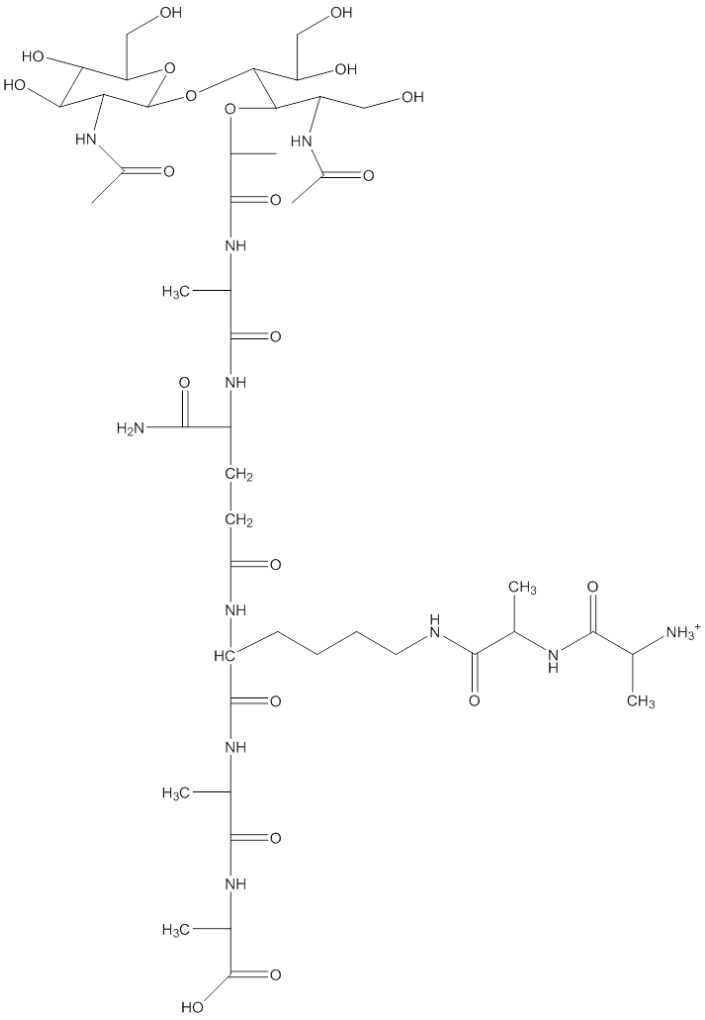

b. Sugar-Linked Peptidoglycan

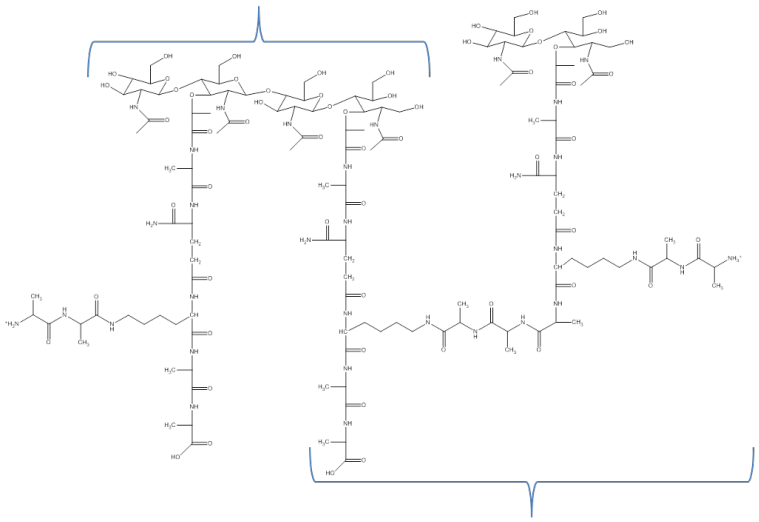

Cross-Linked Peptidoglycan

c.

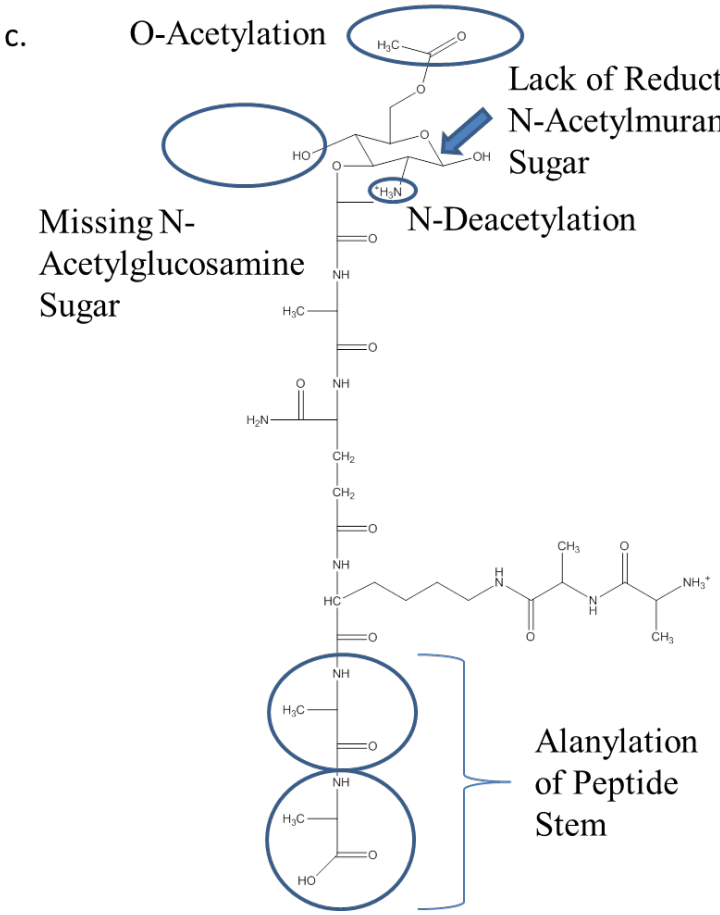
O-Acetylation
Lack of Reduction of the N-Acetylmuramic Acid Sugar
Missing N-Acetylglucosamine Sugar
N-Deacetylation
Alanylation of Peptide Stem

d.

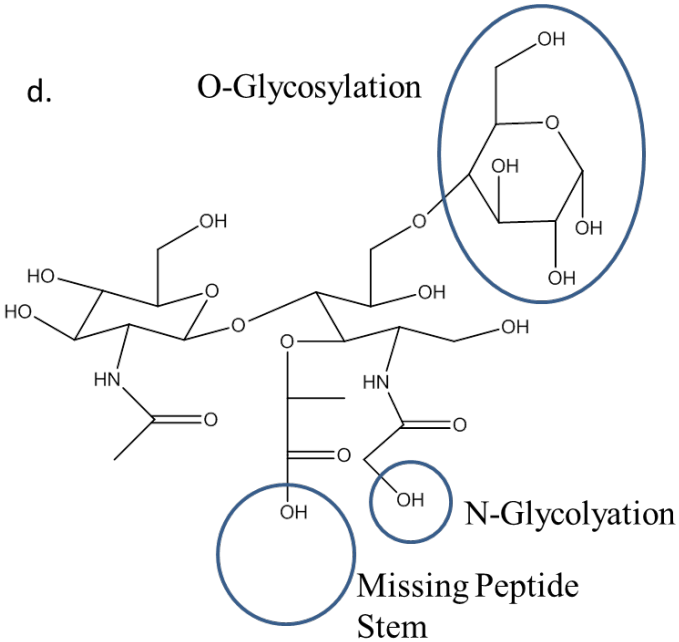
O-Glycosylation
N-Glycolyation
Missing Peptide Stem

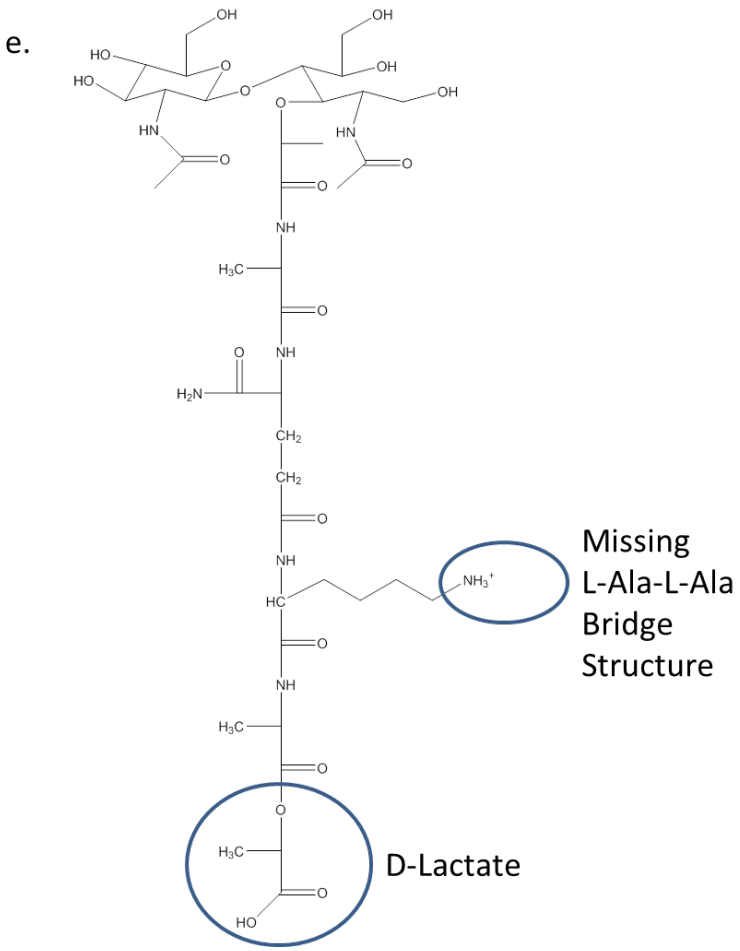

Figure 12: Modifications of the PG Unit. These chemical structures show the modifications considered in the combinatorial generation of the *in silico* PG library used for data analysis. Part (a) shows a monomer without any modifications, for comparison. Part (b) shows a PG trimer with a cross-link and a sugar-link. Part (c) shows an unreduced NAM with O-acetylation and N-deacetylation, and the monomer is also missing the NAG and has two D-alanines on the peptide stem. Part (d) shows O-glycosylation and N-glycolyation of the NAM and a missing peptide stem. Part (e) shows PG missing the L-Alanyl-L-Ala bridge structure and with a terminal D-lactate instead of D-alanine.

PG monomeric units are polymerized by transglycosylases (sugar-linked) and transpeptidases (cross-linked) to form supra-macromolecular structure. The digestion of *E. faecalis* cell wall isolate by mutanolysin hydrolyzes the β(1-4) glycosidic linkage between the N-acetylmuramic acid and the N-acetylglucosamine of the PG. Hence, mutanolysin only cleaves between the PG-repeat units, leaving the cross-links intact.

Although complete cell wall digestion by mutanolysin has been reported, the PG library includes both cross-linked and sugar-linked species because the visible insoluble precipitant following the cell wall digestion by mutanolysin suggests incomplete hydrolysis.

In practice, the presence of both cross-linked and sugar-linked PG species complicates analysis because of difficulty in differentiating between the isomers of cross-linked and sugar-linked species. For cross-linked PG, transpeptidases remove the terminal alanine positioned at the 5^{th} amino acid of the PG stem; whereas, the sugar-linking of PG does not share the D-alanine loss. Nonetheless, cross-linked and sugar-linked species can be isomers with the same number of alanines. For example, a cross-linked dimer has the same mass as a sugar-linked dimer with a tetrapeptide stem. De-alanylation is frequent in mature cell walls of *E. faecalis*, carried out by D,D-carboxypeptidases, which cleave the terminal D-Ala of uncrosslinked PG. The mass ambiguity between the cross-linked and sugar-linked species was resolved by reducing the sugars with sodium borohydride. The only reducible sugar in PG is the terminal NAM. Cross-linked and sugar-linked species have different numbers of reducible sugars (with the sugar-linked species having one fewer reduction per sugar-linkage), and therefore the cross-linked and sugar-linked species can be unambiguously differentiated by both retention time during chromatographic separation and by mass upon the reduction (Figure 13)

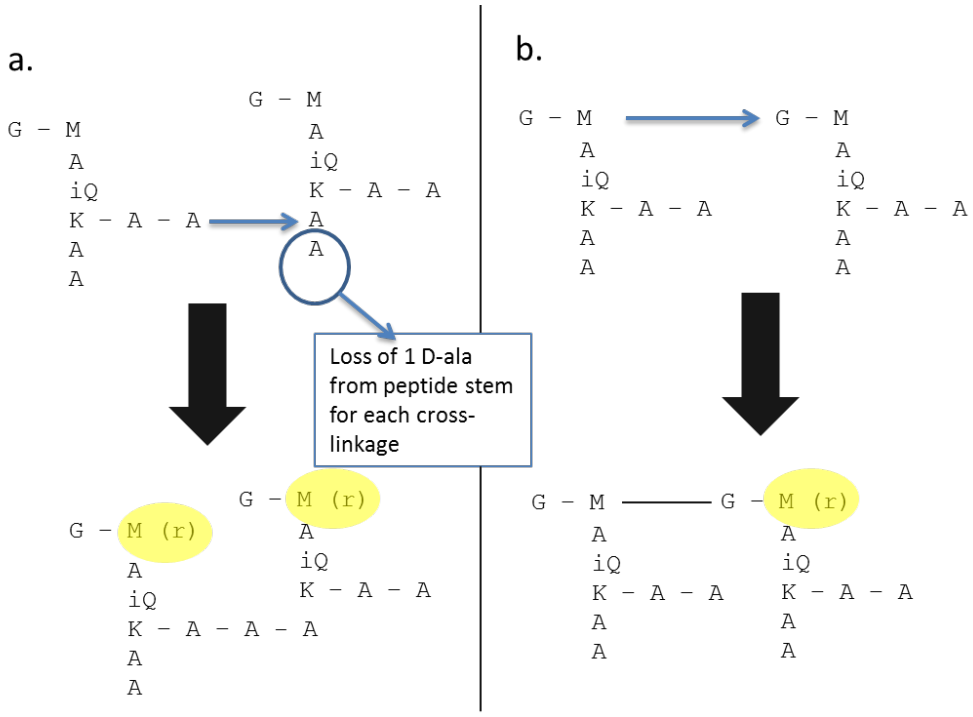

Figure 13: Mass Difference in PG Cross-Linking and Sugar-Linking. This figure shows the formation of PG dimers through cross-linking and sugar-linking of monomers. Part (a) of the schematic shows the loss of alanine involved in the cross-linking of PG units. Part (b) shows that the sugar-linking of PG units does not involve a loss of an alanine. The sugar-linked species has one fewer reduced N-acetylmuramic acid, which allows for differentiation of sugar-linked species from cross-linked species by mass upon reduction of the terminal NAM by sodium borohydride.

The combinatorial library for mutanolysin-digested *E. faecalis* PG fragments was generated using a MATLAB (The MathWorks, Inc.) script by assigning each PG modification a variable with an integer value corresponding to the number of occurrences. For example, the library entry for a cross-linked dimer with only 1 D-alanine on the pentapeptide stem, with 2 O-acetylations to the NAM, and with NAM unreduced would have the following variable assignments: cross-link (C) = 1, sugar-link (S) = 0, Stem_Missing = 0, Ala = 1, Sugar_Missing = 0, Lac-terminated stem (Lac) = 0, O-acetylation (O_Ac) = 2, N-deacetylation (N_DAc) = 0, N-glycolyation (N_Gly) = 0,

O-glycosylation (O_Gly) = 0, Unreduced NAM (Non_Reduction) = 1. The MATLAB script used for library generation is included in the Appendix.

To limit the library to only include structurally possible PG modifications, the upper limits for each variable were set into the script as shown in Table 2 as a function of modifications. For instance, a PG fragment missing the peptide stem (Stem_Missing) cannot have terminal D-alanine modifications by the absence of the stem structure. Similarly, N-deacetylation on the NAG is not permitted for a PG fragment missing NAG. Even with these parameters, the script generated a library containing over a million entries; each entry represented a possible mutanolysin-digested PG fragment.

Table 2: Parameters for Modifications of PG. These upper limits for each modification were incorporated into the MATLAB script to limit the PG library to include only possible PGs as entries.

PG Modifications	Variable Abbreviation	Maximum Number of Modifications
Cross-link	C	N/A
Sugar-link	S	N/A
Stem Missing	Stem_Missing	If C = 0 and S = 0, then max = 1 If C = 0 and S > 0, then max = S + 1 If C > 0, then max = 0
D-Alanine	Ala	(S*2 + 2) – (Stem_Missing*2)
Missing NAG	Sugar_Missing	1 + C
D-Lactate	Lac	(Ala/2) rounded down to nearest whole number value
O-Acetylation	O_Ac	C + S + 1
N-Deacetylation	N_DAc	(C*2 + S*2 + 2) – Sugar_Missing
N-Glycolyation	N_Gly	(C*2 + S*2 + 2) – N_DAc – sugar_missing
O-Glycosylation	O_Gly	(C*2 + S*2 + 2) – O_Ac – Sugar_Missing
Unreduced N-Acetylmuramic Acid Sugars	Non_Reduction	C + 1

After the variable assignments, the masses and mass-to-charge ratios for each entry in the library were generated. The mass of a PG monomer with a tripeptide stem (Figure 14a) calculated with ChemBioDraw 12.0 Ultra software was used as the starting mass (Start_Mass, Formula 1) from which subsequent modifications were added to generate the calculated exact masses. Examples of reduced PG monomer and cross-linked dimer with modifications are shown in Figures 14 b and c, respectively.

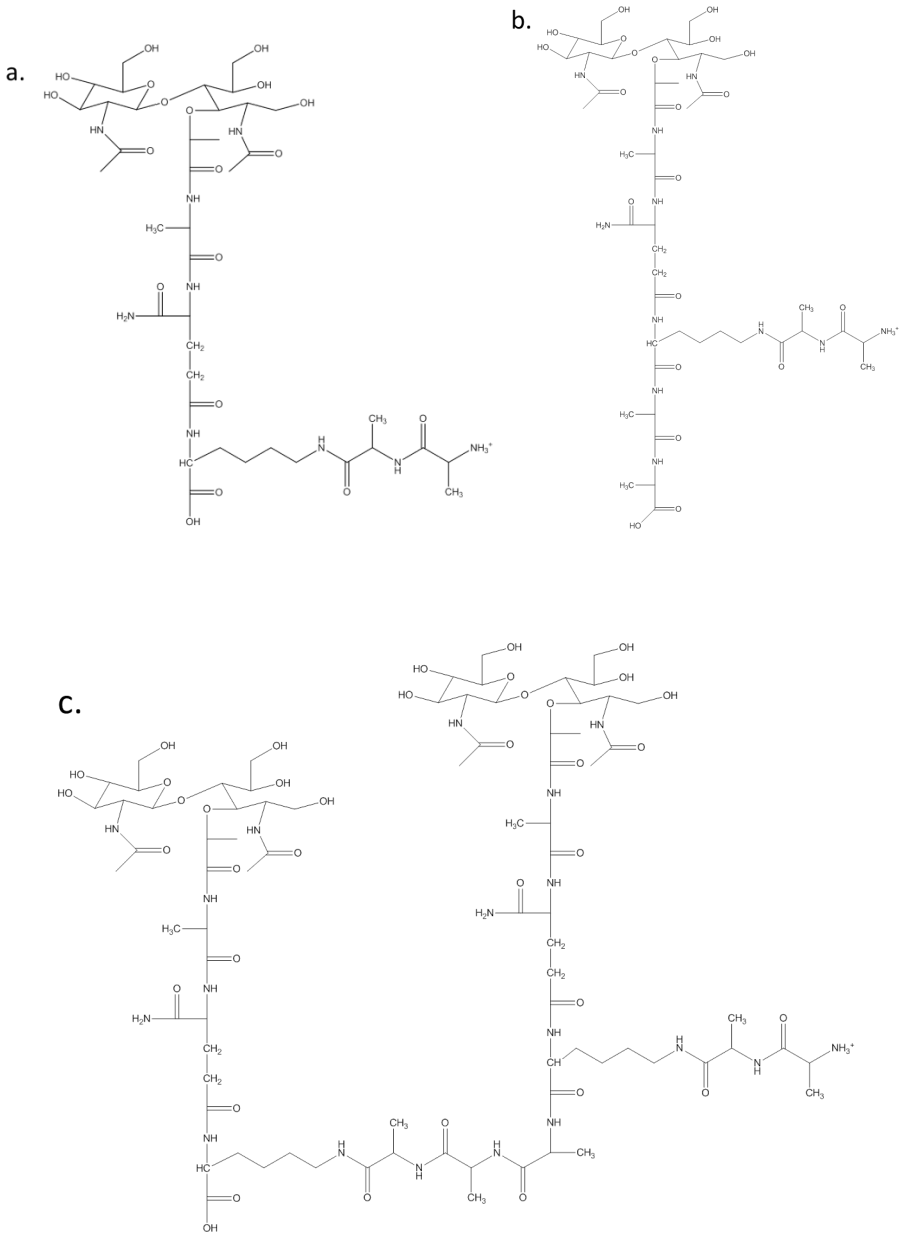

Figure 14: ChemBioDraw PG Fragments Used to Calculate Mass Differences Due to Modifications. Part a) shows the starter PG fragment, part b) shows the PG fragment modified with the addition of 2 alanines, and part c) shows the PG fragment modified with the addition of 1 cross-linkage

The masses corresponding to the chemical formulas in Table 3 assume i) complete reduction of reducible NAG in PG fragments by sodium borohydride, and ii) carboxylic acids and terminal amines of PG are protonated since UPLC separation was

performed at acidic conditions with pH 2.72 (0.1% formic acid by volume). The exact mass for the chemical formula (Table 3, right column) was calculated to ten decimal places using the Molecular Mass Calculator on the Biological Magnetic Resonance Data Bank (www.bmrb.wisc.edu) for mono-isotopic masses with uniform ^{12}C and ^{14}N.

Table 3: Chemical Formulas and Exact Masses for PG Variations.

Modified PG	Chemical Formula	Exact Mass
Monomer without Terminal D-Alanines	$C_{39}H_{70}N_9O_{19}^{+1}$	968.4782475338
Cross-Linked Dimer	$C_{81}H_{142}N_{19}O_{38}^{+1}$	1988.9757677169
Sugar-Linked Dimer	$C_{78}H_{136}N_{18}O_{37}^{+2}$	1916.9302803171
Monomer with 1 Terminal D-Alanine	$C_{42}H_{75}N_{10}O_{20}^{+1}$	1039.5153613216
Monomer with 2 Terminal D-Alanines	$C_{45}H_{80}N_{11}O_{21}^{+1}$	1110.5524751094
Monomer with Terminal Lactate	$C_{45}H_{79}N_{10}O_{22}^{+1}$	1111.5364906942
O-Acetylated Monomer	$C_{41}H_{72}N_9O_{20}^{+1}$	1010.4888122201
N-Deacetylated Monomer	$C_{37}H_{69}N_9O_{18}^{+2}$	927.4749592997
N-Glycolyated Monomer	$C_{39}H_{70}N_9O_{20}^{+1}$	984.4731621559
O-Glycosylated Monomer	$C_{45}H_{80}N_9O_{24}^{+1}$	1130.5310709653
Monomer without N-Acetylglucosamine Sugar	$C_{31}H_{57}N_8O_{14}^{+1}$	765.3988750008
Monomer without Peptide Stem	$C_{19}H_{34}N_2O_{13}$	498.2060891891
Unreduced Monomer	$C_{39}H_{68}N_9O_{19}^{+1}$	966.4625974696

The changes in the exact masses upon chemical modification to the PG starting mass (Start_Mass), designated as "Mass Difference Constant" are shown in Table 4 (right column). For example, the mass of a cross-linked dimer is derived from a sum of the Mass Difference Constants in the following manner: Start_Mass (968.4782475338 Da) + C_Mass (1020.4975201831 Da) = 1998.9757677169 Da. Similarly, the calculated mass for the singly O-acetylated cross-linked dimer would be a sum of the following Mass Difference Constants: Start_Mass (968.4782475338 Da) + C_Mass (1020.4975201831 Da) + O_Ac_Mass (42.0105646863 Da) = 2030.9863324034 Da. Using this method, the total exact mass (Exact_Mass) for all PG modifications (the variables defined in Figure 1) are calculated.

Table 4: Calculating and Defining Mass Difference Constants for PG Library Formula

Calculation of Mass Difference from Modified PG Masses	Defined Mass Variable	Mass Difference Constant (Da)
Monomer	Start_Mass	968.4782475338
(Cross-Linked Dimer) – (Monomer)	C_Mass	1020.4975201831
(Sugar-Linked Dimer) – (Monomer)	S_Link_Mass	948.4520327833
(Monomer with 1 Alanine) – (Monomer)	Ala_Mass	71.0371137878
(Monomer with Terminal Lactate instead of Alanine) – (Monomer with 2 Alanines)	Lac_Mass	0.9840155848
(O-Acetlyated Monomer) – (Monomer)	O_Ac_Mass	42.0105646863
(Monomer) – (N-Deacetylated Monomer)	N_DAc_Mass	41.0032882341
(N-Glycolyated Monomer) – (Monomer)	N_Gly_Mass	15.9949146221
(O-Glycosylated Monomer) – (Monomer)	O_Gly_Mass	162.0528234315
(Monomer) – (Monomer without N-Acetylglucosamine Sugar)	Sugar_Missing_Mass	203.079372533
(Monomer) – (Monomer without Peptide Stem)	Stem_Missing_Mass	470.2721583447
(Monomer) – (Unreduced Monomer)	Non_Reduction_Mass	2.0156500642

Formula 1: Exact Mass for PGs with Modifications. Part (a) includes the abbreviations for the constants given in Table 4, whereas part (b) includes the actual mass difference values in Daltons as the constants.

a. $Exact\_Mass = Start\_Mass + (C * C\_Mass) + (S * S\_Mass) + (Ala * Ala\_Mass) + (Lac * Lac\_Mass) + (O\_Ac * O\_Ac\_Mass) - (N\_DAc * N\_DAc\_Mass) + (N\_Gly * N\_Gly\_Mass) + (O\_Gly * O\_Gly\_Mass) - (Sugar\_Missing * Sugar\_Missing\_Mass) - (Stem\_Missing * Stem\_Missing\_Mass) - (Non\_Reduction * Non\_Reduction\_Mass)$

b. $Exact\_Mass = 968.4782475338\,Da + (C * 1020.4975201831\,Da) + (S * 948.4520327833\,Da) + (Ala * 71.0371137878\,Da) + (Lac * 0.9840155848\,Da) + (O\_Ac * 42.0105646863\,Da) - (N\_DAc * 41.0032882341\,Da) + (N\_Gly * 15.9949146221\,Da) + (O\_Gly * 162.0528234315\,Da) - (Sugar\_Missing * 203.079372533\,Da) - (Stem\_Missing * 470.2721583447\,Da) - (Non\_Reduction * 2.0156500642\,Da)$

The positive terms in Formula 1 designate the modifications to the PG unit resulting in increased mass, such as cross-linking, sugar-linking, alanylation, presence of lactate, O-acetylation, N-glycolyation, and O-glycosylation. In contrast, the negative terms arise from modifications that reduce mass, such as N-deacetylation, a missing NAG, a missing peptide stem, and lack of reduction of NAM.

If the changes in mass due to all of the modifications to the PG are summed together, Formulas 1 can be simplified to Formula 2.

Formula 2: Simplified Formula for Exact Mass of PGs. Part (a) includes the abbreviation for Start_Mass constant given in Table 4, whereas part (b) includes the actual Mass Difference Constant for Start_Mass in Daltons.

a. $Exact\_Mass = Start\_Mass + \sum Modifications$

b. $Exact\_Mass = 968.4782475338\ Da + \sum Modifications$

Formulas 1 and 2 calculate the exact mass of the PG for any entry in the PG library; however, mass spectra do not give exact masses but rather give mass-to-charge ratios. Therefore, in order to predict the values given by the mass spectra for any given entry in the library, a formula must be devised to calculate the mass-to-charge ratios for the various protonation states for a given exact mass.

The amines of PG (ε-nitrogen of L-Lys in PG without bridge attached, or N-terminus of L-Ala of the bridge, and also the amine nitrogen of NAG/NAM after N-deacetylation) under the acidic condition of the column are positively charged, giving PG inherent positive charge. Thus, the initial charge (initial_charge) of a given PG depends on the number of bridge structures that are not participating in a cross-linkage and on the degree of N-deacetylation, as shown in Formula 3. The electrospray ionization process also adds additional protons as part of the ionization process. PGs will thus more heavily charged as a result of electrospray ionization, and this is represented by a variable (column_protonation). The final charge (final_charge) can then be determined by summing the initial charge with the charge acquired by additional protonation using Formula 4. Once the final charge is calculated, the mass-to-charge ratio (m/z) can be determined using Formula 5.

Formula 3: Initial Charge of PG

$$Initial\_Charge = (S + N\_DAc + 1 - Stem\_Missing)$$

Formula 4: Final Charge of PG after Ionization

$$Final\_Charge = Initial\_Charge + Column\_Protonation$$

Formula 5: Mass-per-Charge Ratio for PG

a. $$\frac{m}{z} = \frac{Exact\_Mass + (Mass\_Proton * Column\_Protonation)}{Final\_Charge}$$

b. $$\frac{m}{z} = \frac{Exact\_Mass + (1.0072764522 * Column\_Protonation)}{Final\_Charge}$$

PG Species Identified by LC-MS

An overview of all the identified PG species is given in Table 5, and schematic representations of these PGs are given in Figures 15-21.

Many of the species were observed in more than one charged state, and the larger species tended to be more highly charged. The PG fragments each had an inherent positive charge from the acidic pH (2.72) that caused the terminal carboxylic acids and amines to be in their protonated states. The PGs then acquired further charge during the ionization process through the addition of protons, and larger fragments were more likely to be ionized multiple times. The varying charges for a single species were caused by the ionization process adding variable numbers of protons to identical fragments.

The accuracy of the matches was determined through calculating the ppm differences between the observed and theoretical masses. Most of the PG species were identified within about 10 ppm, and many of the matches were much better than 10 ppm. For the PGs that were observed in two different change states, the ppm difference for the species with the better match is recorded in the table.

The following types of modifications to the basic PG structure were observed: 1) D-Ala-D-Lac instead of D-Ala-D-Ala as the terminal residues on the PG pentapeptide stem, 2) varying degrees of alanylation of the PG pentapeptide stem, 3) varying degrees of cross-linking (monomers through heptamers), and 4) O-acetylation of the NAM.

Table 5: Identified PGs.

	Terminal D-Ala (or D-Lac)	Additional Modifications	Theoretical Mass (Da)	Charge States Observed	Best ppm Match	ID
Monomers	0		967.4700	2	3.1009	a
	1		1038.5070	2	2.3110	b
	2		1109.5442	2	5.9484	c
Dimers	0		1987.9668	2,3	6.7381	d
		1 O_Ac	2029.9775	2,3	2.3646	e
		2 O_Ac	2071.9880	3	1.0135	f
	1		2059.0045	2,3	3.8889	g
		1 O_Ac	2101.0152	2	1.7135	h
	2		2130.0411	2,3	6.5359	i
		1 Lac	2131.0256	2,3	0.3207	j
		1 O_Ac	2172.0522	2,3	2.6703	k
		1 O_Ac, 1 Lac	2173.0355	3	8.4214	l
		2 O_Ac	2214.0623	3	1.2195	m
Trimers	0		3008.4644	3	5.7768	n
		1 O_Ac	3050.4749	3	8.1627	o
	1		3079.5020	2,3	0.5547	p
		1 O_Ac	3121.5119	3	5.3820	q
	2		3150.5391	2,3	1.9695	r
		1 Lac	3151.5226	3	1.7670	s
Tetramers	0		4028.9618	3,4	7.4461	t
		1 O_Ac	4070.9723	3,4	2.8740	u
	1		4099.9985	3,4	1.4199	v
		1 O_Ac	4142.0096	3,4	7.3877	w
	2		4171.0361	3,4	2.6589	x
		1 O_Ac	4213.0461	4	3.6085	y
		1 O_Ac, 1 Lac	1054.5154	4	5.3156	z
Pentamers	0		5049.4589	4	1.6450	aa
		1 O_Ac	5091.4695	4	1.1784	bb
	1		5120.4963	4	1.5623	cc
		1 O_Ac	5162.5067	4	14.2566	dd
	2		5191.5331	4	7.7479	ee
		1 O_Ac	5233.5435	4	2.9043	ff
		1 O_AC, 1 Lac	5234.5275	4	8.1765	gg
Hexamers	0		6069.9563	4	0.0659	hh
	1		6140.9935	4	0.0651	ii
	2		6212.0306	4,5	10.4215	jj
Heptamer	2		7232.5279	5	13.0660	kk

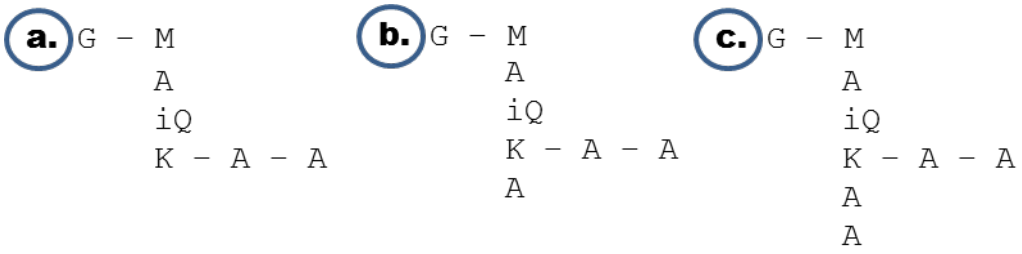

Figure 15: Identified PG Monomers.

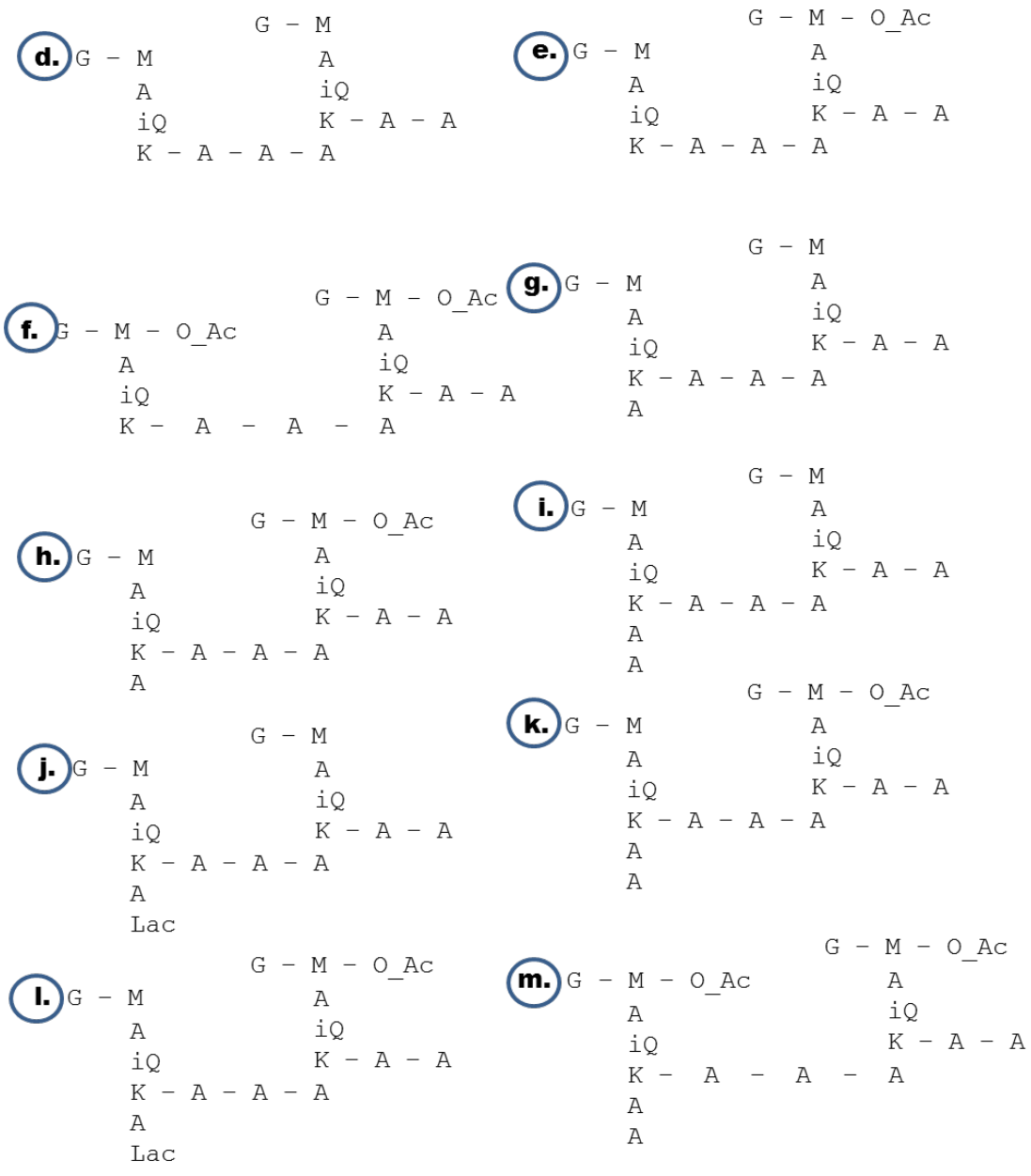

Figure 16: Identified PG Dimers.

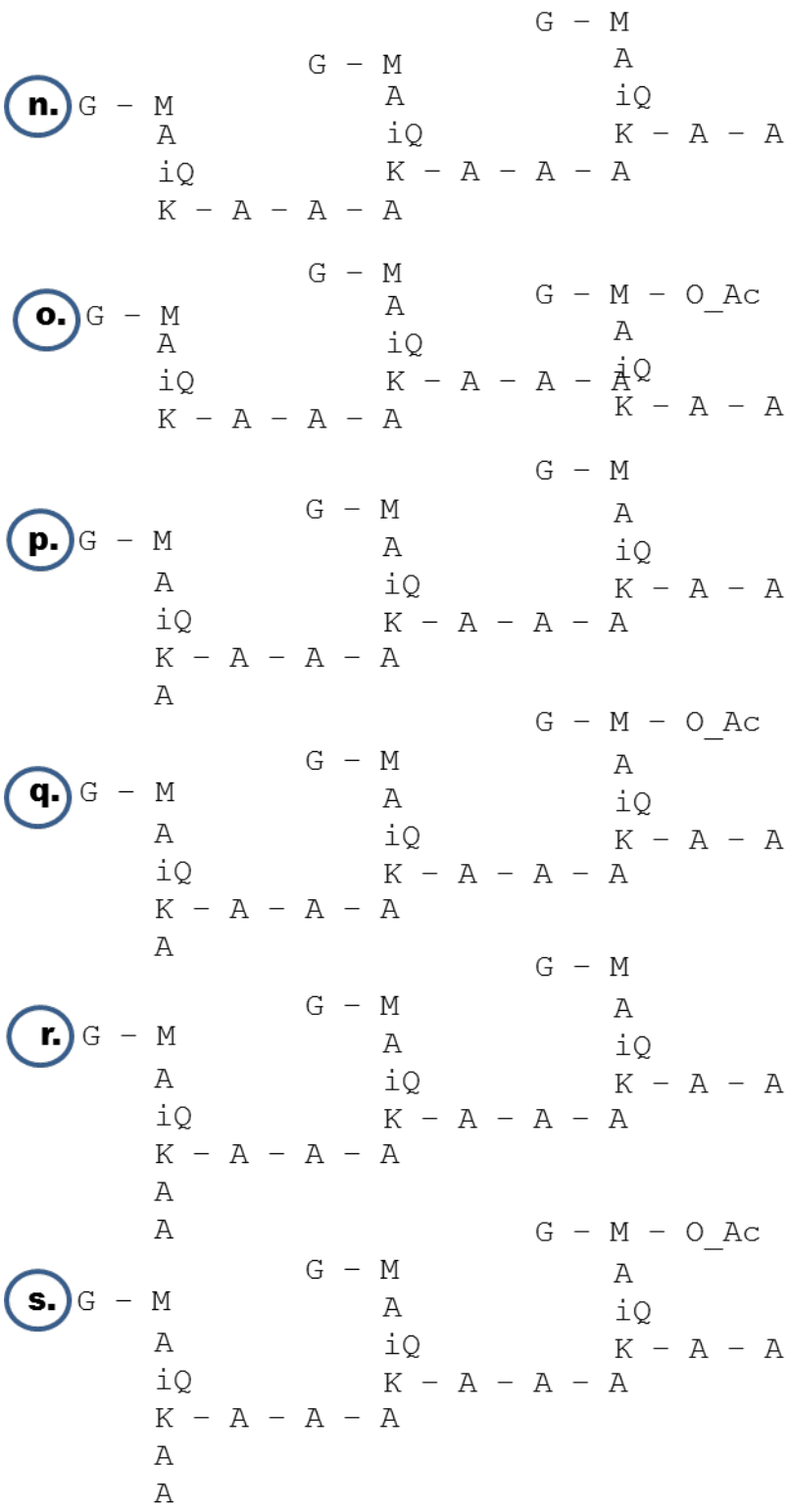

Figure 17: Identified PG Trimers.

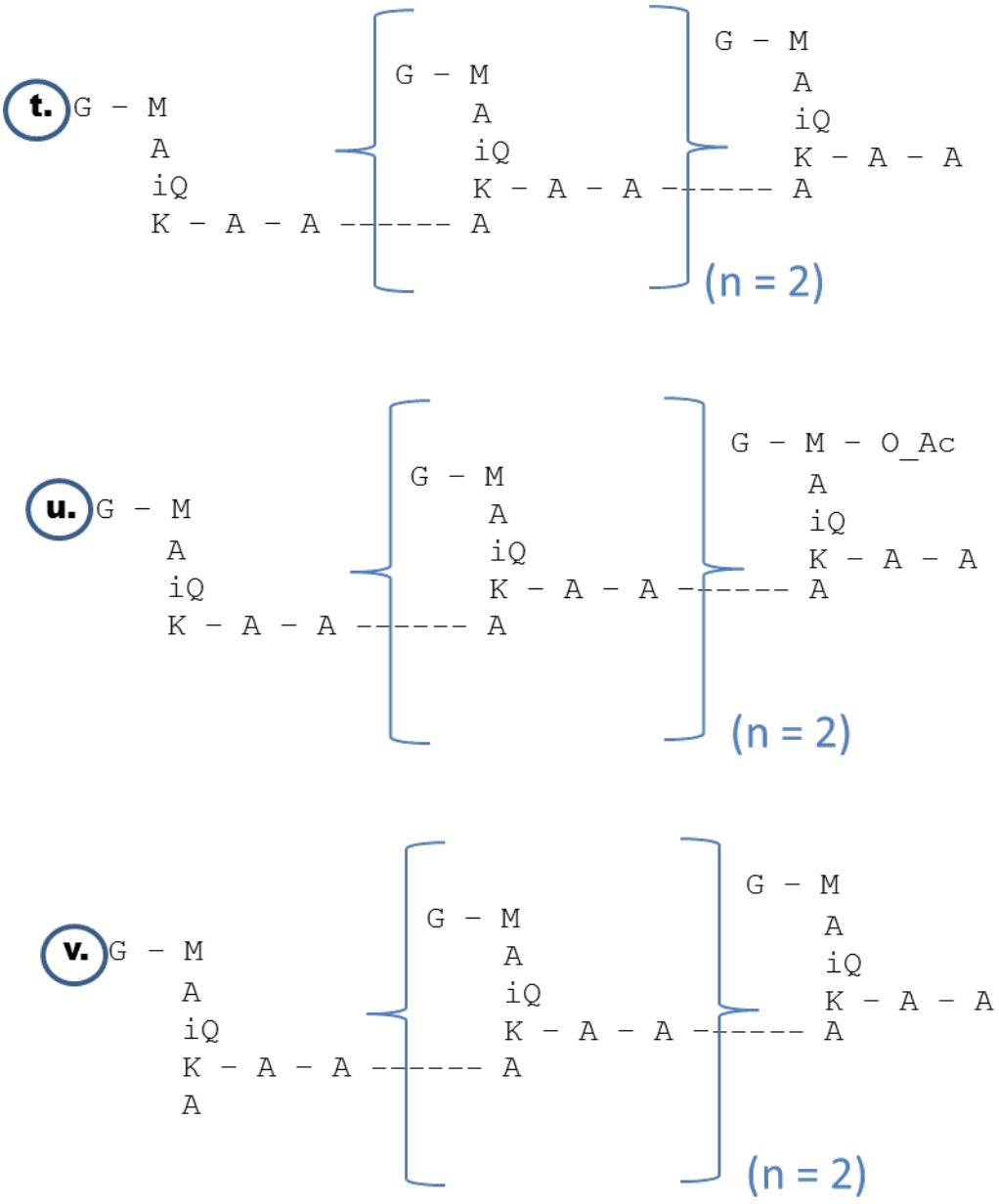

Figure 18a: Identified PG Tetramers (figure continued on the next page).

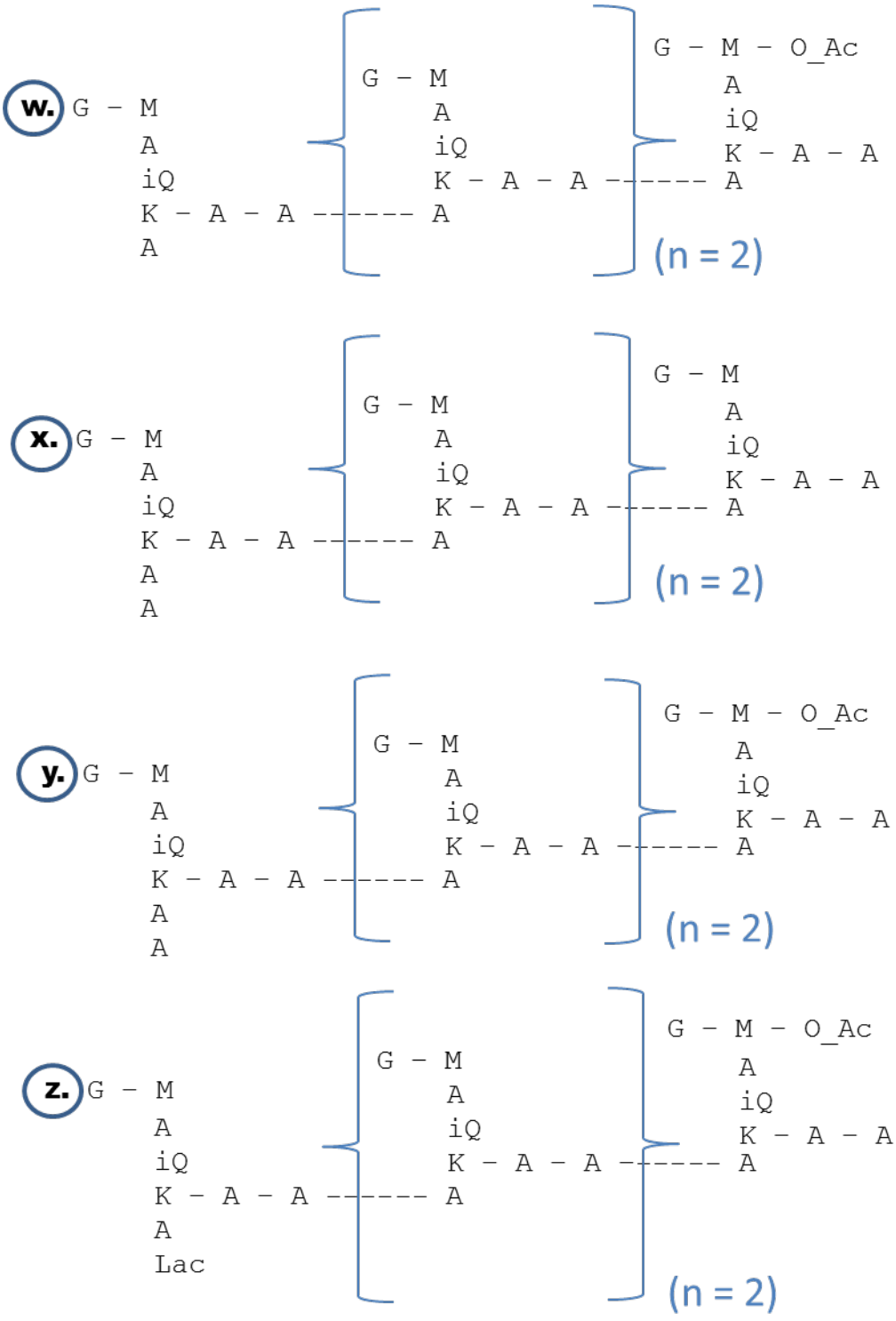

Figure 18b: Identified PG Tetramers (continuation of figure from previous page).

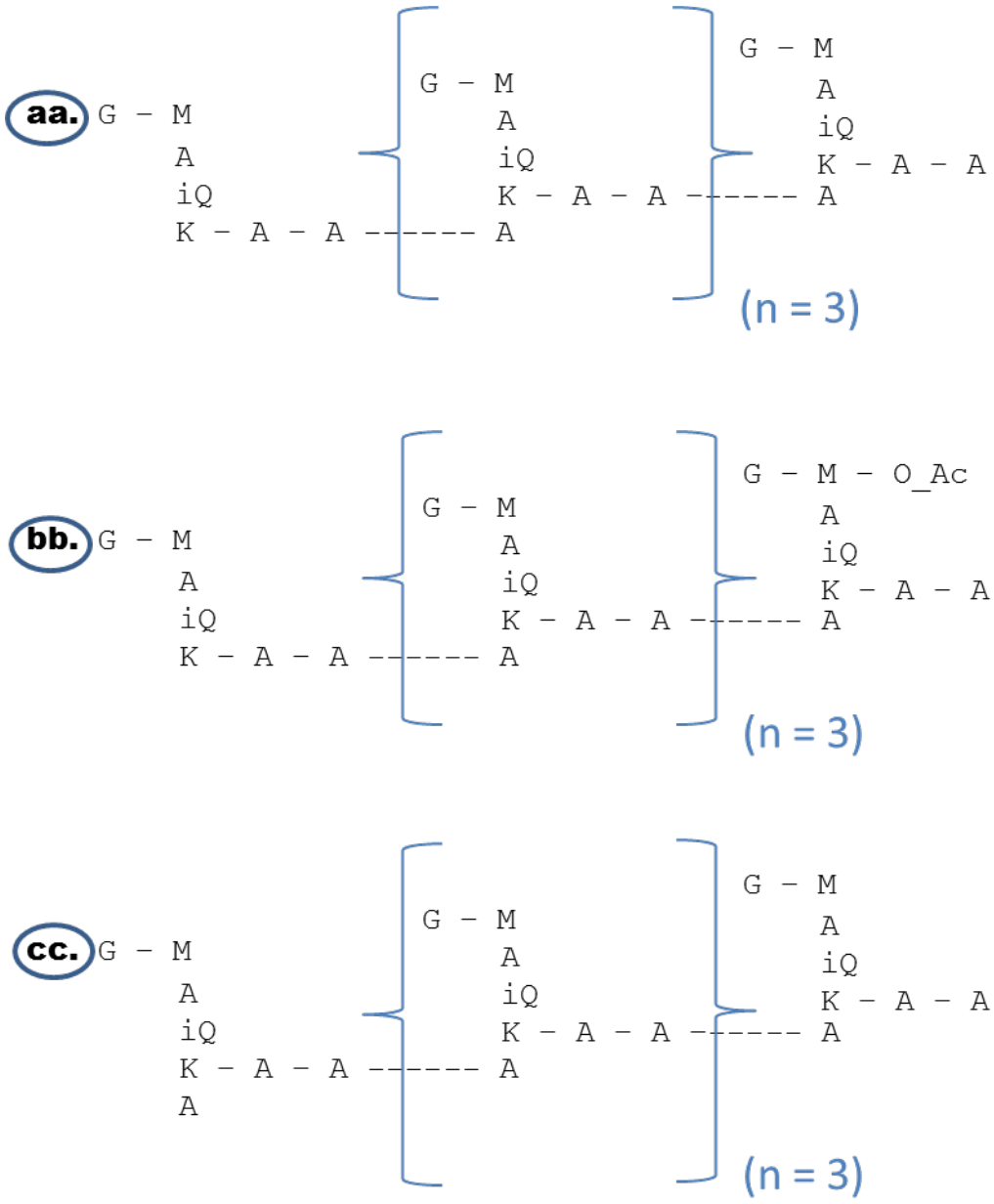

Figure 19a: Identified PG Pentamers (figure continued on next page).

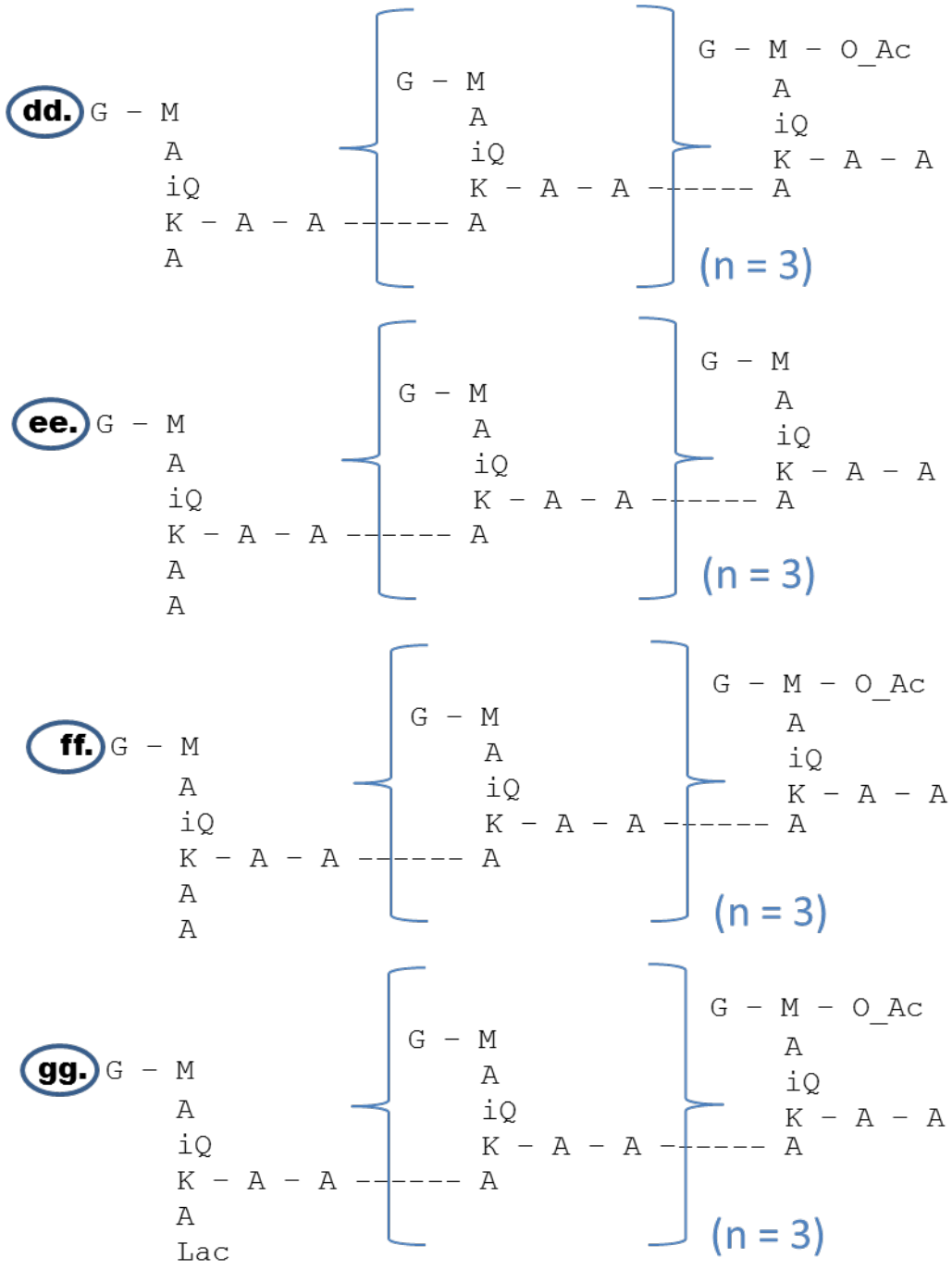

Figure 19b: Identified PG Pentamers (continuation of figure from previous page).

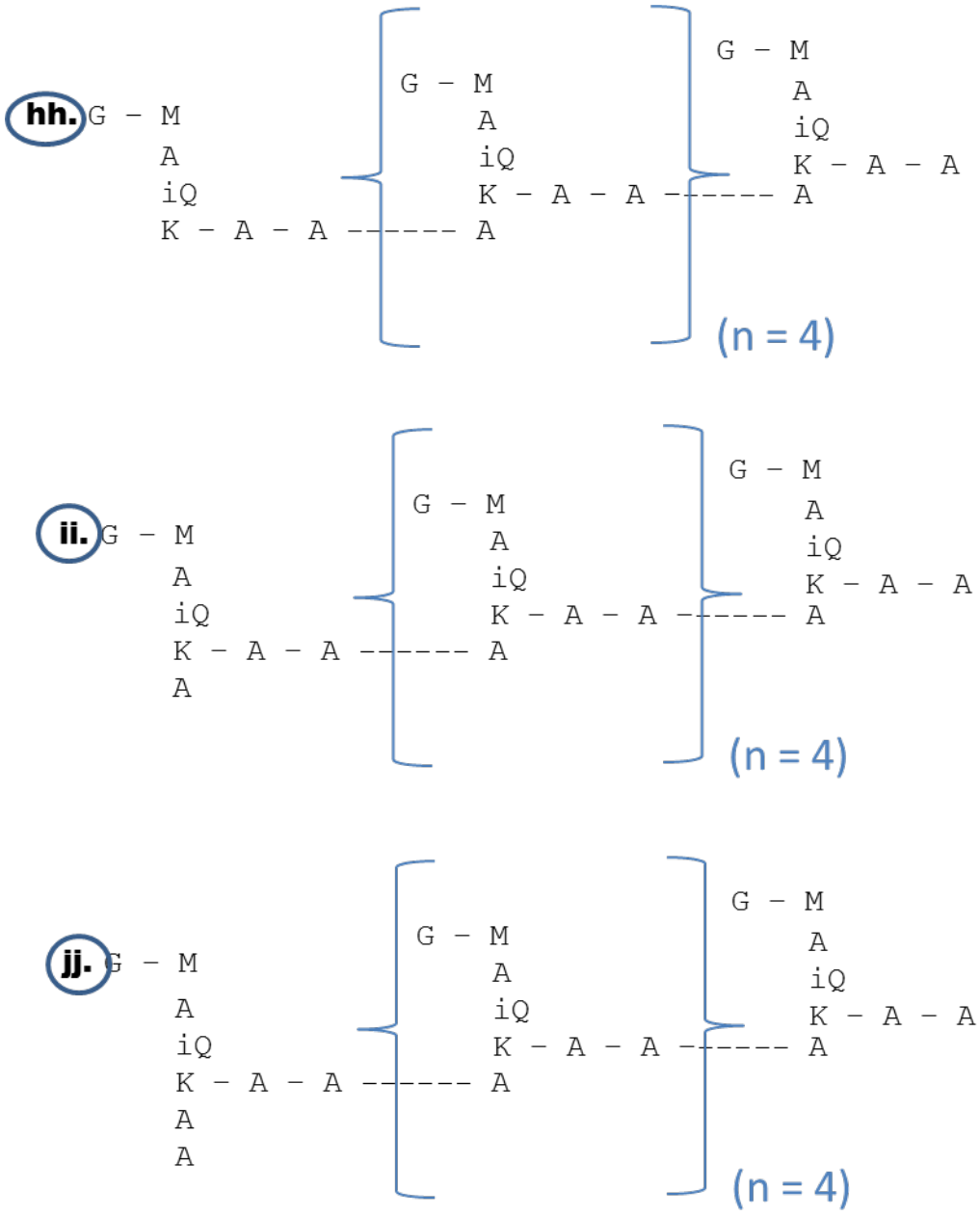

Figure 20: Identified PG Hexamers.

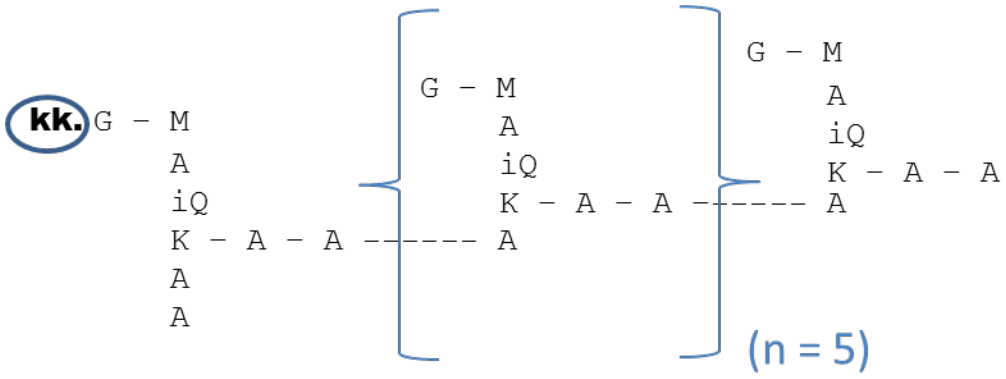

Figure 21: Identified PG Heptamer.

Validation of Methods by Tandem Mass Spectrometry

The PG fragments were subjected to tandem mass spectrometry (MS/MS) with collision-induced dissociation (CID) for further analysis. The relatively low-energy CID did not result in peptide stem fragmentation, but fragmentations between NAG and NAM of disaccharides and within the NAG moiety were observed, consistent with earlier observations (Morelle and Michalski, 2007). The MS/MS spectrum of a doubly-charged PG dimer of *E. faecalis* is shown in Figure 22 with a visible m/z at 204.0942, which corresponds to the NAG fragment (Y_0 or Y_1). Since every PG fragment (regardless of the chemical modification and size) contains at least one NAG, all identified species were validated by the presence of the NAG fragment in the MS/MS spectra. An SIC showing elution of the NAG fragment is given in Figure 23. Note that the NAG fragment elutes from about 5 minutes to 12 minutes, which corresponds to the elution of PG off of the UPLC column from the monomers at 5 minutes to the heptamers at 12 minutes. Furthermore, the large peaks on the SIC for the NAG fragment correspond to the times that the oligomers were also found to elute off of the column.

Additionally, literature suggests that acetylation of PG takes place on the NAM of the disaccharide backbone, rather than on the NAG (Vollmer, 2008). Since the NAG was found to fragment under MS/MS it was possible to distinguish the location of added acetyl groups to the disaccharide. Many NAG fragments were observed, but no acetylated NAG fragments were found. The lack of acetylated NAG fragments confirms that acetylation in VSE and VRE (both with and without vancomycin) takes place preferentially, if not exclusively, on the NAM.

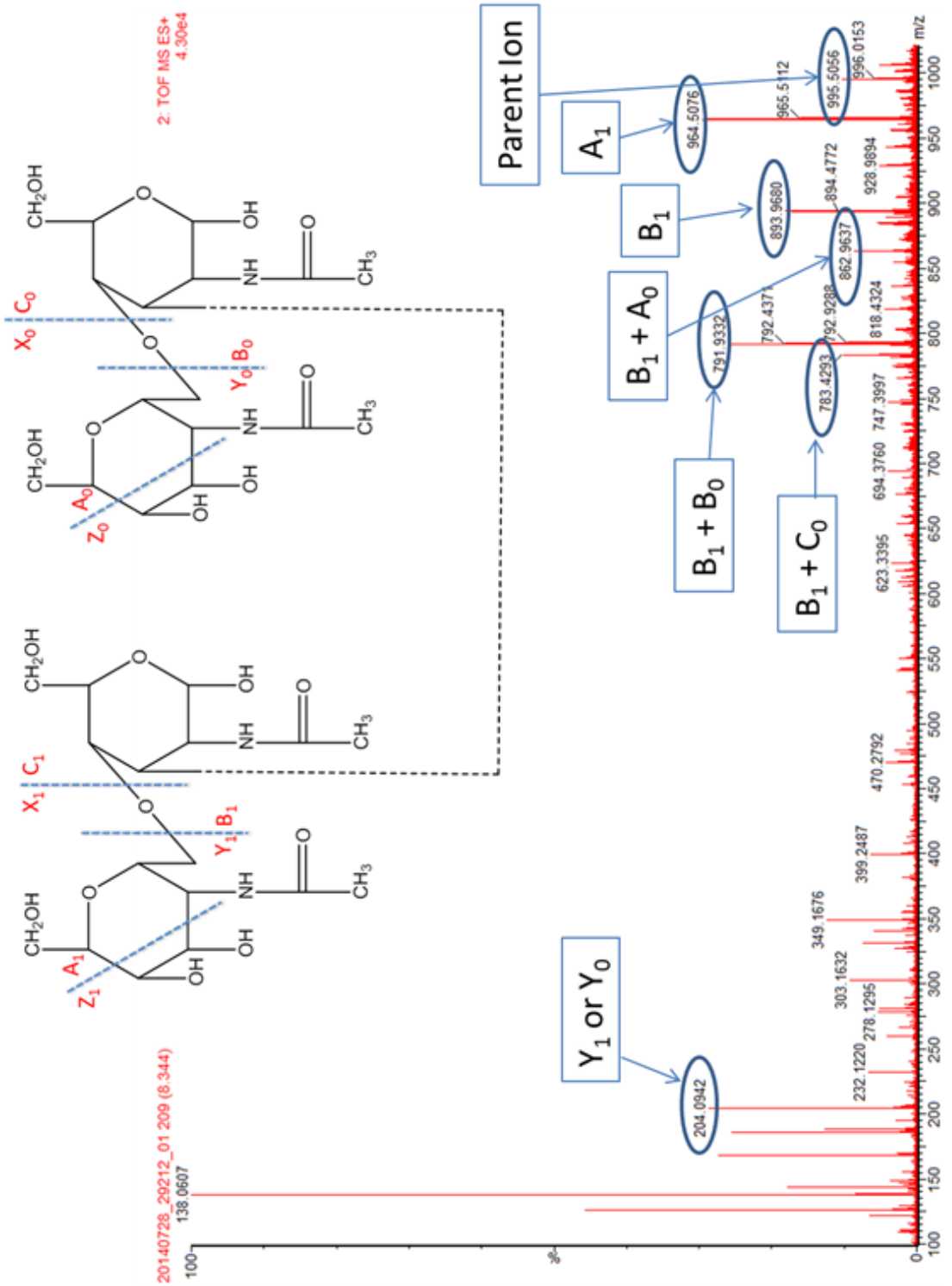

Figure 22: PG Fragmentation. This figure includes an MS/MS spectrum from VSE. It shows the parent ion of a doubly-charged dimer with no terminal D-alanines and numerous fragments of the dimer. Fragmentation occurred between the NAG and NAM of the disaccharide and within NAG moiety. Each fragment peak is labeled corresponding to the schematic of the PG dimer shown above the spectrum.

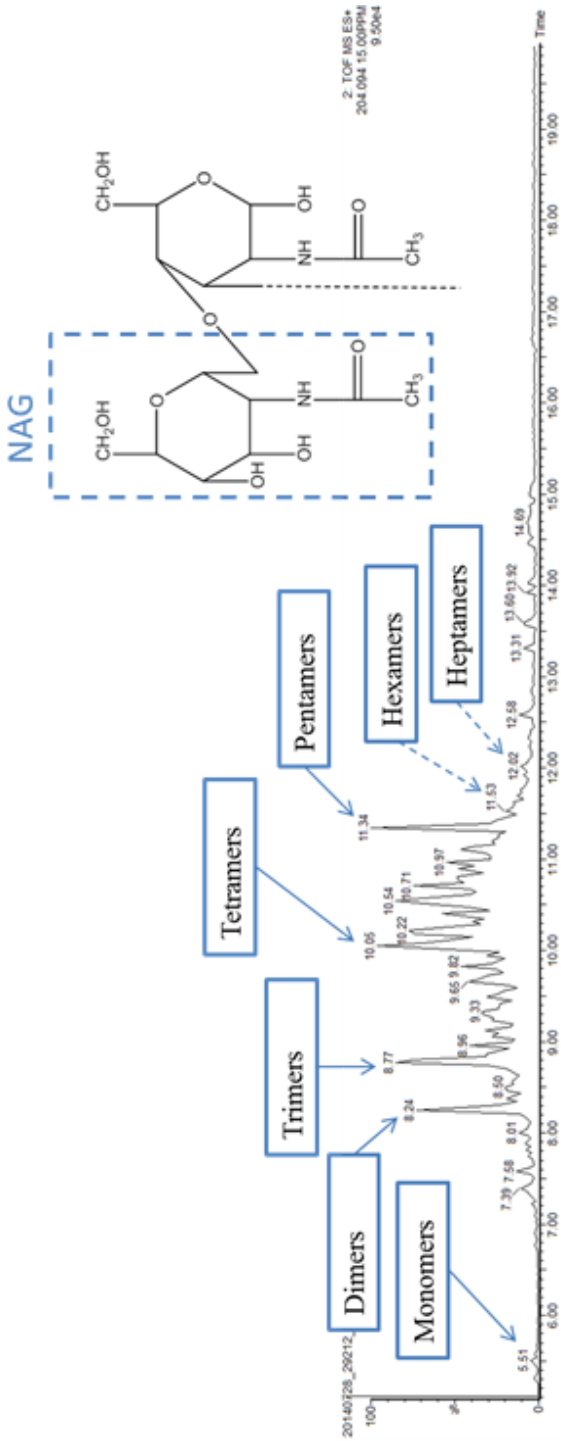

Figure 23: SIC for the N-Acetylglucosamine Fragment. The figure shows the elution profile for the NAG fragment, which tended to match the overall elution for PG, from about 5 to 12 minutes. Moreover, relatively intense peaks are visible on the NAG SIC when each PG oligomer eluted off of the column, as labeled in the figure. The largest oligomers identified (hexamers and heptamers) do not show as distinct peaks on the NAG SIC, indicated by the dotted arrows.

Quantifying Identified PG for Comparative Analysis

For comparative analysis of PG species within and across the experimental groups, it was necessary to quantify the amount of observed PG. Select ion chromatograms (SICs) are used to show the ionization current of a selected m/z from the total ionization current during the chromatographic elution. The integration of an SIC for a particular m/z, the area under the curve, provides an estimate for the amount of PG species analyte. For each PG m/z distribution identified on the mass spectrum, an SIC was generated for the tallest peak, which corresponded to the mass of the most abundant isoptomer. Some of the SICs included species without a sharp, distinct elution time profile, so the integrated values from multiple peaks deemed to be from that particular species were summed to give the total integrated value for that given m/z species.

Since each PG species is represented on the mass spectrum by a distribution of peaks corresponding to the isotopic distribution of the species, it was necessary to adjust the integrated value from that SIC according to the isotopic distributions for the corresponding PG in order to ascertain the overall abundance of each species. Using the chemical formula for the identified PG, a table of relative abundances of each isotopic variation was generated using MATLAB's "isotopicdist" function. The most abundant mass calculated by MATLAB corresponded to the tallest m/z peak of the isotopic distribution. The peak-to-intensity ratio of the most abundant mass to the monoisotopic mass was therefore used as the correction factor. Each integrated SIC value was divided by the correction factor to calculate the SIC value that would result from a monoisotopic species, which is a raw measure of the abundance of that PG species observed. This process of determining the amount of PG observed was done for every identified PG

species at every charge observed, and the process is summarized in Figure 24 and Formula 6.

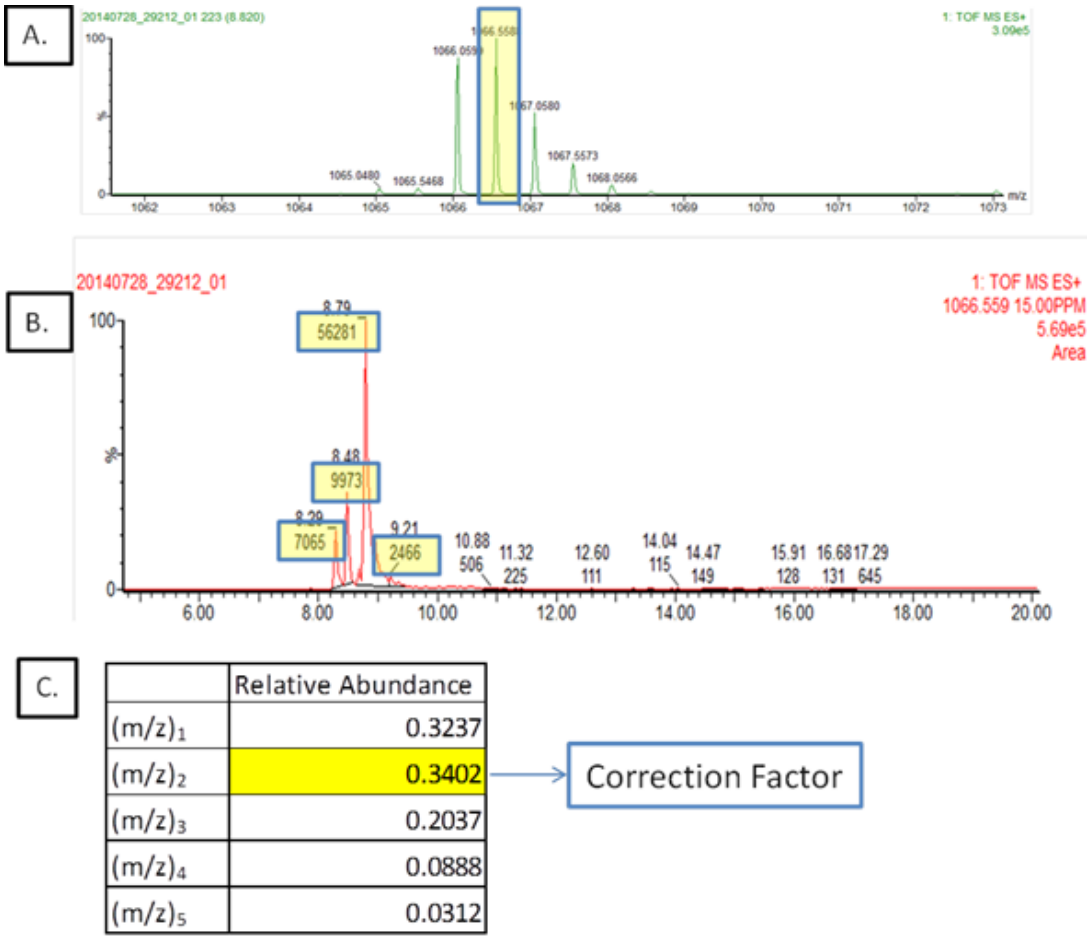

Figure 24: Quantification of PG. In order to describe the amount of PG observed, the tallest peak (highlighted) from the distribution on the mass spectrum (A) was used to generate a select ion chromatogram (SIC) (B). The select ion chromatogram gave integrated values representing the area under the curve for each peak (highlighted), and these values were summed to give a total integrated value from the SIC. Using the isotopic distribution for the species, the relative abundance corresponding to the tallest m/z peak (highlighted) was selected for use as the correction factor (C).

Formula 6: Corrected SIC Value. By dividing the integrated value from the SIC by the correction factor, the corrected SIC value accounts for the total amount of each PG fragment observed of all the isotopes for a particular PG species with a particular charge. The corrected SIC value is useful for comparing relative amounts of PG within an experimental group.

$$Corrected\ SIC\ Value = \frac{Integrated\ SIC\ Value}{Correction\ Factor}$$

This method of determining the actual amount of each PG species observed allowed for accurate comparison of the relative amounts of each PG species observed within an experimental group; however, due to variations in the total amounts of PG observed for each experimental group, the corrected SIC values alone do not allow for comparing the amounts of PG across experimental groups. The data was therefore further normalized for comparison by determining the percentage composition represented by each PG species. Percentage composition was calculated by dividing the raw amount of each type of PG observed by the total amount of PG observed in a given experimental group, as shown in Formula 7.

Formula 7: Percentage Composition. Calculating the percentage composition takes into account the total amount of PG observed for a given experimental group, allowing for comparison of PG across experimental groups.

$$Percentage\ Composition = \frac{Corrected\ SIC\ Value}{\Sigma Corrected\ SIC\ Values}$$

Presence of Terminal D-Alanine-D-Lactate in the PG Stem

PGs with terminal D-Ala-D-Lac were only identified in the cell wall of VRE grown in the presence of vancomycin. In contrast, D-Ala-D-Lac terminated PGs were

not found in the cell wall isolates from VSE and from VRE when grown in the absence of vancomycin. The chemical structures of PG terminating in D-Ala-D-Ala and D-Ala-D-Lac are shown in Figure 25. The only difference is that the D-Ala-D-Lac is a depsipeptide, replacing the NH of the peptide bone by an ester link (highlighted in yellow in Figure 25), which increases the mass by a mere 1 Da. This small difference complicates the differentiation between PG species that terminate in D-alanine from those that terminate in D-lactate as the ^{13}C-isotopic distributions are also separated by 1 Da. Nevertheless, the isotopic distribution of a PG dimer from the cell wall of VRE grown in the presence of vancomycin clearly shows the mass shift by 1 Da in Figure 26. No shift is observed for the PG dimer in isolated cell walls from VSE and from VRE grown in the absence of vancomycin.

The shape of the isotopic distribution was used to determine the amount of PG stems terminating in D-Ala-D-Lac. Figure 27 shows the simulation for the isotopic distribution as the relative amounts of PG stems terminating in D-Ala-D-Lac increases from 0, 20, 40, 80, to 100%. The isotopic distribution line shape of observed PG dimer from the cell wall of VRE grown in the presence of vancomycin, shown in Figure 26, is consistent with 100% of PG pentapeptide stems terminated in D-Ala-D-Lac; however, this was not the case for all of the distributions of D-Ala-D-Lac in VRE with vancomycin.

The modification of PG stems terminating in D-Ala-D-Ala to D-Ala-D-Lac, in addition to shift in mass, also increases the retention time. Figure 28 shows this shift in the SIC profile of a PG dimer in VRE when grown in the presence of vancomycin.

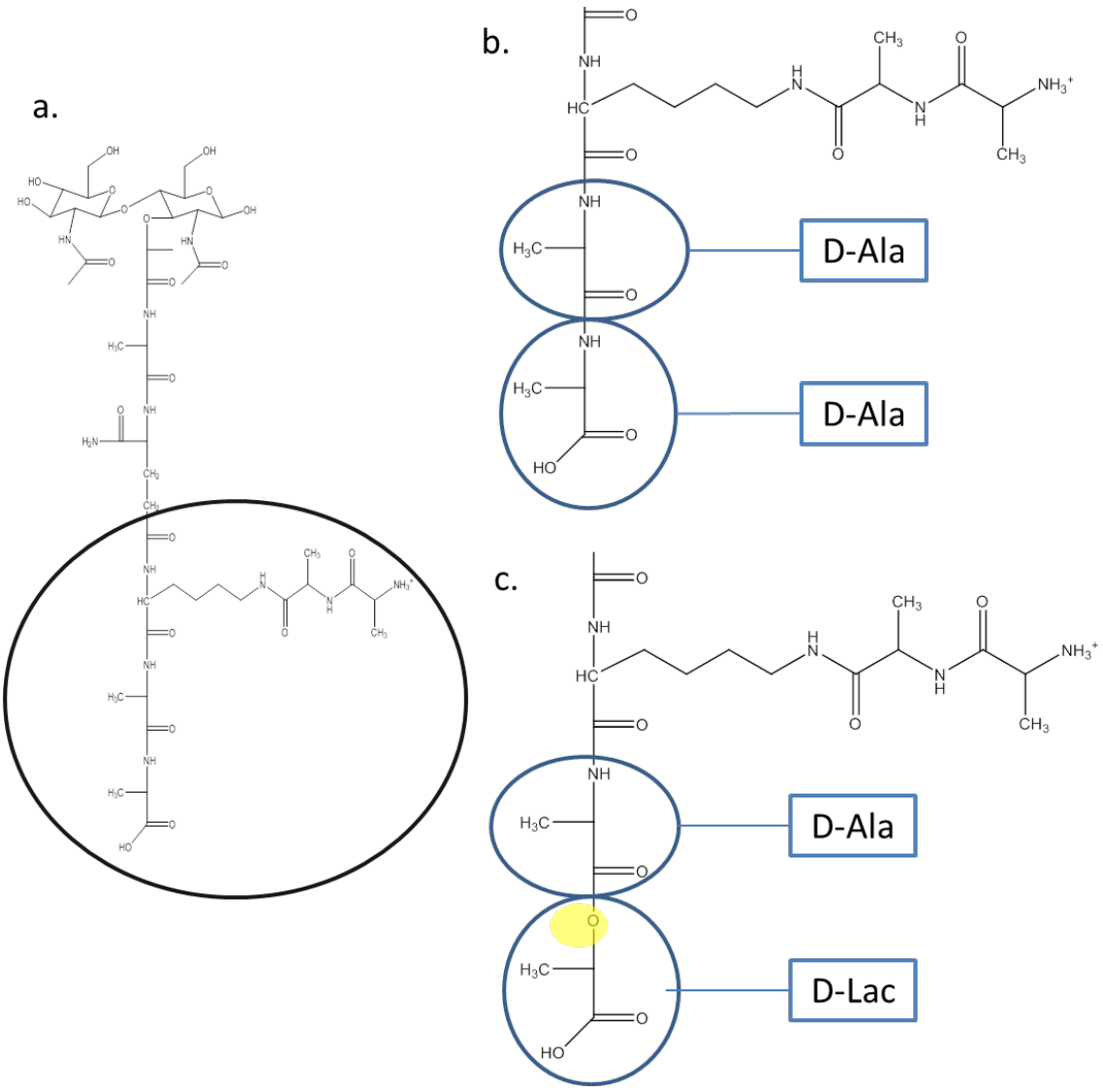

Figure 25: D-Lactate in PG Pentapeptide Stem. Part a) shows the terminal portion of the pentapeptide stem of PG that will be enlarged in parts b and c. Part b) shows PG with unedited D-Ala-D-Ala residues. Part c) shows a PG that has D-Lactate instead of the terminal D-alanine. The only difference between the two is that an oxygen in Lactate (highlighted) replaces the nitrogen and hydrogen in Alanine, making the total mass difference approximately 1 Da.

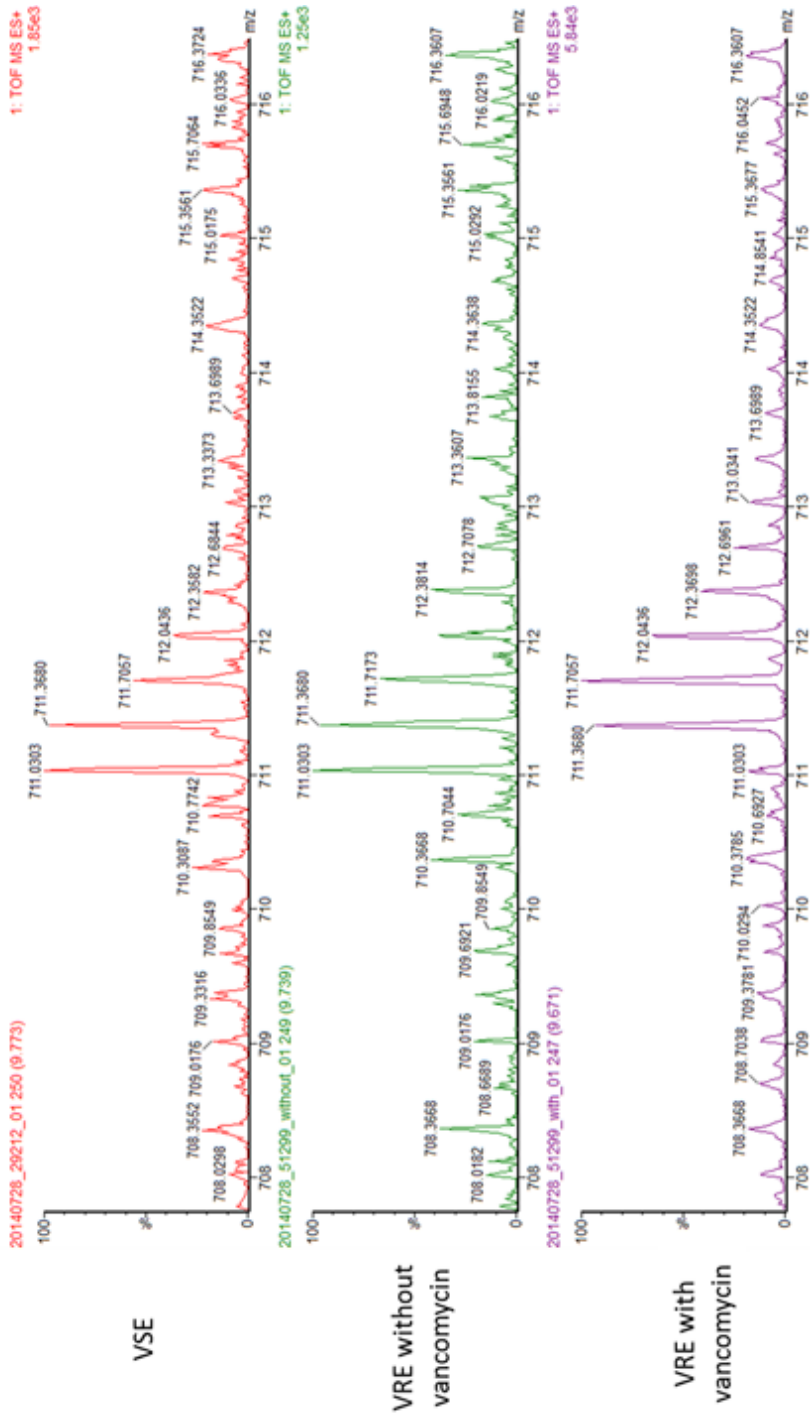

Figure 26: D-Lactate on Mass Spectrum. The mass spectra show distributions representative of triply-charged dimers. The first m/z peak in the distribution for VRE with vancomycin is shifted by 0.33 in comparison to the first peaks for VSE and VRE without vancomycin. Since the species is triply charged, the 0.33 difference in m/z corresponds to a mass difference of 1 Da, indicating the presence of a terminal D-lactate in the VRE with vancomycin PG.

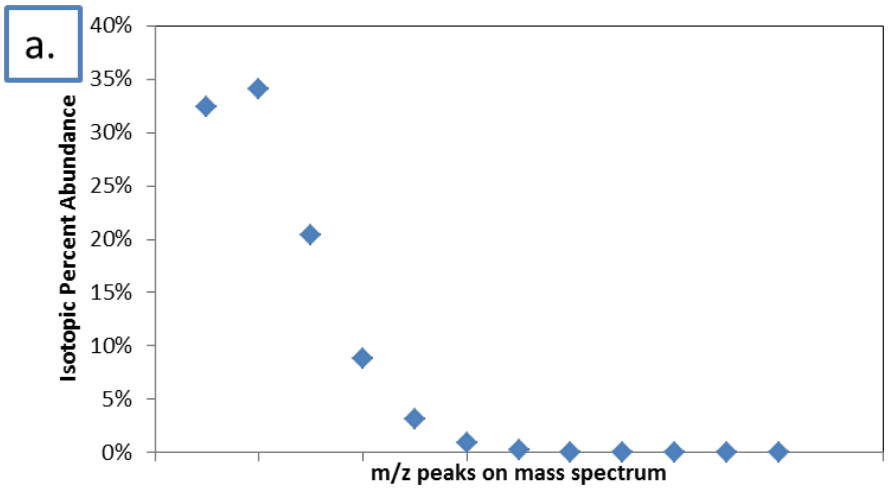
a.
Isotopic Percent Abundance
40%
35%
30%
25%
20%
15%
10%
5%
0%
m/z peaks on mass spectrum

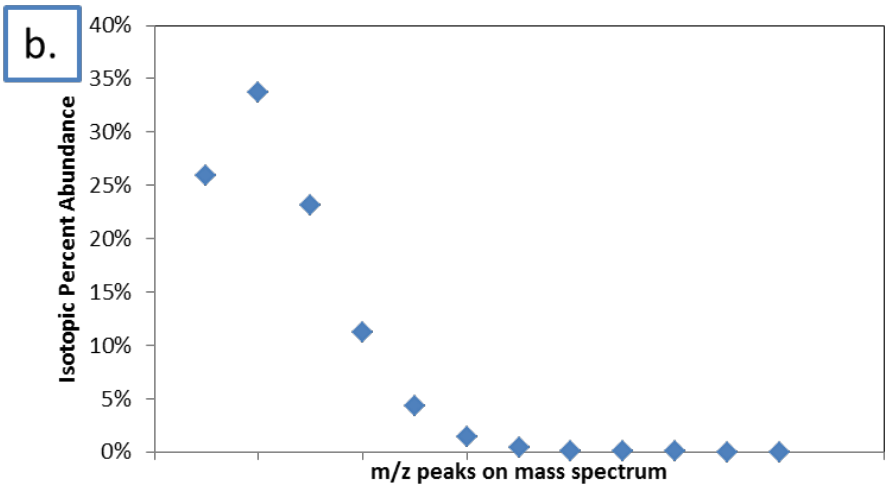
b.
Isotopic Percent Abundance
40%
35%
30%
25%
20%
15%
10%
5%
0%
m/z peaks on mass spectrum

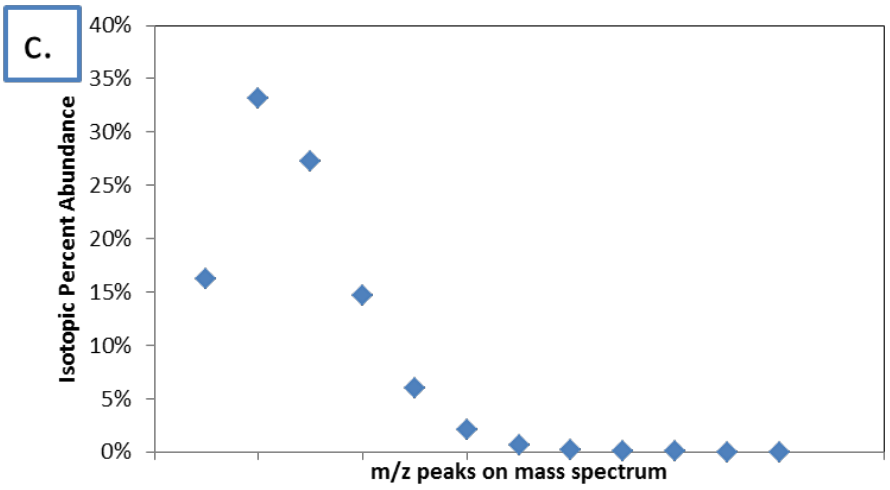
c.
Isotopic Percent Abundance
40%
35%
30%
25%
20%
15%
10%
5%
0%
m/z peaks on mass spectrum

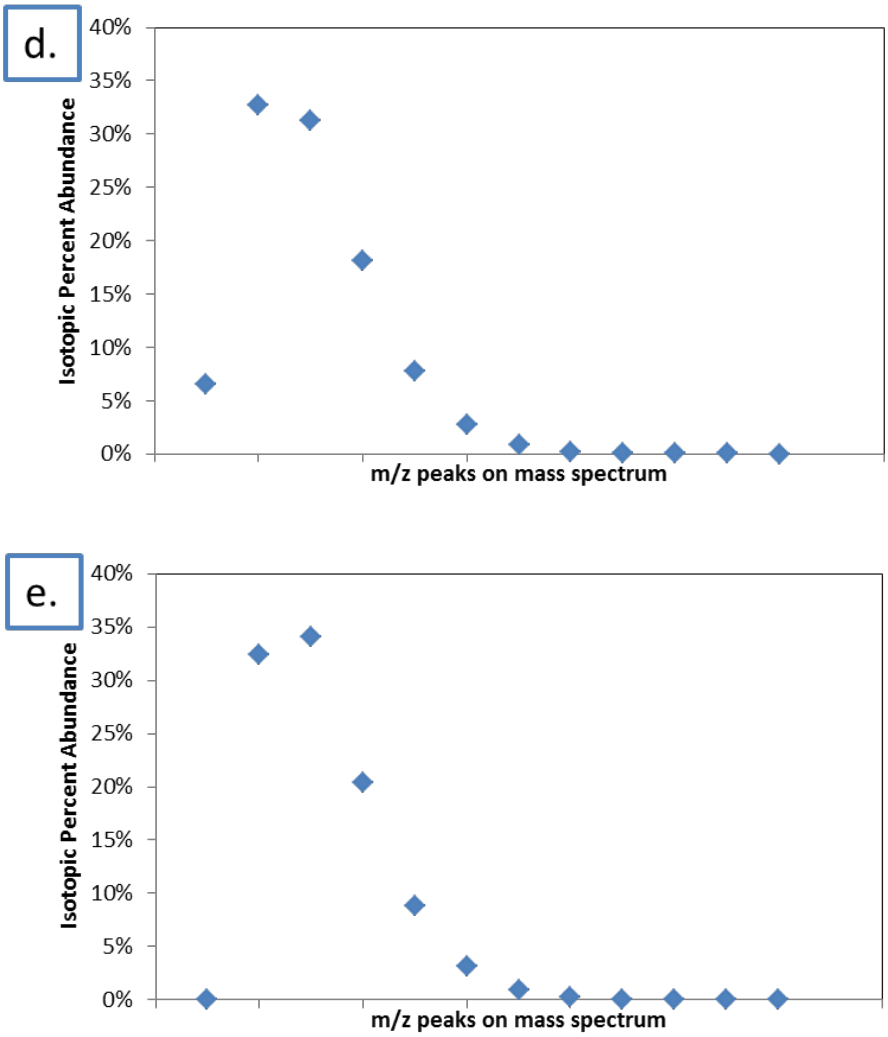

Figure 27: Expected Heights for m/z Peaks on Mass Spectra Based on the Relative Amounts of Terminal D-Ala/D-Lac. While some PG samples may exclusively contain PGs that terminate in either D-Ala-D-Ala or D-Ala-D-Lac, other samples may contain a mixture of the two. The shape of a mass spectrum distribution is dependent upon the relative abundances of the given isotopes. In the figure, the ratio of D-Ala-D-Ala to D-Ala-D-Lac is a) 100:0, b) 80:20, c) 50:50, d) 20:80, and e) 0:100. Note that the first point plotted in part e) is at 0% abundance, meaning that this peak should not be apparent for species that contain exclusively D-Ala-D-Lac.

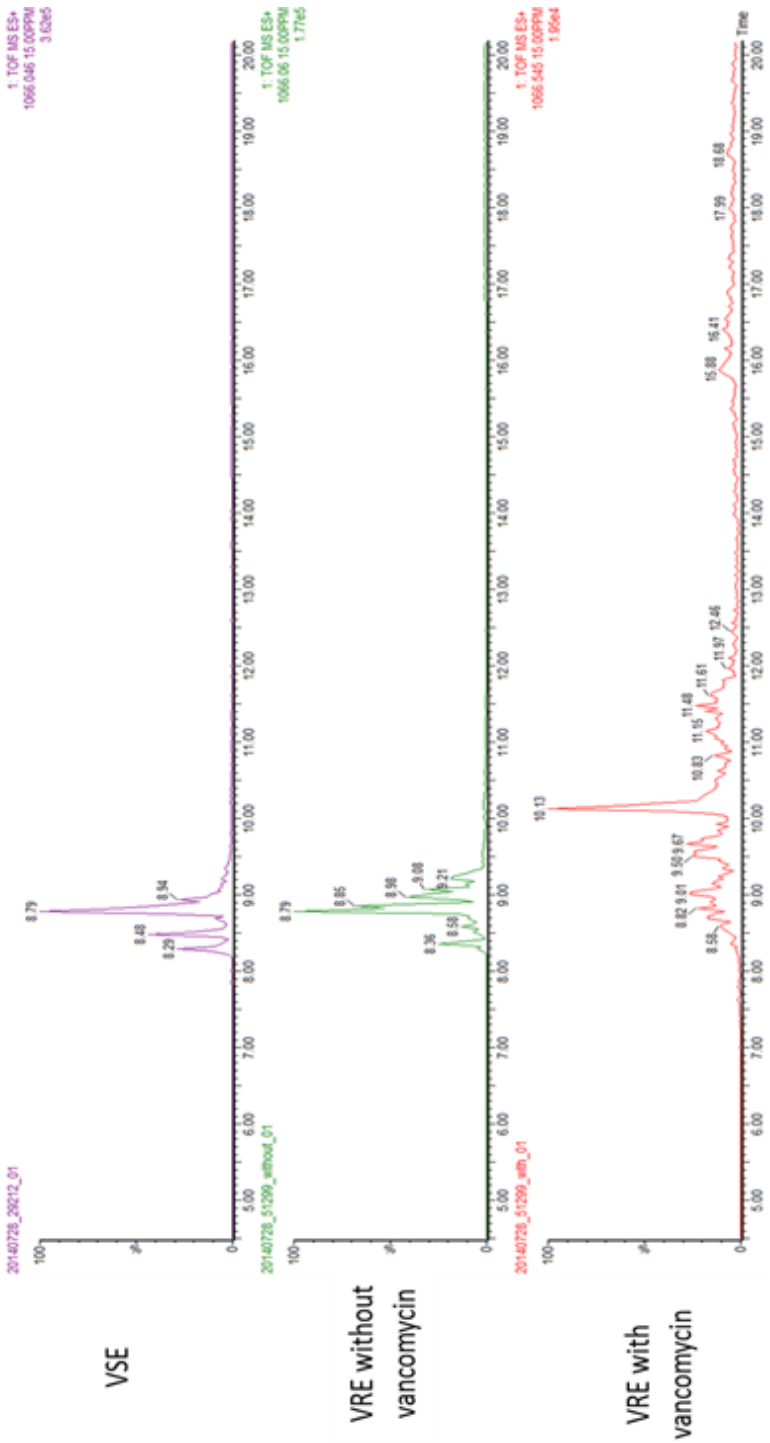

Figure 28: SIC for D-Ala-D-Ala vs. D-Ala-D-Lac. The figure highlights the later elution time for species in the VRE sample with vancomycin containing terminal D-Ala-D-Lac in comparison to corresponding species with terminal D-Ala-D-Ala in the samples from VSE and VRE without vancomycin. In this case for doubly-charged PG dimers, the PGs with D-Ala-D-Ala are eluting most prominently at 8.79 minutes, whereas those with D-Ala-D-Lac are eluting most at 10.13 minutes.

Variations in Alanylation of the PG Peptide Stem

The change in the degrees of PG-stem alanylation was monitored in VRE and VSE. Figure 29 shows mass spectra for doubly-charged PG dimers from VRE and VSE with varying degrees of alanylation. There are only three states of alanylation: pentapeptides (terminating in either D-Ala-D-Ala or D-Ala-D-Lac), tetrapeptides (terminating in D-Ala), and tripeptides (without any terminal D-Ala). PGs in all three states of alanylation were identified.

The alanylation profiles of both VSE and VRE grown in the absence of vancomycin are similar, both having high concentrations of PG with pentapeptide stems terminating in D-Ala-D-Ala and minor concentrations of PG with tripeptide stems. PGs with tetrapeptide stems were also detectable, but significantly less prevalent than PGs with pentapeptide or tripeptide stem structures. In contrast, very few unedited pentapeptides were observed for VRE grown in the presence of vancomycin. Instead, the edited PGs with tetrapeptide and tripeptide stems were both observed abundantly, again with the tripeptides being more common than the tetrapeptides.

The relative amounts of PGs with tripeptide, tetrapeptide, and pentapeptide stem structure found in VSE and VRE grown with and without vancomycin are summed for all identified PG species and are shown as a bar graph in Figure 30 and a heatmap in Figure 32. The relative amounts are encoded using a red/green/black color scale in the heatmap.

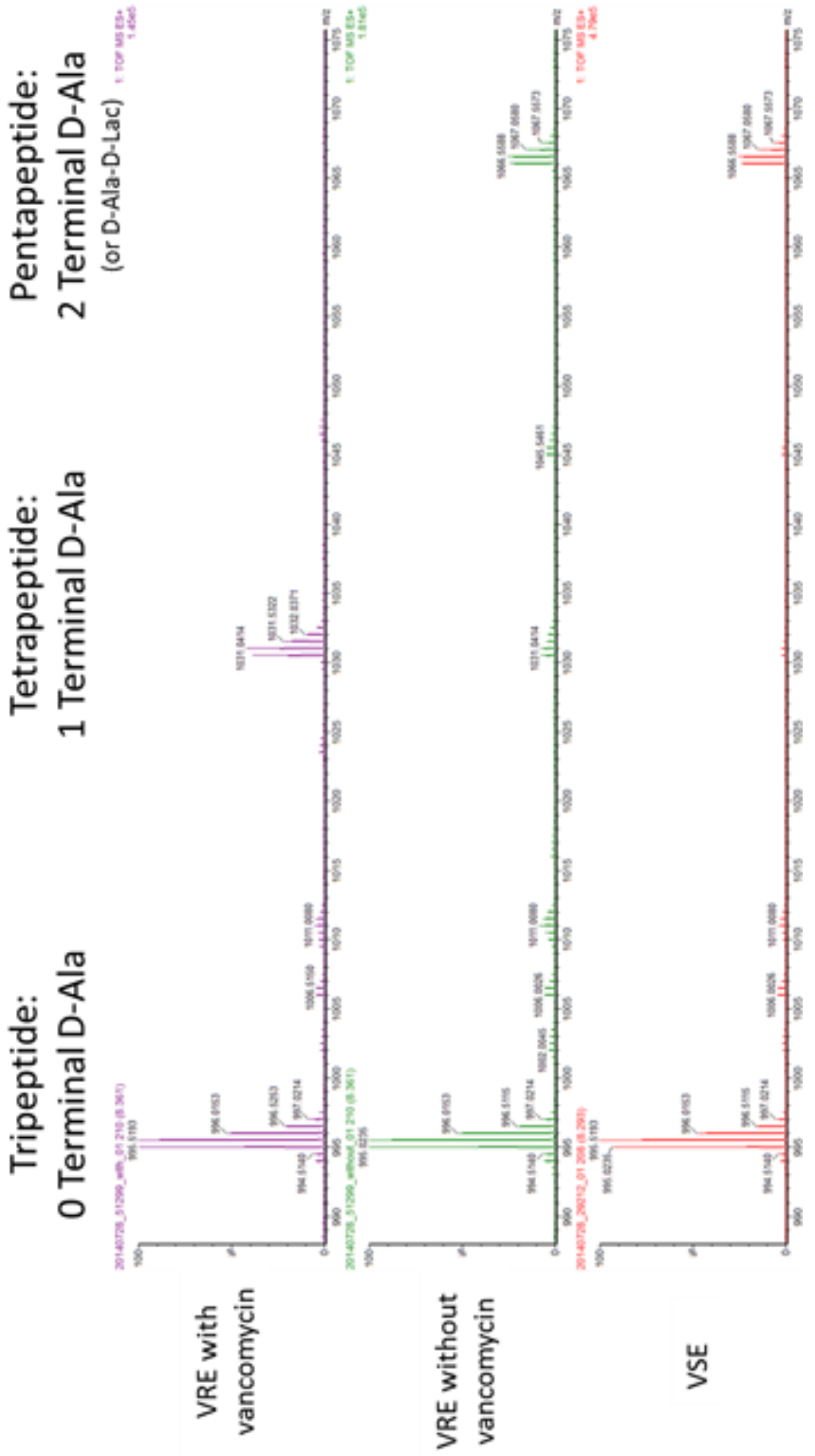

Figure 29: Mass Spectra with Differing Degrees of Alanylation. PGs were observed in the pentapeptide, tetrapeptide, and tripeptide forms, and the figure shows sample mass spectra from doubly-charged PG dimers.

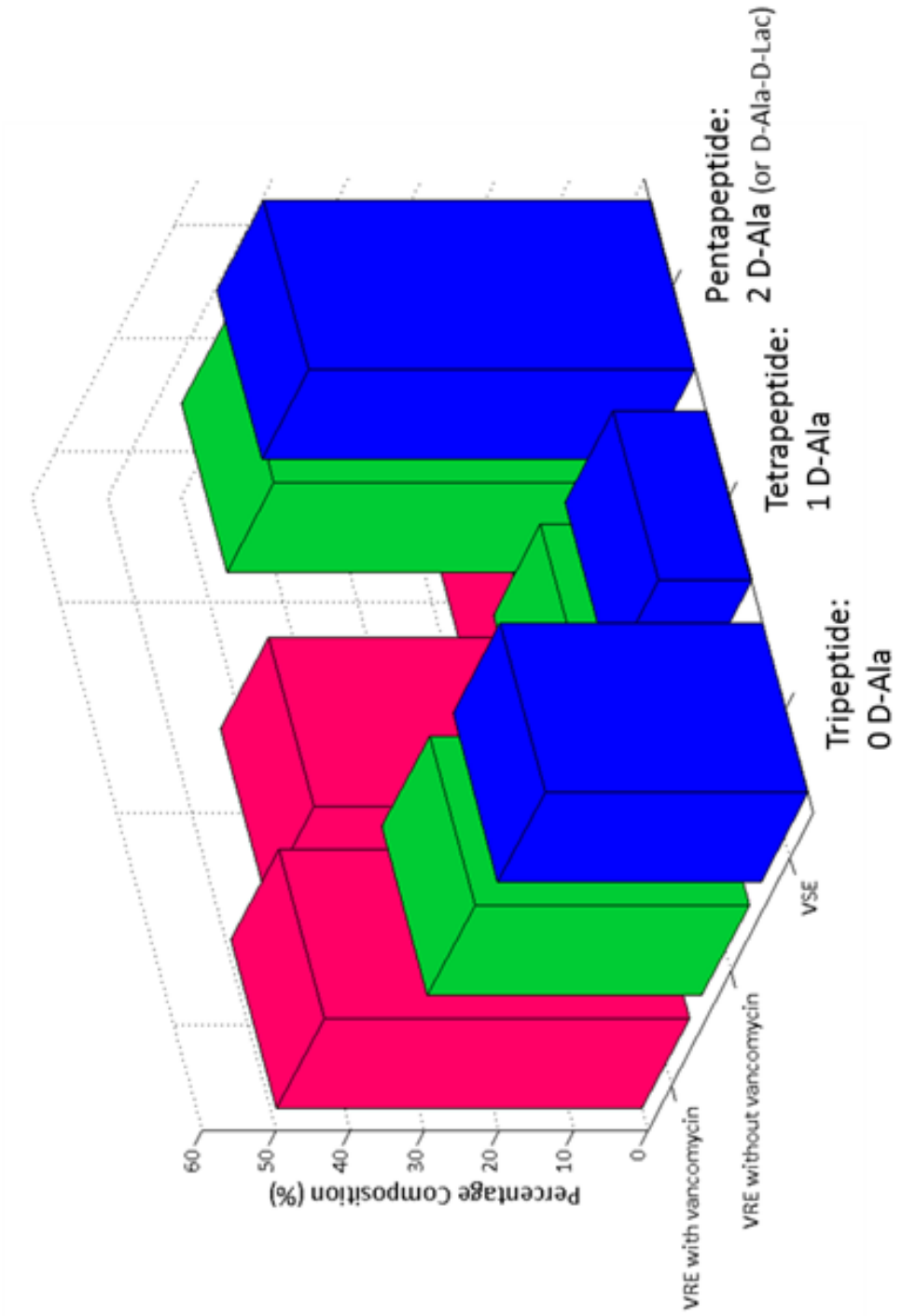

Figure 30: Comparison of PG Pentapeptide Stem Alanylation. The 3D bar graph shows similar patterns of alanylation in VSE and VRE without vancomycin in which the majority of the PG has the unedited pentapeptide stem with two terminal D-alanines. In contrast, the VRE with vancomycin shows increased editing, with the majority of the PG in the tripeptide and tetrapeptide states and a small minority in the pentapeptide form.

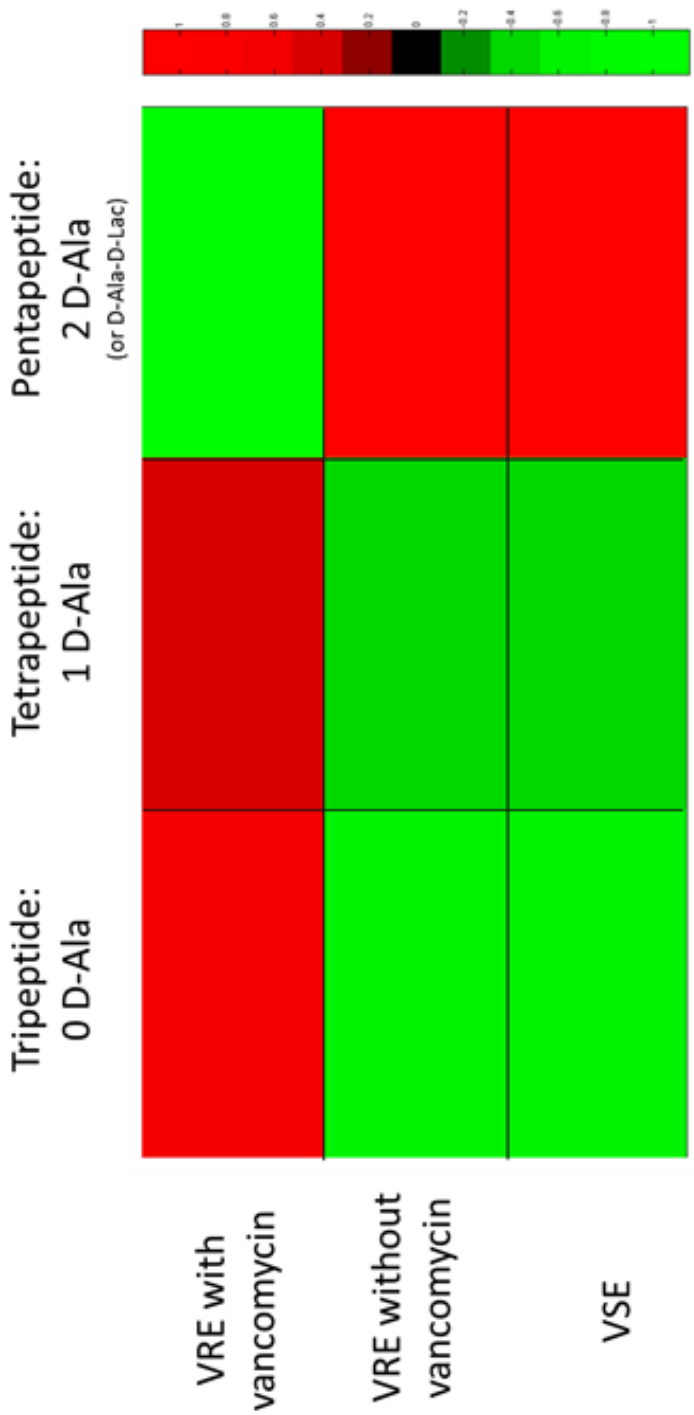

Figure 31: Heatmap Showing Varying Degrees of Alanylation. This heatmap shows the similar patterns of alanylation in VSE and VRE without vancomycin in which the majority of the PG has the unedited pentapeptide stem with two terminal D-alanines. In contrast, the VRE with vancomycin shows increased editing, with the majority of the PG in the tripeptide and tetrapeptide states and a small minority in the pentapeptide form.

Cross-Linking of PG Units to Form Oligomers

In addition to identifying monomers, cross-linked oligomers were identified ranging from dimers through heptamers. As shown through the SICs in Figure 32, the retention time for PG directly correlates with the MW and hence also with the number of cross-links. The monomers are eluted first, followed by the dimers, trimer, tetramers, and subsequent oligomers in order of increasing numbers of cross-linkages.

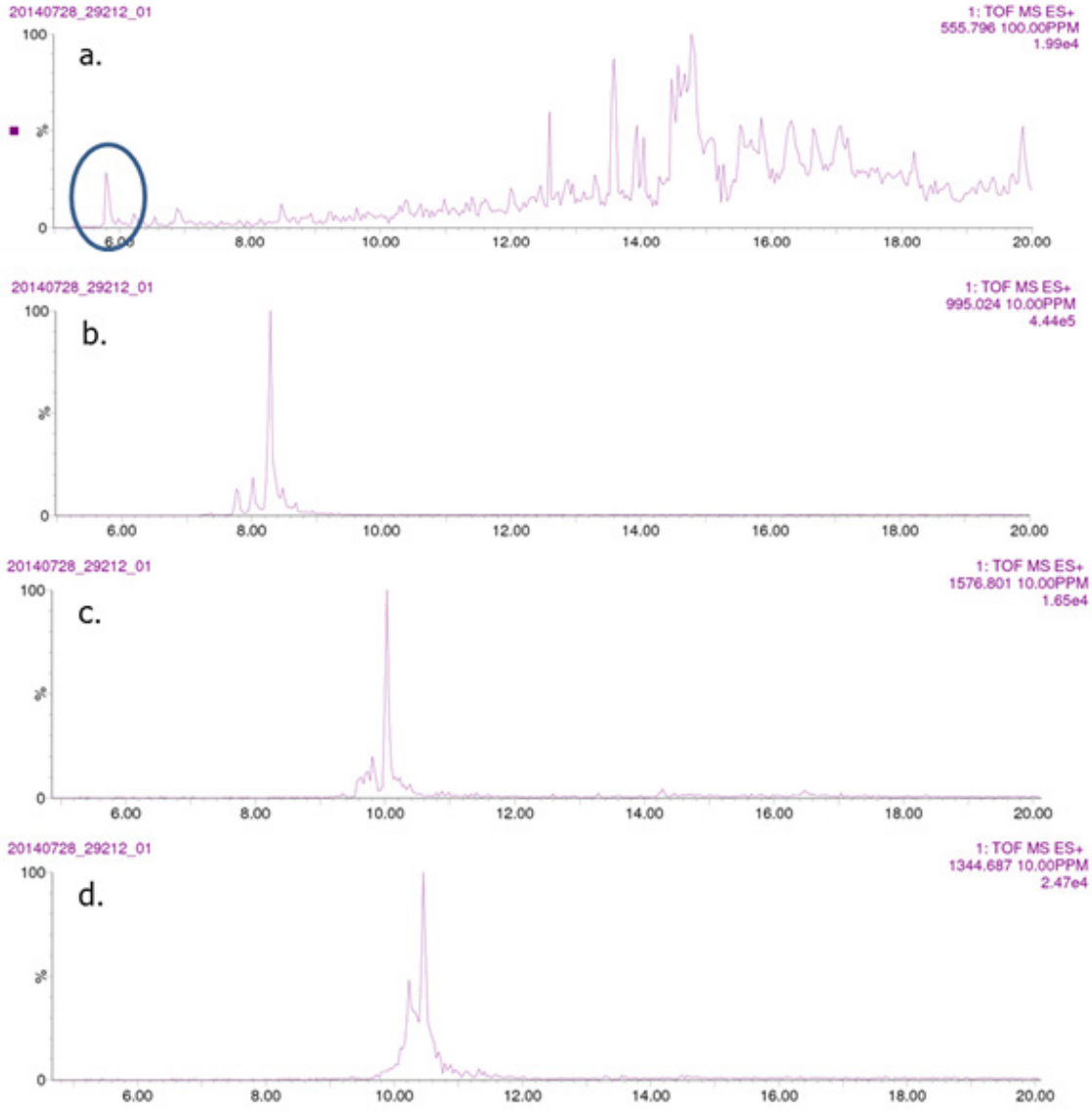

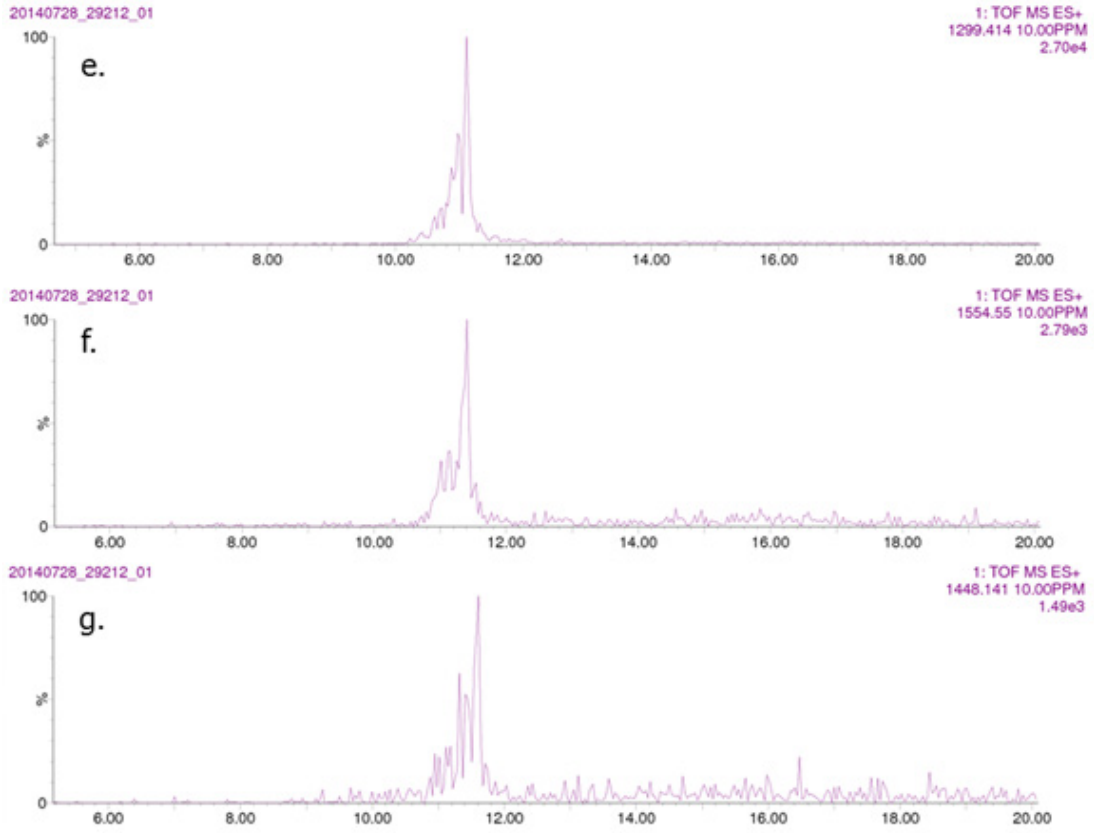

Figure 32: SICs for Cross-Linked PG by Oligomeric Size. Typical elution profiles are given for a) monomers, b) dimers, c) trimers, d) tetramers, e) pentamers, f) hexamers, and g) heptamers. The PG species eluted off the column in order of increasing oligomeric size, with monomers eluting first, dimers eluting second, trimers eluting third, etc. Although monomers were identified, they were not present in very large quantities. All monomers identified were found to elute around 5 minutes, and thus the peak on the SIC at about 5 minutes was circled to draw attention to the portion of the SIC truly attributed to the elution of identified monomers. For simplicity, only SICs from the VSE sample are represented here; however, similar elution profiles were observed for PG oligomers in the VRE samples with and without vancomycin. SICs are shown from about 0 to 20 minutes, although PG was only found to elute between 5 and 12 minutes.

A common way to characterize the overall extent of cross-linking in PG is through calculating the cross-linking efficiency (CE) from the relative amounts of each PG oligomer observed, as shown in Formula 8. The CE is based on comparing the number of cross-links observed with the number of possible cross-links, and observed

and possible cross-links are defined by whether or not existing cross-linking bridges are actively engaged in cross-linking, as shown in Figure 33.

Formula 8: Cross-Linking Efficiency of PG. The definition for PG CE is shown in a) and b). The expression is reduced to the sum shown in c) where the subscript *i* represents the number of PG subunits in the oligomer. The observed value for *i* ranged from 1 (monomer) to 7 (heptamer). Each k_i represents the corrected integrated SIC value for the given oligomer species.

a. $$CE = \frac{number\ of\ cross{-}links\ observed}{number\ of\ possible\ cross{-}links}$$

b. $$CE = \frac{dimers+(2*trimers)+(3*tetramers)+\ \ldots}{monomers+(2*dimers)+(3*trimers)+(4*tetramers)+\ \ldots}$$

c. $$CE = \frac{\sum_{i=1}^{7}(i-1)k_i}{\sum_{i=7}^{7} ik_i}$$

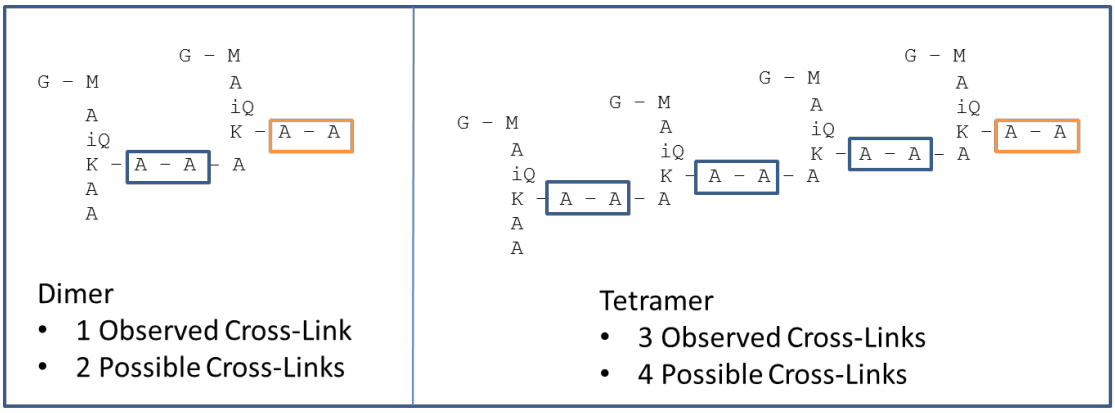

Figure 33: Observed and Possible Cross-Links for Determining CE. Observed cross-links are boxed in blue, whereas possible cross-links that were not formed are boxed in orange. A dimer, for example, has 2 cross-linking bridges (one for each monomeric subunit), but only one of the cross-linking bridges is actively involved in a cross-link, giving 1 cross-link observed out of 2 possible cross-links. Similarly, a tetramer has 4 cross-linking bridges, only 3 of which are involved in cross-links, giving 3 observed cross-links out of 4 possible cross-links.

The calculated CEs are shown in Table 6. For all practical purposes, the CEs are identical in all three samples with a mere difference of 0.2% between the highest to the lowest CEs. VSE and VRE without vancomycin had the lowest CE's. The CE for VSE was slightly above VRE without vancomycin (by 0.1%) and slightly below VRE with vancomycin (by 0.1%). For VRE, a slight increase in the cross-linking (of 0.2%) was observed with the addition of vancomycin.

Table 6: Measured Cross-Linking Efficiencies. Nearly identical cross-linking efficiencies were observed for all three experimental groups.

VSE	58.2%
VRE without vancomycin	58.1%
VRE with vancomycin	58.3%

Cross-linking efficiency, although a useful way to summarize cross-linking data with a single number, is not sufficiently detailed enough to thoroughly describe trends in cross-linking. The details of the cross-linking trends can be described better through graphs that display the PG observed by oligomer size.

The oligomeric distributions by experimental group are shown individually in Figure 34. These individual bar graphs emphasize the similarities in the cross-linking across experimental groups since all three graphs show a similar pattern of having very few monomers in the sample, having a large majority of the sample consist of dimers, and having the abundance of larger oligomers decrease with increasing size of the oligomer.

Figure 35 graphs the same oligomeric distributions from all of the experimental groups and overlays them on one graph, which highlights the subtle differences in the

distributions. For instance, VRE with vancomycin has a reduced number of dimers and an increased number of trimers in contrast to the VRE without vancomycin. Likewise, adding vancomycin to VRE reduces the number of tetramers but increases the number of pentamers. These small differences in which VRE with vancomycin has slightly more of the larger oligomers and slightly fewer of the smaller oligomers could perhaps account for the slight increase in CE observed upon the addition of vancomycin to VRE.

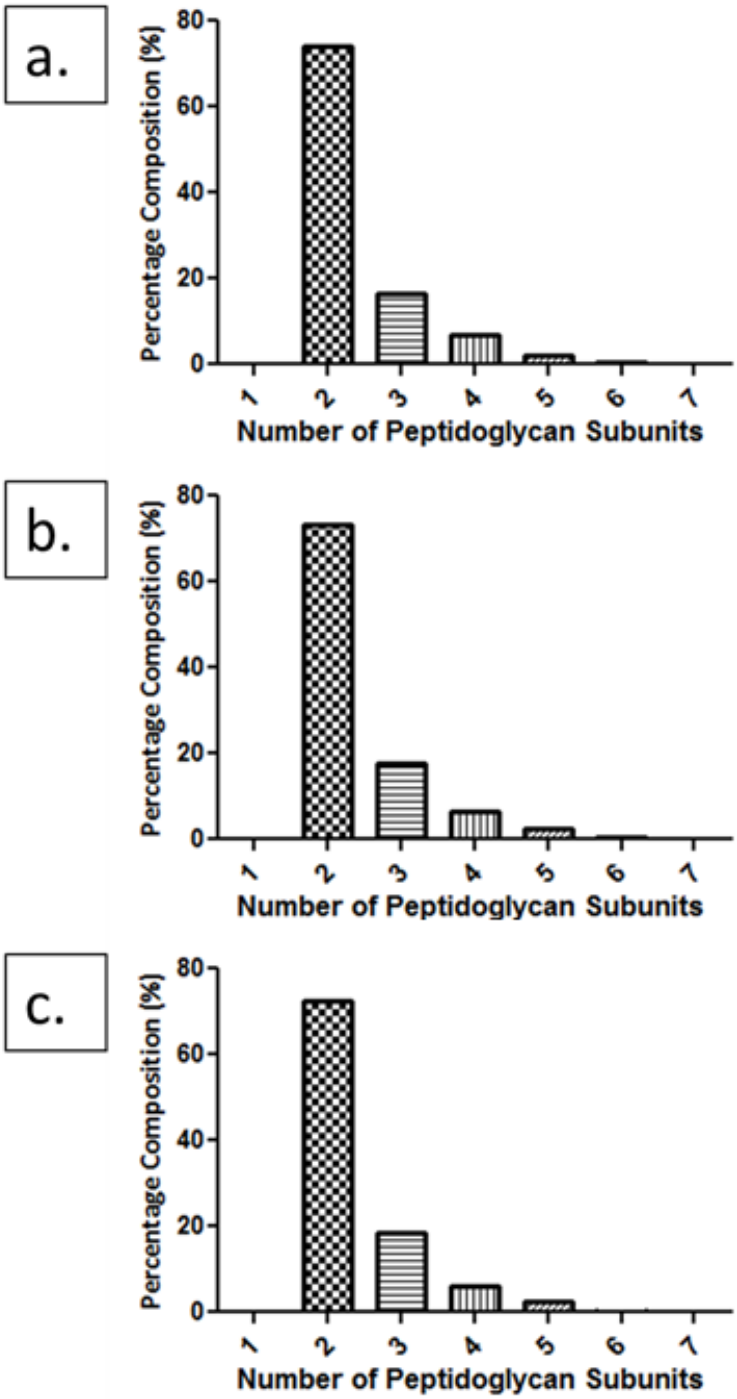

Figure 34: Oligomeric Distributions for Cross-Linked PG by Experimental Group. The bar graphs above represent the cross-linked species observed for a) VSE, b) VRE without vancomycin, and c) VRE with vancomycin. All three show very similar patterns, with the most abundant species being the dimers. Monomers were observed only sparsely, and larger oligomers were observed less abundantly as a function of increasing size.

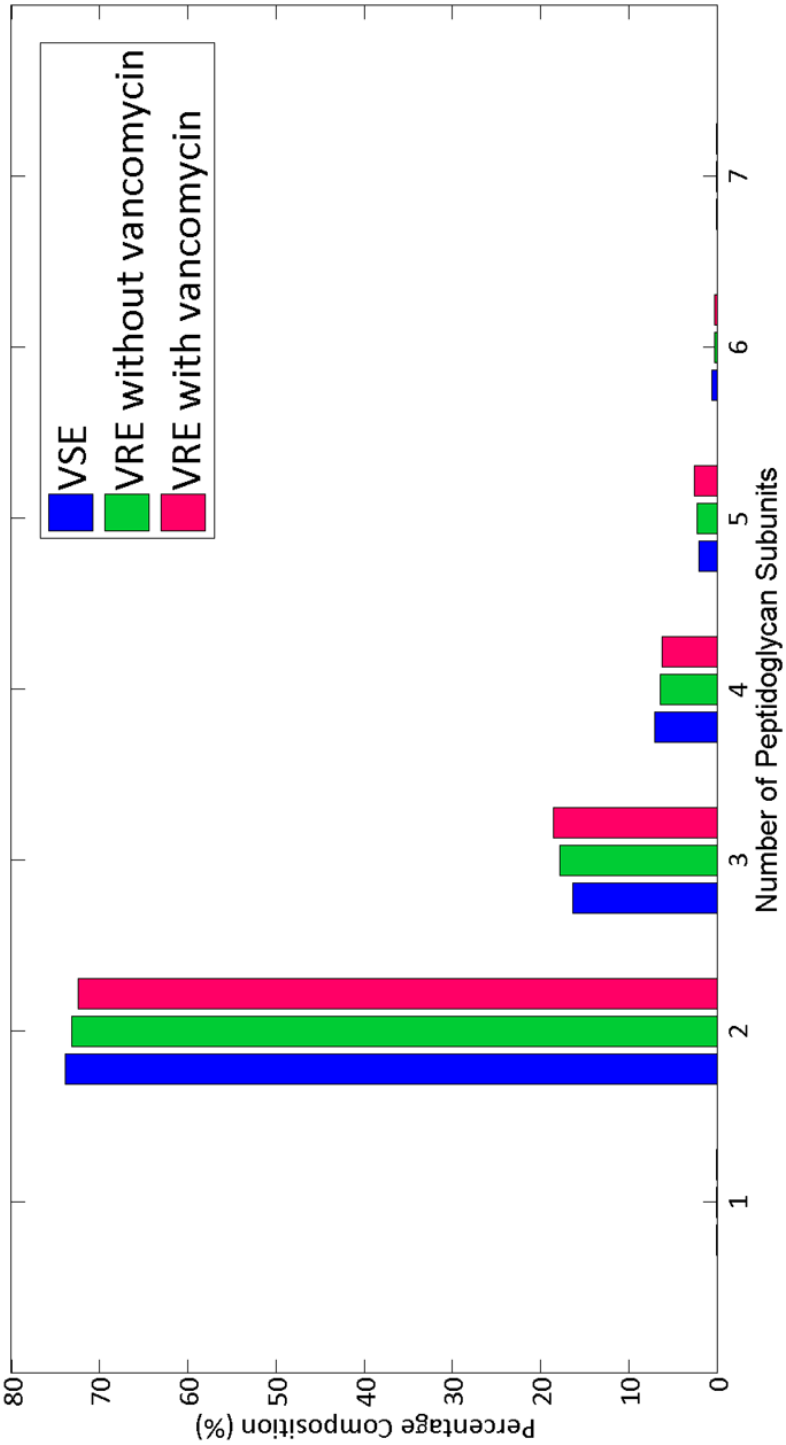

Figure 35: Oligomeric Distributions for Cross-Linked PG. Slight differences in cross-linking are highlighted by the figure. For instance, adding vancomycin reduces the number of dimers and increases the number of trimers. Likewise, adding vancomycin to VRE reduces the number of tetramers but increases the number of pentamers. These changes could perhaps account for the slight increase in CE observed upon the addition of vancomycin to VRE.

O-Acetylation of PG NAM

The structures of PG with and without O-acetylation are shown in Figure 36. NAM (rather than NAG) is generally assumed to be the target of this modification. Although it is not possible to discern with only exact mass which sugar in the disaccharide receives the acetyl group, the MS/MS data supported that O-acetylation takes place on the NAM.

PG dimers, trimers, tetramers, and pentamers were observed in the acetylated form. Some of the dimers observed were even doubly acetylated. The identification of these doubly-acetylated dimers was perhaps aided from the relative abundance of dimers in the PG samples. Identification of the O-acetylated species was carried out by searching for species that differed by 42 Da, which is the increase in mass that corresponds to the addition of an acetyl group. O-acetylated PG is also distinct because of its markedly later elution time for PG from the UPLC column in comparison to species lacking the O-acetyl group. These differences in mass and elution time are shown in Figure 37. O-acetylated monomers, hexamers, and heptamers were not identified, which is perhaps due to the low abundance of these oligomers in general in the PG samples.

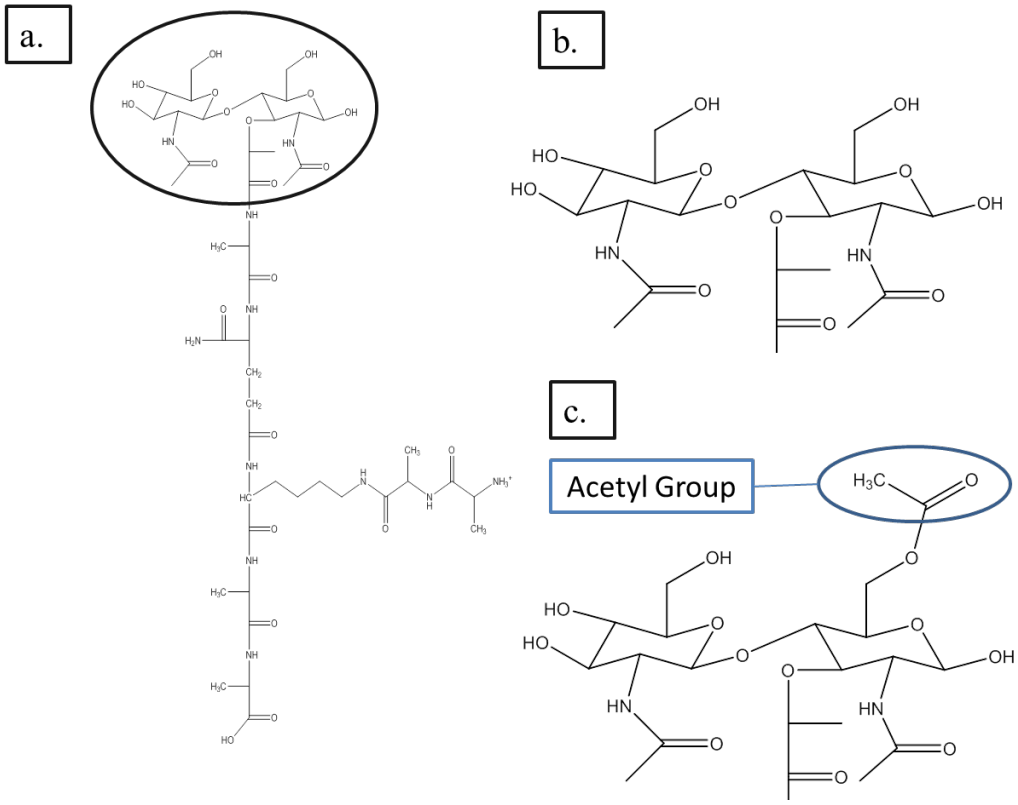

Figure 36: O-Acetylated N-Acetylglucosamine of PG. Part a) shows the N-acetylglucosamine and N-acetylmuramic acid disaccharide enlarged in parts b and c. Part b) shows NAM without O-acetylation, and part c) shows 1 O-acetylation on the NAM.

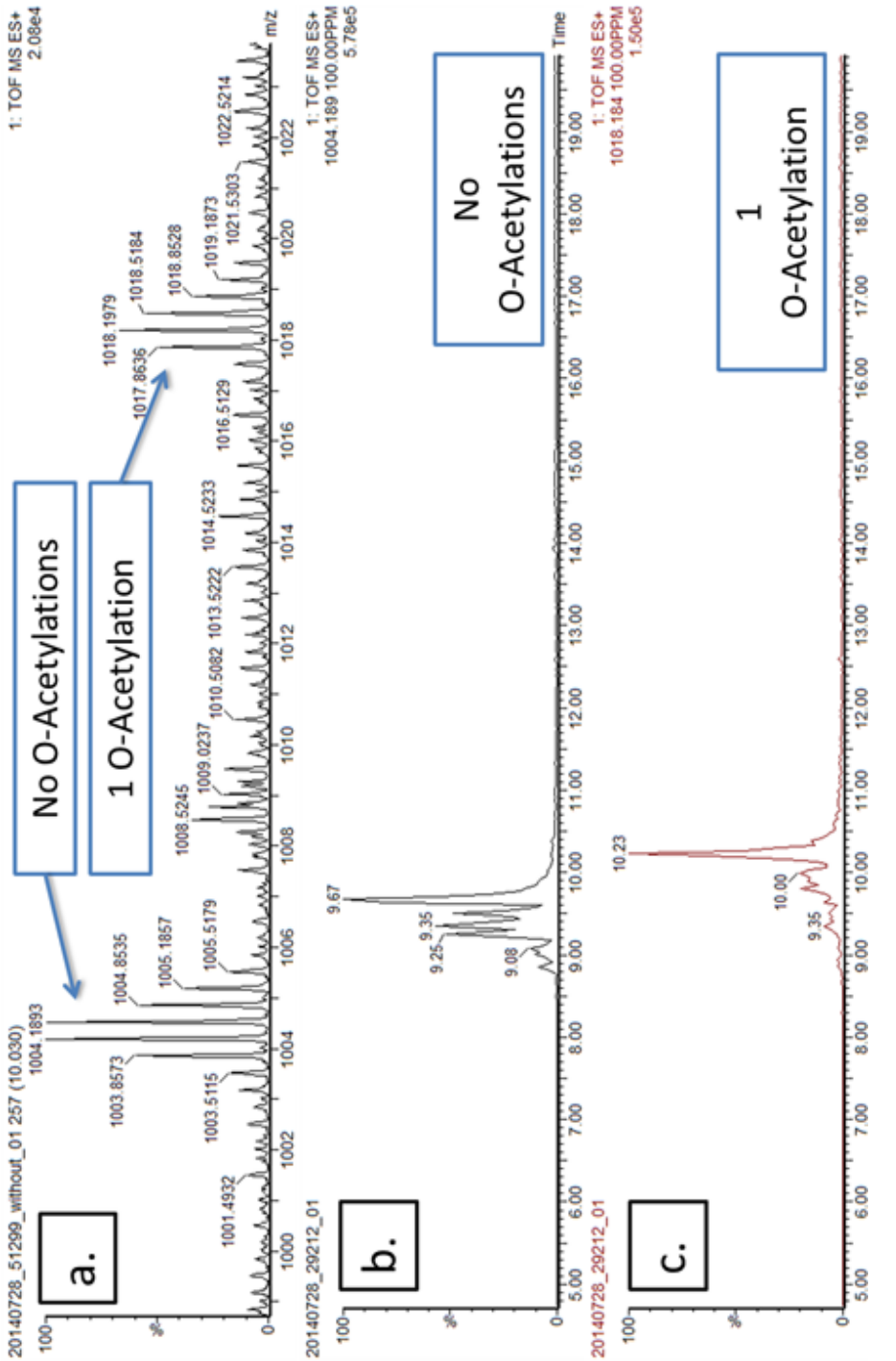

Figure 37: Sample Spectrum and Chromatograms for O-Acetylation. This figure includes a the following spectrum and chromatograms of a PG trimer with no terminal D-alanines: a) mass spectrum showing species with and without an O-acetylation, b) SIC of PG without an O-acetylation, and c) SIC of PG with one O-acetylation. Notice that the species with the O-acetylation not only shows a mass shift of about 42 Da in the spectrum but also has a shifted elution time (at about 10.23 minutes instead of 9.67 minutes).

Figure 38 shows the percentage of the PG species that were observed to be acetylated in each experimental group. In general, VSE and VRE without vancomycin had about the same level of O-acetylation, although VRE was slightly less O-acetylated than VSE. VRE, however, showed an increase in O-acetylation upon the presence of vancomycin.

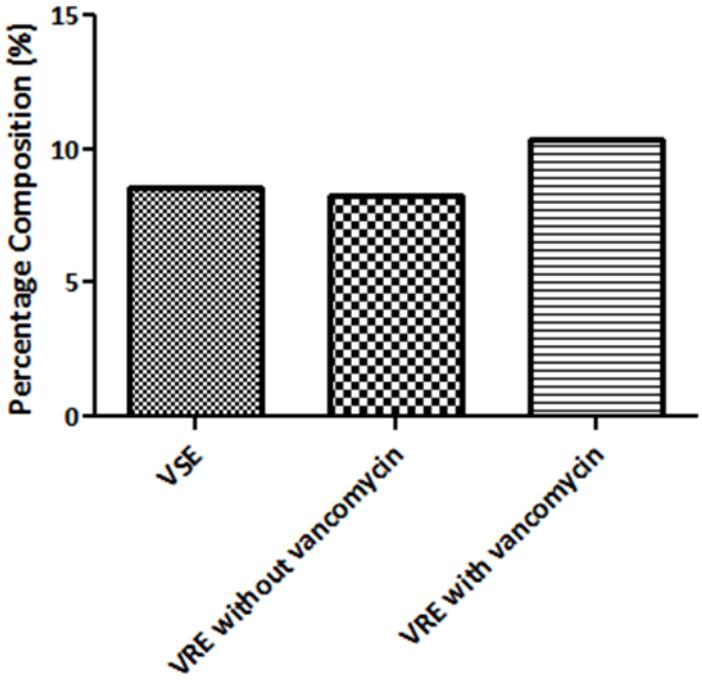

Figure 38: Degrees of PG O-Acetylation. The bar graph shows the percentage of the PG species that were O-acetylated for each experimental group. VSE and VRE without vancomycin had relatively similar degrees of O-acetylation, with VSE being slightly more acetylated. With VRE, the degree of O-acetylation increased when vancomycin was added.

The same pattern of O-acetylation increasing in VRE in the presence of vancomycin is especially noticeable in the larger oligomers when the O-acetylation data is broken down by the oligomeric size of the PG fragments, as shown in Figure 39. High relative abundance of dimers masks the changes in the degree of O-acetylation as a response of vancomycin, as this change is very minor in the case of a dimer. However,

when the larger oligomeric species are singled out, the increase in the degree of O-acetylation upon the addition of vancomycin becomes more readily apparent.

Figure 39 also shows that the percentage of the fragments containing at least one O-acetylation increased as a function of the size of the oligomer, with the largest oligomers also having the highest degrees of O-acetylation. It is sensible that larger oligomers are more likely to have at least one O-acetylation since the larger oligomers have more NAMs that can possibly be acetylated.

To more objectively compare O-acetylation across oligomeric sizes, the percentage of O-acetylated NAMs was calculated by oligomeric size (Figure 40). Interestingly, different trends were observed for VSE and VRE. For VSE, relatively equal percentages of NAM were O-acetylated regardless of the size of the oligomer. Hence, the apparent increase in O-acetylation for larger oligomers observed in Figure 39 is simply due to the larger oligomers containing more NAMs available for O-acetylation, and all NAMs are O-acetylated with equal frequency independent of the size of the oligomer. In contrast, for VRE a trend was observed in which the proportion of O-acetylated NAM's increased with increasing oligomer size. Although this pattern held true for VRE both with and without vancomycin, the presence of vancomycin exaggerated the trend since a greater percentage of O-acetylated NAM was observed for each size of oligomer when vancomycin was added during growth.

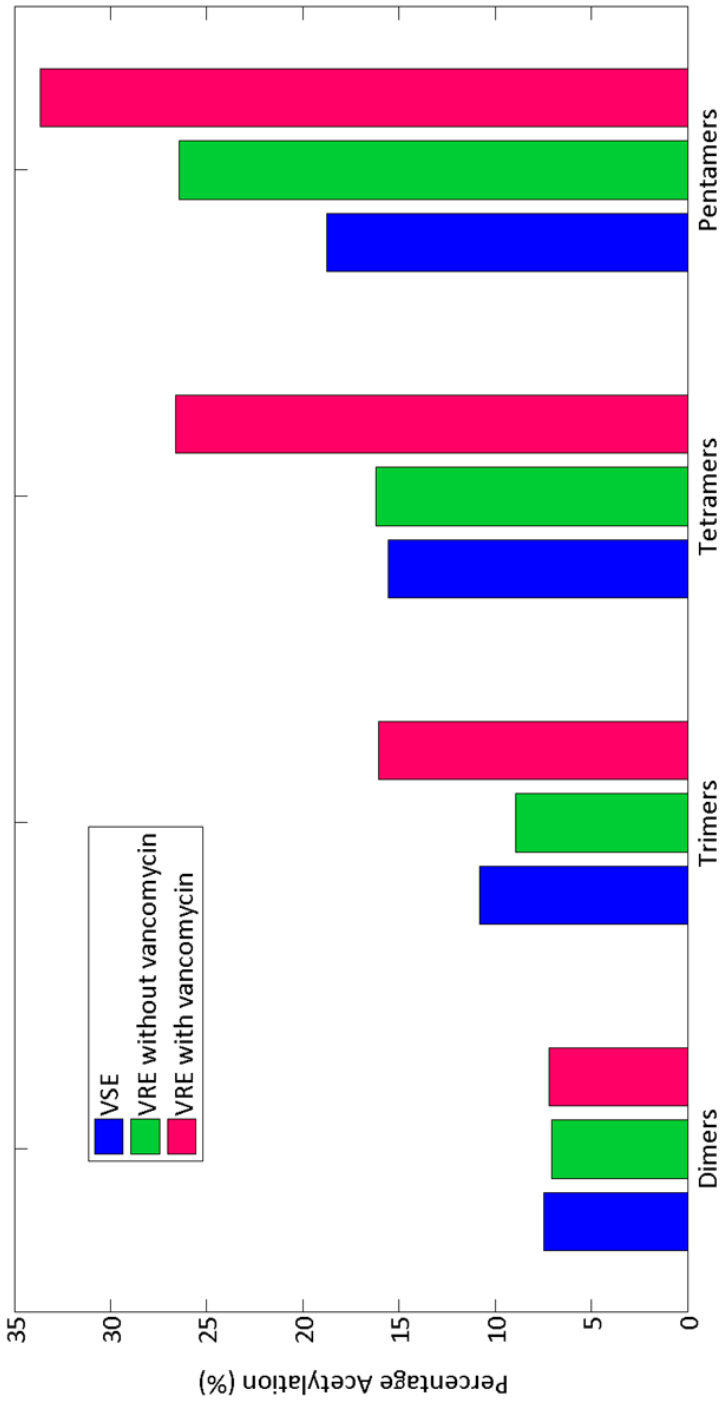

Figure 39: O-Acetylation by Oligomeric Size. For each oligomeric size, the O-acetylation of VRE increases in the presence of vancomycin. The percentage of the PG samples that are O-acetylated also is shown to increase as the size of the oligomer increases.

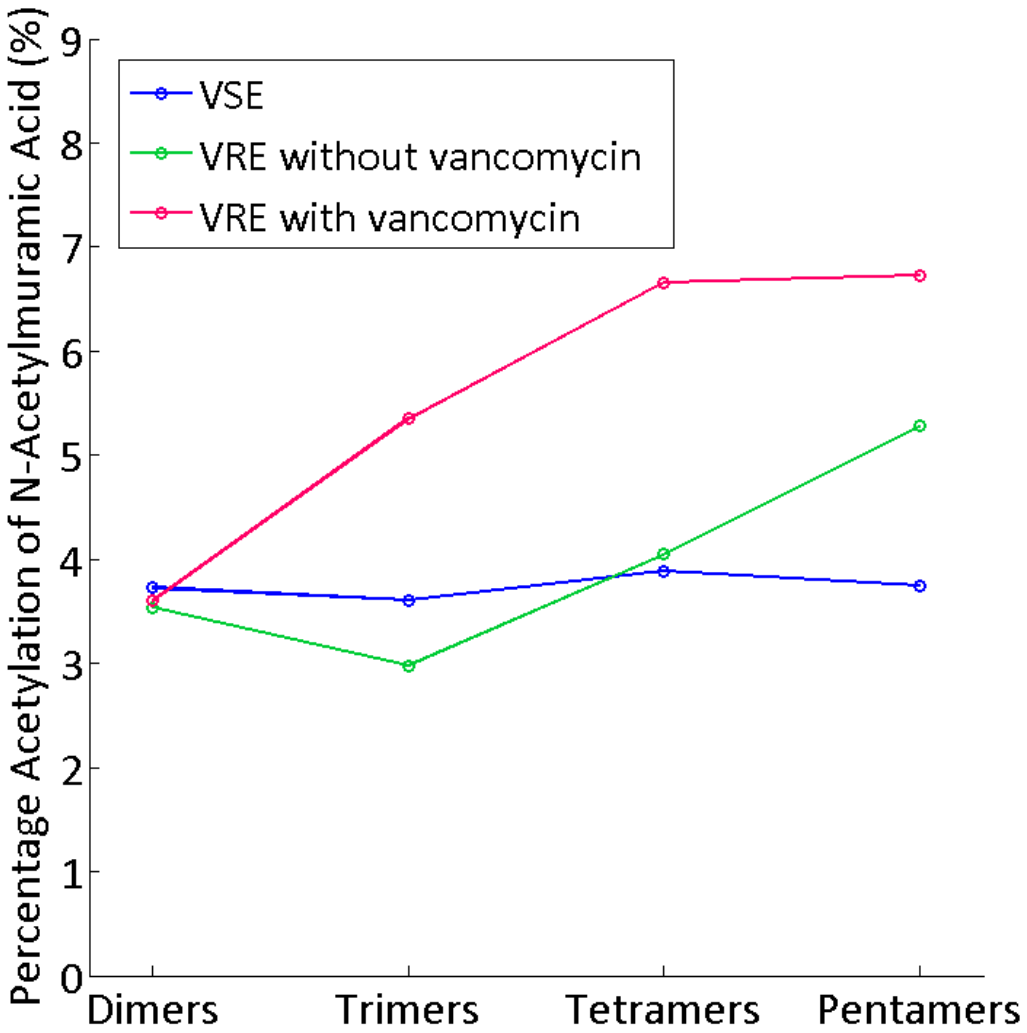

Figure 40: Percentage of NAM O-Acetylated by Experimental Group. By calculating the percentage of the NAM's that are O-acetylated for each oligomer size, it is possible to objectively compare the degree of O-acetylation across oligomer sizes. The degree of O-acetylation stays relatively constant across oligomer sizes for VSE. For VRE, however, the degree of O-acetylation tends to increase as the oligomer size increases, both in the presence and absence of vancomycin.

CHAPTER FOUR

Discussion and Conclusions

The major success of this project was the application of a novel method for PG analysis in which a combinatorial PG mass library was generated *in silico* and applied to liquid chromatography-mass spectrometry data. This method allowed for more efficient and thorough identification and quantification of the mutanolysin-digested PG fragments. This approach was successful in identifying the following types of modifications to vancomycin-resistant *E. faecalis* PG: 1) terminal D-Ala-D-Lac, 2) differential alanylation of the peptide stem, 3) cross-linking to form oligomers, and 4) O-acetylation of NAM. The quantification of the PG species showed that some of these modifications are indeed dependent upon the presence of vancomycin.

Presence of Terminal D-Lactate upon Addition of Vancomycin

It was expected that the presence of vancomycin would cause induction of the *vanB* operon, upregulating the expression of $VanH_B$, $VanX_B$, and VanB proteins and consequently leading to the incorporation of D-Ala-D-Lac as the terminal portion of the PG pentapeptide stems. As expected, terminal D-Ala-D-Lac was observed in VRE only when it was grown in the presence of vancomycin, which can be attributed to the induction of the *vanB* operon by vancomycin. Terminal D-Ala-D-Lac was not observed in VRE grown in the absence of vancomycin and was not observed for VSE, which can

be attributed to suppression of the *vanB* operon by the lack of vancomycin in the VRE sample growth without vancomycin and the absence of the operon altogether in VSE.

Moreover, the currently accepted mechanism for the induction of *vanB* theorizes the activating of the operon by vancomycin bound to the terminal D-Ala-D-Ala of PG, implying that some PGs terminating in D-Ala-D-Ala must remain in the cell wall of VRE even in the presence of vancomycin. Indeed, a complete replacement of terminal D-Ala-D-Ala by D-Ala-D-Lac was not observed even when vancomycin was present during growth. Rather, the pentapeptide PGs from the VRE sample grown in vancomycin included a mixture of terminal D-Ala-D-Ala and D-Ala-D-Lac.

Having both D-Ala-D-Ala and D-Ala-D-Lac pentapeptide stems in the same sample presented a challenge for definitive differentiation of the species by mass due to D-Ala and D-Lac differing in mass by only one Da. Due to the relatively large number of carbon atoms in PG combined with the 1% natural abundance of ^{13}C, PGs on the mass spectra do not appear as just one peak but rather present themselves as a distribution of isoptomers. With isoptomers each differing in mass by one Da and D-Ala-D-Ala and D-Ala-D-Lac also differing in mass by one Da, it is difficult to distinguish PG with D-Ala-D-Lac from a PG D-Ala-D-Ala isoptomer with one additional ^{13}C. We were thus unable to reliably differentiate D-Ala-D-Ala from D-Ala-D-Lac by mass alone and had to also rely on chemical property differences that resulted in chromatographic separation on the UPLC column. Further experiments that wish to easily identify PGs terminating in D-Ala-D-Lac by mass could do so by increasing the mass difference between PGs with D-Ala-D-Ala and D-Ala-D-Lac by isotopically labeling lactate. Labeling of lactate could be accomplished by growing the bacteria with labeled pyruvate since the lactate

incorporated into the PG peptide stem comes from the conversion of pyruvate by $VanH_B$. Alternatively, differentiating PGs with D-Ala-D-Ala from those with D-Ala-D-Lac by mass would also be simplified if the PGs appeared on the mass spectra as one peak and did not show an isotopic distribution, which could be accomplished by growing the bacteria in uniformly labeled ^{12}C media.

Increased Editing of the PG Stem upon Addition of Vancomycin

Another protein encoded by the *vanB* operon is $VanY_B$, a D-D carboxypeptidase that cleaves the terminal D-alanine residue of a PG precursor, converting the pentapeptide stem of the precursor into a tetrapeptide stem. Hence, the presence of vancomycin was expected to increase editing of PG pentapeptides and result in additional tetrapeptides. As expected, the presence of vancomycin during the growth of VRE drastically decreased the quantities of PG pentapeptides and markedly increased the quantities of PG tetrapeptides.

An unforeseen effect of vancomycin on VRE was the increase in the quantities of tripeptide PG stems with both of the terminal D-alanines edited off. The creation of PGs with tripeptide stems is thought to result from the initially synthesized pentapeptide PG serving as the substrate for the sequential actions of D,D and L,D-carboxypeptidases; the D,D-carboxypeptidase first creates a tetrapeptide from a pentapeptide by cleaving the peptide bond between the terminal two D-alanines, followed by the L,D-carboxypeptidase then cleaving the penultimate amide bond between the L-Lysine and the D-alanine to create a tripeptide from a tetrapeptide (Korza and Bochtler, 2005). Tripeptides were observed both in the presence and absence of vancomycin, so

L,D-carboxypeptidases have a basal activity; however, the relative amount of tripeptides increased in the presence of vancomycin. This increase in tripeptides suggests that the L,D-carboxypeptidase activity, like the D,D-carboxypeptidase activity, could be somehow mediated by the presence of vancomycin and that the presence of vancomycin causes an increase in the L,D-carboxypeptidase activity. Since very few L-D carboxypeptidases have even been identified and their regulatory mechanisms have certainly not yet been elucidated, such a hypothesis would not be unreasonable (Hoyland, Aldrige, Cleverley, Duchene, Minasov, Onopriyenko, Sidiq, Stogios, Anderson, Daniel, Savchenko, Vollmer, and Lewis, 2014). Alternatively, since the substrates for the L,D-carboxypeptidases are the tetrapeptide PGs, maybe the increase in PG tripeptides in the presence of vancomycin is simply a result of having increased tetrapeptide substrate available due to the upregulated activity of the D,D-carboxypeptidases.

Increased O-Acetylation upon Addition of Vancomycin

Since O-acetylation is not thought to be regulated by the *vanB* operon that is induced by the presence of vancomycin, the extent of O-acetylation was expected to be independent of the presence of vancomycin during the growth of VRE. Nevertheless, O-acetylation was observed to increase in VRE in the presence of vancomycin. This trend is not only noticeable when considering the overall O-acetylation of the sample, but it is evident to an even greater extent with considering exclusively the O-acetylation of the trimers, tetramers, and pentamers. Hence, it is abundantly clear from the data that there is a definite correlation between growing VRE in the presence of vancomycin and the increased O-acetylation of the PGs.

O-acetylation of PG NAM in *E. faecalis* is known to be carried out by the O-acetyltransferase EF0783, which is homologous to the more well-known OatA O-acetyltransferase in *S. aureus* (Vollmer, 2007). Additionally, removal of O-acetyl groups from PG is known to occur via O-acetylpeptidoglycan esterases (Pfeffer and Clark, 2012). Hence, increased O-acetylation of PG in the presence of vancomycin could be due either to the increased activity of O-acetyltransferases or to the decreased activity of O-acetylpeptidoglycan esterases, and it is not possible to determine from the LC-MS data alone which mechanism is more prevalent in increasing O-acetylation. Either way, there clearly seems to be a yet-unexplored modulation of O-acetylation by the presence of vancomycin during growth.

Not only did O-acetylation increase in the presence of vancomycin, but O-acetylation was also observed to increase with the increasing of oligomeric size. This trend was observed in VRE both in the presence and absence of vancomycin but was not observed in VSE. It could be suggested that this trend in O-acetylation is merely an artifact of digestion in which mutanolysin less thoroughly digested the more densely O-acetylated regions of the cell wall. However, the control group of VSE was also subject to the identical mutanolysin digestion procedure and did not show the trend of increasing O-acetylation of the larger oligomers. Instead, O-acetylation in VSE was shown to be independent of the oligomer size. The data therefore suggests that O-acetylation in VRE varies across PG structure, with parts that are heavily cross-linked also being subject to greater O-acetylation. Transpeptidases are therefore likely somehow related to O-acetyltransferases (or perhaps to O-acetylpeptidoglycan esterases) in VRE. This data is consistent with other sources that have also suggested a yet-unexplained correlation

between the action of O-acetyltransferases and the action of transpeptidases in antibiotic-resistant bacteria (Vollmer, 2007). Future research should seek to elucidate the connection between O-acetylation and transpeptidation in VRE.

Transpeptidation as Independent of the Presence of Vancomycin

Transpeptidation, or the cross-linking of PGs by penicillin-binding proteins, is not thought to be one of the processes regulated by the *vanB* operon, and thus the degree of cross-linking was expected to be independent of the presence of vancomycin. Indeed, very similar trends in transpeptidation were observed for VRE in the presence and absence of vancomycin. In fact, the following trend was observed in all three experimental groups: very few monomers, incredibly abundant dimers, and increasingly fewer larger oligomers (trimers through heptamers) as oligomeric size increased.

Since consistency was observed among the oligomeric distributions, any oddities in the oligomeric data may have been the result of systematic, procedural factors. And in fact, there were some aspects of the oligomeric distributions that suggest areas in which the procedure could be improved for future experiments. For instance, although monomers were identified, the quantity of monomers identified was very low. Other literature sources that explore PG structure of similar enterococcal species using LC-MS report monomers as composing a much larger sector of the identified PGs. For instance, one study on *Enterococcus faecium* reported that 47% of the identified PGs were monomers (Patti, Chen, Schaefer, and Gross, 2008). One explanation for obtaining fewer monomers is that the monomers were retained by the instrument (particularly in the matrix of the UPLC column); however, this explanation is unlikely since the monomers

were abundant enough to allow for positive identification. If there was a systematic flaw in the chromatography that resulted in monomers being retained in the column, then one would expect to not see any monomers at all, which was not the case. Additionally, species retained by the column would be expected to have later elution than species not retained by the column, but the PGs eluted from the column in order of increasing oligomeric size, with the PG monomers eluting before all of the other species. It also could be suggested that the mutanolysin digestion was not thorough enough to produce abundant monomers. This explanation is also unlikely because an incomplete digestion would have resulted in sugar-linked PGs in the sample. Although the PG mass library included sugar-linked species, none were observed, indicating that the mutanolysin digestion was complete. The more likely explanation is that the PG in our bacteria was mature, heavily cross-linked PG due to letting the culture grow for a full 24 hours and then harvesting the bacteria during the stationary phase of growth. Other studies of bacterial PG by LC-MS that have observed substantially more monomers grew the bacteria for a fraction of the time and then harvested the bacteria in the mid-exponential to late-exponential phase (Patti, Chen, Schaefer, and Gross, 2008; De Jonge, Handwerger, and Gage, 1996). Hence, further research should compare the stationary phase samples against those harvested earlier, perhaps in the mid-exponential or late-exponential growth phase.

Additionally, the observed quantities of the largest oligomers observed were likewise minimal. Perhaps this finding accurately represents the true prevalence of the larger oligomers in the sample; however, it is more likely that bias in the mass spectrometry prevented identification of many of the larger oligomers since some notable

oligomers that were likely present in the sample were not identified. For instance, doubly-acetylated dimers were identified but no doubly-acetylated species for oligomers larger than dimers were identified, although such double-acetylation is theoretically more likely for the larger species since acetylation was observed to increase as a function of oligomeric size. The likely bias in the instrument is due to the increasing range of the isotopic distribution and the subsequently decreasing relative intensities of the individual peaks as the species get larger. In other words, larger species are more likely to incorporate more variable numbers of ^{13}C atoms, which produces more peaks on the mass spectra since each peak represents an isoptomer. This spreading out of the distribution on the mass spectrum in turn diminishes the peak heights even if the overall amount of the species is identical to a smaller species. For identified peaks, the method used to quantify PG corrected for any diminishing in the peak height due to the isotopic distribution by use of a correction factor that served to calculate the intensity that would have resulted from a monoisotopic species. However, it is probable that many distributions of larger oligomers on the mass spectra had such diminished peak heights that these peaks were lost in the noise of the instrument and thus were not able to be identified. This challenge inherent to observing larger species with LC-MS could perhaps be circumvented by growing the bacteria in uniformly ^{12}C labeled media. Without any available ^{13}C for the bacteria to incorporate into the PGs, the species would appear on the mass spectra as a single monoisotopic peak rather than as a distribution of isoptomers, and the larger oligomers could then be better identified above the noise.

Final Conclusions

The liquid chromatography-mass spectrometry analysis of isolated, mutanolysin-digested cell wall peptidoglycans was accomplished through a method that applied a combinatorial PG mass library generated *in silico*. The PG structures in *vanB*-type VRE were consistent with the proposed induction of *vanB* by the presence of vancomycin, including the vancomycin-induced presence of terminal D-Ala-D-Lac in PG pentapeptide stems and the increased editing of the PG pentapeptides to form tetrapeptides by D,D-carboxypeptidases in the presence of vancomycin. The presence of vancomycin was also observed to elicit additional effects not thought to be related to *vanB*, including increased L,D-carboxypeptidase activity and increased O-acetylation of PGs. O-acetylation in VRE was also observed to be positively correlated with increasing oligomer size, independent of vancomycin's presence. Further modifications to the PG architecture, such as N-deacetylation and N-glycolyation, were not observed in *E. faecalis* in any of the experimental condition groups.

The most prominent findings are the vancomycin-dependent changes to PG structure that are unexplained by induction of the *vanB* operon by vancomycin. Further research is necessary to explain the role of vancomycin in mediating increased L,D-carboxypeptidase activity and increased O-acetylation of PG in VRE. Perhaps *vanW* (the portion of the *vanB* operon that is uncharacterized as of yet) has a function in PG editing by L,D-carboxypeptidases and/or functions in O-acetylation. Alternatively, vancomycin may have inducible and/or repressible effects that cause the observed increase in L,D-carboxypeptidase activity and O-acetylation through mechanisms outside of induction of *vanB*.

Future research could also be instrumental in improving the characterization of PG by LC-MS. The approach to PG analysis that used LC-MS in combination with an *in silico* PG mass library generated combinatorially by considering all possible combinations of known and theoretical modifications could be further established and refined in future studies. A more thorough isolation of the PG could be accomplished through the acid-mediated removal of the all teichoic acid, and having a purer sample might provide easier and more accurate identification of PGs. Labeling the lactate through growing the bacteria in media with labeled pyruvate would provide for clearer identification of the terminal D-Lac in VRE in the presence of vancomycin. Growing the bacteria in uniformly labeled ^{12}C media would also provide for better identification of terminal D-Lac while also perhaps providing better identification of the larger oligomers. Harvesting the bacteria in the mid-exponential or late-exponential phase of growth would perhaps allow for identification of a larger proportion of monomers while also allowing for identification of the difference in the PG composition in response to the bacterial population density.

APPENDIX

MATLAB Script for PG Library Generation and Matching

The following is an example of a MATLAB script generated *in sitio* that was used for the following two purposes: 1) to generate all of the possible combinations of the known and hypothetical modifications to the PGs and 2) to match the observed mass-per-charge (m/z) ratios from the mass spectra with the corresponding PGs. For the portion of the script that generated the PG mass library, arbitrary maximum values were set for cross-linking and sugar-linking to limit the size of the library. In this particular example, PGs were limited to a maximum of 6 cross-links and a maximum of 3 sugar-links, which gave 3,708,976 entries total in the PG mass library. For the matching portion of the script that identified the m/z peaks from the mass spectra, an arbitrary maximum difference tolerance was set so that all of the identified matches were within a certain PPM range of the calculated values. In this example, the tolerance is set at 50 PPM.

```
% Enterococcus faecalis modification possibility library script
% with m/z matching

clear all
clc

% Initializing the library matrix
Modification_variables = 21;
Number_of_variations = 5000000;
Library(Number_of_variations,Modification_variables) = 0;

% Minimum variation parameters and maximum cross/sugar linker numbers
crosslink_minimum = 0;
crosslink_maximum = 6;
sugarlink_minimum = 0;
sugarlink_maximum = 3;
crosslink_sugarlink_maximum = 0;
sugar_missing_minimum = 0;
alanine_minimum = 0;
lactate_minimum = 0;
O_acetylation_minimum = 0;
N_deacetylation_minimum = 0;
N_glycosylation_minimum = 0;
O_glycosylation_minimum = 0;
stem_missing_minimum = 0;
non_reduction_minimum = 0;
```

```
cyclization_minimum = 0;
query_charge_limit = 8;
starting_charge_column = 15;
Library_count = 0;

% Mass parameters for Enterococcus faecalis
mass_proton = 1.0072764668;
start_mass = 968.4782475338;
cross_link_mass = 1020.4975201831;
sugar_link_mass = 948.4520327833;
alanine_mass = 71.0371137878;
lactate_addition_mass = 0.9840155848;
O_Ac_mass = 42.0105646863;
N_DAc_mass = 41.0032882341;
N_Gly_mass = 15.9949146221;
O_Gly_mass = 162.0528234315;
sugar_missing_mass = 203.079372533;
stem_missing_mass = 470.2721583447;
cyclization_mass = 2.0389109316;

% Looping crosslinks
for c = crosslink_minimum:crosslink_maximum

  % Looping sugarlinks
  sugarlink_maximum = crosslink_sugarlink_maximum - c;
  if (crosslink_sugarlink_maximum - c) < 0
     sugarlink_maximum = 0;
  end

  for s = sugarlink_minimum:sugarlink_maximum

    % Looping for missing stems
    stem_missing_maximum = s;
    if c == 0 && s == 0
      stem_missing_maximum = 1;
    end
    if c == 0 && s > 0
      stem_missing_maximum = s + 1;
    end

    for stem_missing = stem_missing_minimum:stem_missing_maximum

      % Looping crosslinker cyclization
      cyclization_maximum = s + 1 - stem_missing;
      for cyclization = cyclization_minimum:cyclization_maximum

        % Looping missing sugars
        sugar_missing_maximum = 1 + c;
        for sugar_missing = sugar_missing_minimum:sugar_missing_maximum

          % Looping alanine
          alanine_maximum = (s*2 + 2) - (stem_missing*2);
          for ala = alanine_minimum:alanine_maximum;

            % Looping lactate
```

```
lactate_maximum = floor(ala/2);
if lactate_maximum < 0
  lactate_maximum = 0;
end
for lactate = lactate_minimum:lactate_maximum

  % Looping O-Acetylation
  O_acetylation_maximum = c + s + 1 - sugar_missing;
  for O_Ac = O_acetylation_minimum:O_acetylation_maximum

    % Looping N-Deacetylation
    N_deacetylation_maximum = c*2 + s*2 + 2 -
     sugar_missing;
    for N_DAc =
     N_deacetylation_minimum:N_deacetylation_maximum

      % Looping N-Glycosylation
      N_glycosylation_maximum = (c*2 + s*2 + 2) - N_DAc -
       sugar_missing;
      for N_Gly =
       N_glycosylation_minimum:N_glycosylation_maximum

        % Looping O-Glycosylation
        O_glycosylation_maximum = (c*2 + s*2 + 2) - O_Ac -
         sugar_missing;
        for O_Gly =
        O_glycosylation_minimum:O_glycosylation_maximum

          % Looping non-reduction
          non_reduction_maximum = c + 1;
          for non_reduction =
          non_reduction_minimum:non_reduction_maximum

            % Entering the variation values for the current
            % library index
            Library_count = Library_count + 1;
            Library(Library_count,1) = c;
            Library(Library_count,2) = s;
            Library(Library_count,3) = ala;
            Library(Library_count,4) = lactate;
            Library(Library_count,5) = O_Ac;
            Library(Library_count,6) = N_DAc*(-1);
            Library(Library_count,7) = N_Gly;
            Library(Library_count,8) = O_Gly;
            Library(Library_count,9) = sugar_missing*(-1);
            Library(Library_count,10) = stem_missing*(-1);
            Library(Library_count,11) = non_reduction;
            Library(Library_count,12) = cyclization;

            % Calculating the exact mass and charge
            exact_mass = start_mass + (c*cross_link_mass) +
             (s*sugar_link_mass) + (ala*alanine_mass) +
             (lactate*lactate_addition_mass) +
             (O_Ac*O_Ac_mass) + ((N_DAc*(-1))*N_DAc_mass) +
             (N_Gly*N_Gly_mass) + (O_Gly*O_Gly_mass) +
```

```
                        ((sugar_missing*(-1))*sugar_missing_mass) +
                        ((stem_missing*(-1))*stem_missing_mass) +
                        (non_reduction*(-1)*(mass_proton*2)) +
                        (cyclization*(-1)*cyclization_mass);
                      Library(Library_count,13) = exact_mass;
                      initial_charge = (s + N_DAc + 1 - stem_missing
                       - cyclization);
                      Library(Library_count,14) = initial_charge;

                      % Filling out the m/z columns
                      for charge_count = 0:query_charge_limit
                        Library(Library_count,(starting_charge_column
                        + charge_count)) = ((exact_mass +
                        charge_count * mass_proton) / (initial_charge
                        + charge_count ));
                      end

                    end

                  end

                end

              end

            end

          end

        end

      end

    end

end

% Reading the combinatorically generated library
target_index_size = Library_count;
target = Library(1:target_index_size,:);

% Reading the manually picked m/z targets of interest from Excel
% Note: xlsread has syntax xlsread(filename,sheet,xlrange)
[mz_query] = xlsread('E faecalis found peaks',1,'E29:H35');
mz_query_index_size = length(mz_query);

% Defining search parameters and initializing the targets
% tolerance in ppm
tolerance = 50;
match(5000,20) = 0;
```

```
match_index = 1;

% Search algorithm
for mz_query_index = 1:mz_query_index_size

  % Setting the m/z query targets
  current_query_mz = mz_query(mz_query_index,3);
  current_query_charge = mz_query(mz_query_index,4);

  % Moving the target from one to another while making the comparison
  for target_index = 1:target_index_size

    % Calculating the ppm difference between the query and library
    target_charge_column = current_query_charge + 14 -
     (target(target_index,14) - 1);
    mz_difference = current_query_mz -
    target(target_index,target_charge_column);
    mass_difference = mz_difference*current_query_charge;
    ppm_difference = (mass_difference/target(target_index,13))*1000000;

    % Comparing the difference and adding to the matches if it is
    % within the ppm tolerance
    if abs(ppm_difference) < tolerance && current_query_charge >=
     target(target_index,14)
      match(match_index,1) = target_index;
      match(match_index,2) = mz_query(mz_query_index,1);
      match(match_index,3:15) = target(target_index,1:13);
      match(match_index,16) = current_query_charge;
      match(match_index,17) = mz_query(mz_query_index,2);
      match(match_index,18) = mz_query(mz_query_index,3);
      match(match_index,19) =
       target(target_index,target_charge_column);
      match(match_index,20) = ppm_difference;
      match_index = match_index + 1;
    end

  end

end
```

BIBLIOGRAPHY

Ashford, P.; Bew, S.P. Recent advances in the synthesis of new glycopeptide antibiotics. *Chemistry Society Reviews* **2012**, *41*, 957-978.

Arias, C. A.; Murray, B. E. The rise of Enterococcus: beyond vancomycin resistance. *Nature Reviews Microbiology* **2012**, *10*, 266-278.

Benachour, A.; Labjouzi, R.; Jeune, A. L.; Hébert, L.; Thorpe, S.; Courtin, P.; Chapot-Chartier, M.; Prajsnar, T. K.; Foster, S. J.; Mesnage, S. The Lysozyme-Induced Peptidoglycan N-Acetylglucosamine Deaccetylase PgdA (EF1843) Is Required for Enterococcus faecalis Virulence. *Journal of Bacteriology* **2012**, *194*(22), 6066-6073.

Betinkaya, Y.; Falk, R.; Mayhall, C. G. Vancomycin-Resistant Enterococci. *Clinical Microbiology Reviews* **2000**, *13*, 686-707.

Bouhss, A.; Josseaume, N.; Severin, A.; Tabei, K.; Hugonnet, J.; Shlaes, D.; Mengin-Lecreulx, D.; Heijenoort, J. V.; Arthur, M. Synthesis of the L-Alanyl-L-alanine Cross-bridge of *Enterococcus faecalis* Peptidoglycan. *Journal of Biological Chemistry* **2002**, *277*(48), 45935-45941.

Bugg, T. D. H.; Braddick, D.; Dowson, C. G.; Roper, D. I. Bacterial cell wall assembly: still an attractive antibacterial target. *Trends in Biotechnology* **2011**, *29*(4), 167-173.

Butler, M.S.; Hansford, K. A.; Blaskovich, M. A. T.; Halai, R.; Cooper, M. A. Glycopeptide antibiotics: Back to the furture. *The Journal of Antibiotics* **2014**, *67*, 631-644.

Centers for Disease Control and Prevention. Antibiotic Resistance Threats in the United States, 2013. http://www.cdc.gov/drugresistance/threat-report-2013/ (accessed March 22, 2015).

De Jonge, B.L; Handwerger, S.; Gage, D. Altered Peptidoglycan Composition in Vancomycin-Resistant *Enterococcus faecalis*. *Antimicrobial Agents and Chemotherapy* **1996**, *40*(4), 863-869.

Depardieu, F.; Courvalin, P.; Msadek, T. A six amino acid deletion, partially overlapping the VanSB G2 ATP-binding motif, leads to constitutive glycopeptide resistance in *VanB*-type *Enterococcus faecium*. *Molecular Microbiology* **2003**, *50*(3), 1069-1083.

Heijenoort, J.V. Lipid Intermediates in the Biosynthesis of Bacterial Peptidoglycan. *Microbiology and Molecular Biology Reviews* **2007**, *71*(4), 620-635.

Hoyland, C.N.; Aldrige, C.; Cleverley, R. M.; Duchene, M.; Minasov, G.; Onopriyenko, O.; Sidiq, K.; Stogios, P. J.; Anderson, W.F.; Daniel, R.A.; Savchenko, A.; Vollmer, W.; Lewis, R. J. Structure of the LdcB LD-Carboxypeptidase Reveals the Molecular Basis of Peptidoglycan Recognition. *Structure* **2014**, *22*, 949-960.

Korza, H. J; Bochtler, M. *Pseudomonas aeruginosa* LD-Carboxypeptidase, a Serine Peptidase with a Ser-His-Glu Triad and a Nucleophilic Elbow. *The Journal of Biological Chemistry* **2005**, *280*(49), 40802-40812.

Kwun, M.J.; Novotna, G.; Hesketh, A. R.; Hill, L.; Hong, H. In Vivo Studies Suggest that Induction of VanS-Dependent Vancomycin Resistance Requires Binding of the Drug to D-Ala-D-Ala Termini in the Peptidoglycan Cell Wall. *Antimicrobial Agents and Chemotherapy* **2013**, *57*(9), 4470-4480.

Meziane-Cherif, D.; Stogios, P. J.; Evdokimova, E.; Savchenko, A.; Courvalin, P. Structural basis for the evolution of vancomycin resistance D,D-peptidases. *Proceedings of the National Academy of Sciences* **2014**, *111*(16), 5872-5877.

Morelle, W.; Michalski, J. Analysis of protein glycosylation by mass spectrometry. *Nature Protocols* **2007**, *2*(7), 1585-1602.

Patti, G.J.; Chen, J.; Schaefer, J.; Gross, M. L. Characterization of Structural Variations in the Peptidoglycan of Vancomycin-Susceptible *Enterococcus faecium*: Understanding Glycopeptide-Antibiotic Binding Sites Using Mass Spectrometry. *Journal for the American Society for Mass Spectrometry* **2008**, *19*, 1467-1475.

Pfeffer, J. M.; Clark, A. J. Identification of the First Known Inhibitors of O-Acetylpeptidoglycan Esterase: A Potential New Antibacterial Target. *ChemBioChem* **2012**, *13*(5), 722-731.

Rice, L. B. Emergence of Vancomycin-Resistant Enterococci. *Emerging Infectious Diseases* **2001**, *7*(2), 183-187.

Tong, G.; Pan, Y.; Dong, H.; Pryor, R.; Wilson, G. E.; Schaefer, J. Structure and Dynamics of Pentaglycyl Bridges in the Cell Walls of *Staphylococcus aureus* by ^{13}C-^{15}N REDOR NMR. *Biochemistry* **1997**, *36*, 9859-9866.

Vollmer, W. Structural variation in the glycan strands of bacterial peptidoglycan. *FEMS Microbiology Reviews* **2008**, *32*, 287-306.

Werner, G.; Strommenger, B.; Witte, W. Acquired Vancomycin Resistance in Clinically Relevant Pathogens. *Future Microbiology* **2008**, *3*(5), 547-562.